Florian Adanitsch

Synthesis of Biological Active Carbohydrates and Analogues

DIPLOMARBEIT

Zur Erlangung des akademischen Grades
eines Diplom-Ingenieurs

an der

Technischen Universität Graz

Betreuerin: Assoc. Prof. Dipl.-Ing. Dr. *techn*. Tanja M. Wrodnigg
Institut für Organische Chemie
Technische Universität Graz

2010

Diese Arbeit wurde in Zusammenarbeit mit Dr. Peter C. Tyler (Industrial Research Limited, Lower Hutt, New Zealand) und Dr. Vern L. Schramm (Albert Einstein College of Medicine, New York, USA) durchgeführt.

Meinen Eltern

Dank

Mein besonderer Dank gilt Prof. Dr. Tanja Wrodnigg und Prof. Dr. Arnold Stütz für die Aufnahme in die Glycogroup, die Themenstellung, die Hilfe bei der Organisation des Neuseeland Aufenthalts, die hervorragende Betreuung, die Geduld und die vielen Gespräche und Aktivitäten in und um die Glycogroup.

Weiters gilt mein Dank allen meinen Glyco-Mitstreitern Gerit, Georg, Uwe, Kathi, Verena, Martin und Patrick.

Allen Kollegen am Institut für Organische Chemie danke ich für die gute Zusammenarbeit und das tolle Umfeld. Bei Birgit Krenn möchte ich mich herzlich für die Hilfe bei den Nitrilsynthesen bedanken. Carina Illaszewicz-Trattner und Prof. Dr. Jörg Weber danke ich für die Unterstützung bei der NMR-Spektroskopie.

Dr. Richard Furneaux, Dr. Peter Tyler, Dr. Gary Evans und Dr. Alistair Longshaw danke ich für die Möglichkeit eine kurze Zeit an ihrer interessanten Forschung mitarbeiten zu dürfen, für die ausgezeichnete Betreuung und ihre Geduld.

Des Weiteren möchte ich mich beim gesamten IRL „Carbo-Team“ für die herzliche Aufnahme, für die Unterstützung bei der Arbeit und vor allem für die zahlreichen Hilfestellungen und Aktivitäten abseits der Labors bedanken.

Dr. Vern Schramm und seinem Team vom Albert Einstein College of Medicine, New York danke ich für die biologischen Tests der von mir hergestellten Verbindungen.

Dem Büro für Internationale Beziehungen und Mobilitätsprogramme der TU Graz, der Fakultät für Technische Chemie, Verfahrenstechnik und Biotechnologie der TU Graz, dem Land Steiermark und Prof. Dr. Rolf Breinbauer danke ich für die großzügige finanzielle Unterstützung.

All meinen Freunden danke ich für ihre Unterstützung, Motivation und die schöne Zeit in allen Lebenslagen.

Meinen Eltern und meiner Schwester gilt mein besonderer Dank für ihre Unterstützung, ihr Vertrauen und ihre Liebe.

Deutsche Fassung:
Beschluss der Curricula-Kommission für Bachelor-, Master- und Diplomstudien vom 10.11.2008
Genehmigung des Senates am 1.12.2008

EIDESSTATTLICHE ERKLÄRUNG

Ich erkläre an Eides statt, dass ich die vorliegende Arbeit selbstständig verfasst, andere als die angegebenen Quellen/Hilfsmittel nicht benutzt, und die den benutzten Quellen wörtlich und inhaltlich entnommene Stellen als solche kenntlich gemacht habe.

Graz, am …… ……..
(Unterschrift)

Englische Fassung:

STATUTORY DECLARATION

I declare that I have authored this thesis independently, that I have not used other than the declared sources / resources, and that I have explicitly marked all material which has been quoted either literally or by content from the used sources.

…… ……..
date (signature)

Abstract

The presented Diploma Thesis is divided into two parts and investigates synthetic approaches towards biological active carbohydrate anlogues.

Part 1: Glycoproteins and glycopeptides are ubiquitous biomolecules that are involved in many biological processes such as cell-cell recognition and communication or immune response. Convenient and efficient access to these glycoconjugates in large quantities is necessary in order to explore their biological relevance as well as to exploit the glycoconjugates functions for the development of new therapeutical methods. The applicability of the Amadori rearrangement for a short and convenient synthesis of glycosylated *C*-glycosyl type glycocoproteins and glycopeptides is investigated.

Part 2: Enzyme inhibitors that closely mimic the transition state structure of the natural substrate are very powerful and show great potential for the development of new pharmaceutical applications. The human and bacterial enzymes 5'-methylthioadenosine phosphorylase (MTAP) and 5'-methylthioadenosine nucleosidases (MTANs) are involved in carcinogenesis as well as bacterial virulence factors. This work presents the synthesis and the biological evaluation of a series of transition state analogue inhibitors for MTAP and MTANs.

Zusammenfassung

Im Zuge dieser Arbeit wurden in zwei Teilen Synthesemethoden für biologisch aktive Kohlenhydrate und Kohlenhydratanaloga untersucht.

Teil 1: Glycoproteine und Glycopeptide gehören zur Substanzklasse der Glycoconjugate und sind wichtige Biomoleküle, die an vielen biologischen Prozessen, wie Zell-Zell Erkennung und Kommunikation oder an Immunreaktionen beteiligt sind. Um ihre Funktionen zu erforschen und für neue therapeutische Ansätze ausnützen zu können, ist es nötig Glycoproteine und Glycopeptide in größerem Maßstab auf einem kurzen und effizienten Weg zu synthetisieren. Dieser Arbeit untersucht die Anwendbarkeit der Amadori Umlagerung für die kurze und einfache Synthese von glycosylierten *C*-glycosyl ähnlichen Glycoproteinen und Glycopeptiden.

Teil 2: Enzyminhibitoren welche den Übergangszustand der natürlichen Substrate nachahmen, sind sehr aktiv und zeigen großes Potential zur Entwicklung neuer pharmazeutischer Wirkstoffe. Die menschlichen und bakteriellen Enzyme 5'-Methyladenosin Phosphorylase (MTAP) und 5'-Methylthioadenosin Nucleosidase (MTAN) sind in Stoffwechselprozesse involviert, die die Cancerogenese und krankheitserregende Wirkung pathogener Bakterien fördern. Dieser Teil der Arbeit zeigt die Synthese und biologische Evaluierung neuer Inhibitoren für diese Enzyme.

Abbreviatons

AI	autoinducer
AMP	adenosine monophosphate
APCI	atmospheric pressure chemical ionisation
aq	aqueous
Asn	asparagine
ATP	adenosine triphosphate
BOC	*tert*-butoxycarbonyl
BzCl	benzoyl chloride
Cbz	carboxybenzyl
CC	column chromatography
$CDCl_3$	deuterochloroform
CH	cyclohexane
d	doublet
d_6-DMSO	deuterated dimethyl sulfoxide
DBU	1,8-diazabicyclo[5.4.0]undec-7-ene
DCM	dichloromethane
dd	doublet-doublet
ddd	doublet of doublets of doublets
DIPEA	*N,N*-diisopropylethylamine
DMAP	4-dimethylaminopyridine
DMF	dimetyhl formamide
DMSO	dimethyl sulfoxide
DTPM	[1,3-dimetyhl-2,4,6 (1H,3H,5H)-trioxopyrimidine-5-ylidene]methyl
E_a	activation energy
equiv	equivalent
ESI	electrospray inonization
Et_2O	diethyl ether
Et_3N	triethylamine
EtOAC	ethyl acetate
EtOH	ethanol
Gal	D-galactose
GalNac	*N*-acetyl-D-galactosamine
Glc	D-glucose
GlcA	D-glucuronic acid
GlcNAc	*N*-acetyl-D-glucosamine
GPI	glycophosphatidylinositol
HPLC	high performance liquid chromatography
HRMS	high resolution mass spectrum
IAG-NH	inosine-adenosine-guanosine nucleoside hydrolase
Imm	Immucillin
IU-NH	inosine-uridine nucleoside hydrolase
K_I	inhibition constant
KIE	kinetic isotope effect
L-Ara	L-arabinose
L-Fuc	L-fucose
L-IdoA	L-iduronic acid
LRMS	low resolution mass spectrum
M	molar
m	multiplett
Man	D-mannose
MeOD	deuterated methanol
mp	melting point
MT	methylthio

MTA	5'-methylthioadenosine
MTAN	5'-methylthioadenosine/S-adenosylhomocysteine nucleosidase
MTAP	5'-methylthioadenosine phophorylase
MW	molecular wight
NANA	*N*-acetylneuraminic acid
NaOMe	sodium methoxide
NBS	*N*-bromosuccinimide
n-BuLi	n-butyl lithium
nM	nanomolar
NMR	nuclear magnetic resonance
$Pd/BaSO_4$	palladium on barium sulfate
Pd/C	palladium on carbon
PMBA	4-methoxy-benzylamine
PNP	purine nucleoside phosphorylase
rf	retention factor
rt	room temperature
s	singlet
SAH	S-adenosylhomocysteine
SAM	S-adenosylmethionone
sat	saturated
Ser	seronine
SRH	S-ribosyl-homocysteine
t	triplet
TBDMS-Cl	*tert*-butyldimethylsilyl chloride
TFA	trifluoroacetic acid
THF	tetrahydrofuran
Thr	threonine
TLC	thin layer chromatography
p-TSA	*p*-toluenesulfonic acid
UV	ultra violett
Xyl	D-xylose
µM	micromolar

Part 1

1 Synthesis of glycosylated C-glycosyltype Glycoconjugates via the Amadori Rearrangement

1.1 Introduction

1.1.1 Carbohydrates

Together with proteins, nucleic acids and lipids carbohydrates constitute the four major classes of biomolecules. Formally carbohydrates are regarded as polyhydroxy aldehydes (aldoses) or ketones (ketoses) with chain lengths between four and six carbon atoms. In fact, many carbohydrates contain more than six carbon atoms and also show a broad variety of functional groups. For instance the *N*-acetylneuraminic acid has a carbon-backbone of nine carbon atoms and contains an *N*-acetyl group as well as a carboxylic acid function (Figure 1).

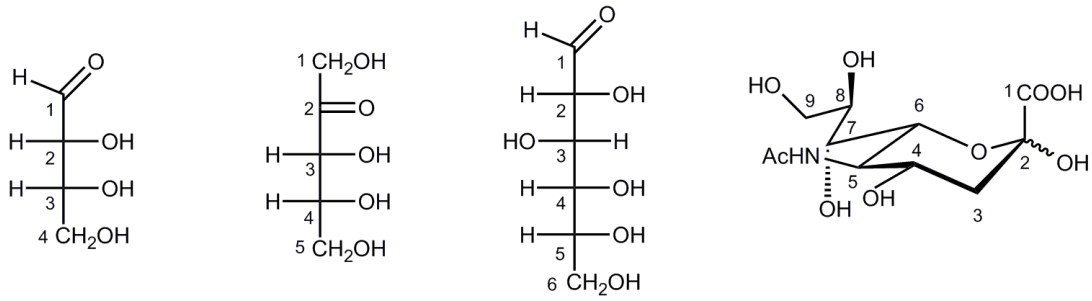

Figure 1: Examples for the different structures of carbohydrates, showing aldoses (D-erythrose and D-glucose) and a ketose (D-ribulose), different chain lengths of the carbon backbone as well as different functional groups (*N*-acetylneuraminic acid).

One characteristic feature of carbohydrates is that they usually do not occur as open chain molecules but form more stable 5- and 6-membered heterocyclic rings. The ring closure takes place between the carbonyl C-atom and one of the hydroxyl groups and as a consequence the carbonyl group is replaced by a hemiacetal. This hemiacetalic group, also referred to as the anomeric centre, is a key feature of carbohydrates and is responsible for their distinctive chemical behaviour (Figure 2).

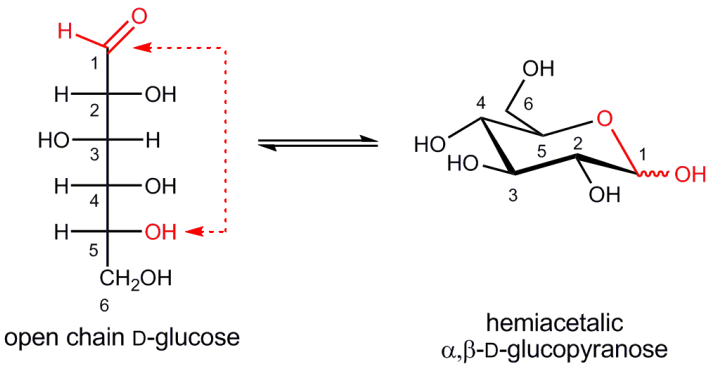

Figure 2: Formation of α,β-D-glucopyranose from the open chain form of D-glucose, by formation of a hemiacetal between C-1 and O-5.

The carbohydrate-monomers also form oligo- and polysaccharides by linkage of different monosaccharides units with each other. This formation of oligo- and polysaccharides has two important characteristics. First: the monosaccharide units can be linked with each other by various linkage types. Second: the formed polymers can be highly branched. For example, starch, the plants major energy store, and cellulose, the major constituent of the plant cell wall. Both polysaccharides consist of several thousand D-glucose monosaccharide units and differ from each other by the type of the monosaccharide linkage through the anomeric centre as well as by branching. Starch is composed of two different polysaccharides, namely amylose and amylopectin. In amylose the D-glucose units are linked by α-(1→4) glycosidic bonds with each other. In amylopectin the monosaccharide units are linked by α-(1→4) glycosidic bonds as well but there are additional branches at position C-6 of the D-glucose units. At these branching points other α-(1→4) linked D-glucose chains are attached to the main polysaccharide. In cellulose the D-glucose units are linked with each other by a β-(1→4)-glycosidic bond and the polysaccharide is not branched (Figure 3). As a consequence of the different linkage of the monosaccharide units and the branching the two polysaccharides have considerably different properties. For instance, starch forms linear and helical structures and the molecules are arranged in granules, whereas cellulose is strictly linear and adopts rod-like, stiff structures.

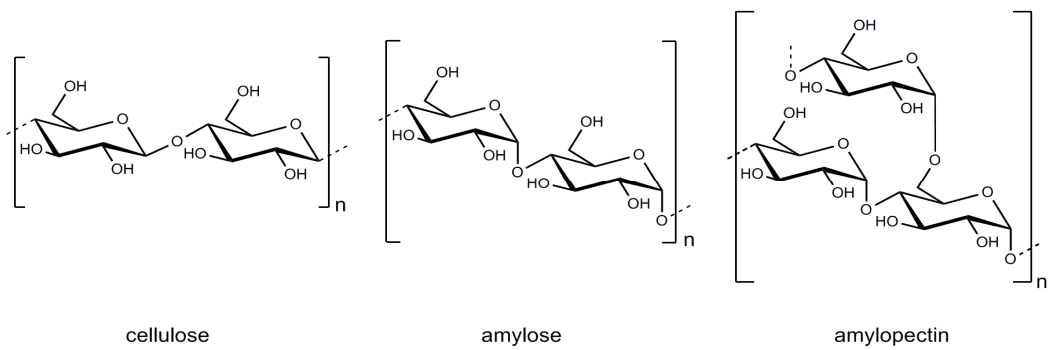

Figure 3: The structures of the polysaccharides cellulose and amylose as well as amylopectin, which form starch.

The various linking types as well as the branching possibilities distinguish polysaccharides from the other two classes of biopolymers, thus the nucleic acids and the proteins. The latter only have one distinctive type of linkage (the phosphodiester bond for nucleic acids and the amide bond for proteins) and, therefore, are linear.[1] The broad variety of linking possibilities allows carbohydrates to occur in almost unlimited structural variations and their functional diversity is as manifold as their structural variety.

In contrast to other biomolecules, such as proteins and nucleic acids, relatively less attention was paid to carbohydrates for a long time. This was mainly caused by two reasons. First, simple and fast structural determination of carbohydrate structures was not possible for a long time due to the lack of analytical tools that were capable to account for complexity of carbohydrate structures. Second, the biological role of carbohydrates was simply underestimated. They were believed to address only two major functions. First: to serve as the major source of energy for all higher living organisms such as plants and animals and second: to structurally constitute the major organic component of the exoskeletons of arthropods (insects, crustaceans, etc.) as well as of the plant cell wall.

This point of view changed in the 1960s, when it was discovered that carbohydrates, either bound to proteins or lipids, so called glycoconjugates, are ubiquitous constituents of extracellular matrices and of the cell surface.[2, 3] There they are essentially involved in cell-cell recognition,[4] cellular differentiation[5] as well as immune response.[6] The discovery of these important roles of glycoconjugates suggested that the understanding of their functions is important for the overall understanding of life related processes and furthermore gives rise for new therapeutic approaches. For example, influenza is initiated by the binding of the virus' heamagglutinin (a carbohydrate-binding membrane protein) to oligosaccharides on the surface of host cells. Molecules with high affinity for the heamagglutinin have the potential to act as competitive inhibitors for hemagglutinin and therefore are potent candidates for influenza blockers.[7]

1.1.2 Glycoconjugates

The glycoconjugates found on cell surfaces and extracellular matrices consist of oligo- and polysaccharides covalently attached to proteins and lipids. Hence, the resulting

[1] Dwek, R.A. Glycobiology: Toward understanding the function of sugars. *Chem. Rev*. **1996**, *96*, 683-720.
[2] Cipolla, L.; La Ferla, B.; Nicotra, F.; Peri, F. Glycoconjugate and oligosaccharide mimetics by chemoslective ligation. *C. R. Chimie* **2003**, *6*, 635-544.
[3] Robyt, J.F. Essentials of carbohydrate chemistry. Springer Verlag, Inc. New York, **1998**, 262-289.
[4] Irvine, K.D.; Okajima, T. Regulation of notch signalling by *O*-linked fucose. *Cell* **2002**, *111*, 893-904.
[5] Nishiwaka, K. et al. An NDPase links ADAM protease glycosylation with organ morphogenesis in *C. elegans. Nat. Cell Biol*. **2004**, *6*, 31-37.
[6] Lowe, J.B. Glycosylation, immunity and autoimmunity. *Cell* **2001**, *104*, 809-812.
[7] Nishimura, S.-I. *et al*. Glycotentacles: Synthesis of cyclic glycopeptides, toward a tailored blocker of influenza virus hemagglutinin. *Angew. Chem. Int. Ed*. **2003**, *42*, 5186-5189.

glycoconjugates are for example glycolipids, lipopolysaccharides, glycoproteins as well as glycopeptides (Figure 4).

Glycolipids are glycoconjugates with a diacylglyceride or a ceramide as the lipid moiety. The carbohydrate part can be a mono-, di- or a branched oligosaccharide. Glycolipids occur primarily in the outer leaflet of the cell membrane and participate in adhesion, signalling and cellular recognition.[8] Lipopolysaccharides are part of the outer membrane of Gram-negative bacteria. They are macromolecular glycoconjugates and consist of three parts: the lipid A, where fatty acids are attached to a disaccharide, the core oligosaccharide and a large, branched polysaccharide. Lipopolysaccharides contribute to the stabilization of the membrane and protect the cell against chemical and physical stress, evoked by the environment of the bacteria.[9] In glycoproteins and glycopeptides the carbohydrate moiety is bound to a protein usually via an *O*- or an *N*-glycosidic linkage to serine, threonine or asparagine, respectively. More seldom also *C*-glycosyl type linkages are found.[10]

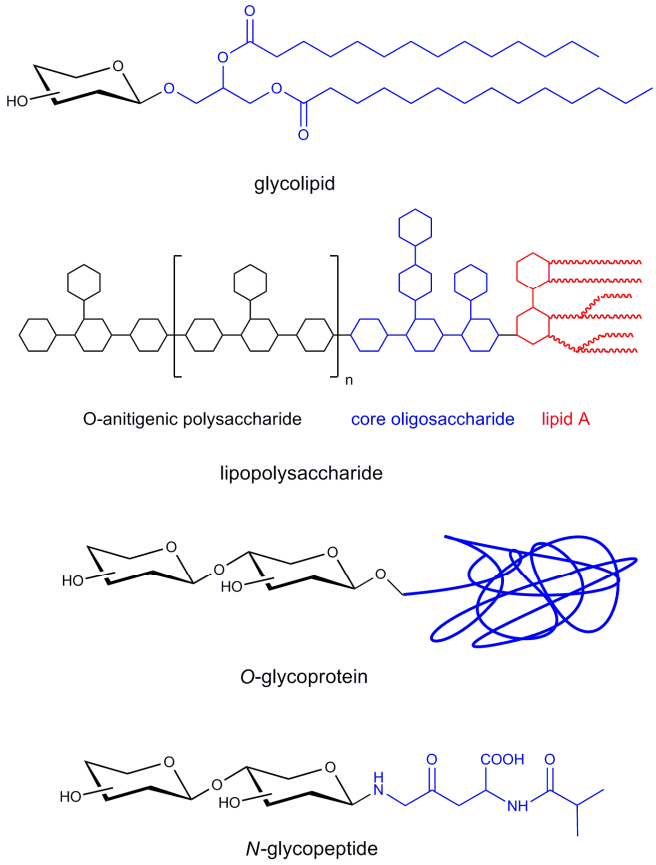

Figure 4: Schematic representations of a glycolipid, a lipopolysaccharide, a glycoprotein as well as a glycopeptide.

[8] Ariga, T.; Yanagisawa, M.; Yu, R. K. in Comprehensive Glycosience. From chemistry to systems biology. Vol.1. Kamerling, J.P. ed., Elsevier Ltd. Oxford, **2007**, p. 73
[9] Holst, O.; Müller-Loennies, S. in Comprehensive Glycosience. From chemistry to systems biology. Vol.1. Kamerling, J.P. ed., Elsevier Ltd. Oxford, **2007**, 123-126.
[10] Talyor, C.M. Glycopeptides and Proteins: Focus on the glycosidic linkage. *Tetrahedron*, **1998**, *54*, 11317-11362.

Among glycoconjugates, especially glycoproteins and glycopeptides have gained valuable interest, since they play an important role in various biological processes such as inflammatory response, cancer metastasis, and bacterial as well as viral infection. Furthermore, the co- and posttranslational modification of proteins with carbohydrates has a crucial impact on the proteins structure, stability and function.[11]

1.1.3 Glycoproteins

In glycoproteins and glycopeptides there are different types of linkage between the carbohydrate moiety, also referred to as the glycan, and the protein or the peptide, also referred to as the aglycon. The most common linkages are the connection via an *O*-glycosidic bond to serine or threonine, the connection via an *N*-glycosidic bond to asparagine and a linkage via a glycophosphatidylinositol anchor (GPI-anchor). A GPI-anchor is a linkage between the *C*-terminal of an amino acid and ethanolamine phosphate as well as a glycan attached to posphatidylinositol. Beside these, also some more uncommon linkages are known, such as phosphodiester-bridges or *C*-glycosyl type linkages (Figure 5).[10, 12, 13]

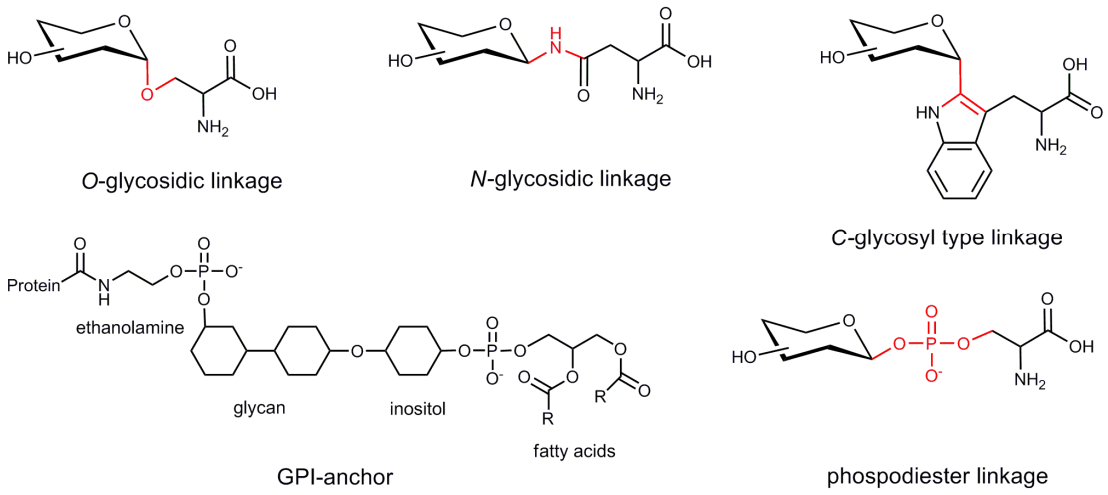

Figure 5: Schematic representation of common *O*-glycosidic, *N*-glycosidic and GPI-anchor linkages in glycoconjugates as well as more uncommon linkage types, such as C-glycosyl type linkage and phosphpdiester bridges**.**

The form of the carbohydrate part as well as the number of the glycosylation sites on the protein are not subjected to any boundaries. The glycan may consist of a single monosaccharide up to a complex and highly branched oligosaccharide or even a

[11] Seeberger, P.H.; Werz, D.B. Carbohydrates as the next frontier in pharmaceutical research. *Chem. Eur. J.* **2005**, *11*, 3194-3206.
[12] Wittmann, V. in Glycosience. Chemistry and Biology. Vol. 3. Fraser-Reid, B.O.; Tatsuta, K.; Thiem, J. eds. Springer-Verlag, Berlin, Heidelberg, **2001**, 2254-2287
[13] Dondoni, A.; Marra, A.; Massi, A. Design and use of an oxazolidine silyl enol ether as a new homoalanine carbanion equivalent for the synthesis of carbon-linked isosteres of *O*-glycosyl serine and *N*-glycosyl asparagine. *J. Org. Chem*. **1999**, *64*, 933-944.

polysaccharide, consisting of several hundreds of monosaccharide units. The number of glycans present on a single glycoprotein varies also from one single residue up to more than one hundred.[12]

Despite the fact that the flexibility in both glycan structure and glycan attachment sites seems to give rise to an inapprehensible possible number of different glycoproteins, it is found that nature only uses a distinctive set of monosaccharides to construct the glycans and that many glycans share common core structures.

The most common monosaccharide building blocks are D-galactose, D-glucose, D-mannose, *N*-acetyl-D-glucosamine, *N*-acetyl-D-galactosamine, L-fucose, L-arabinose, D-xylose, D-glucuronic acid, L-iduronic acid and *N*-acetylneuraminic acid (Figure 6).[3, 11]

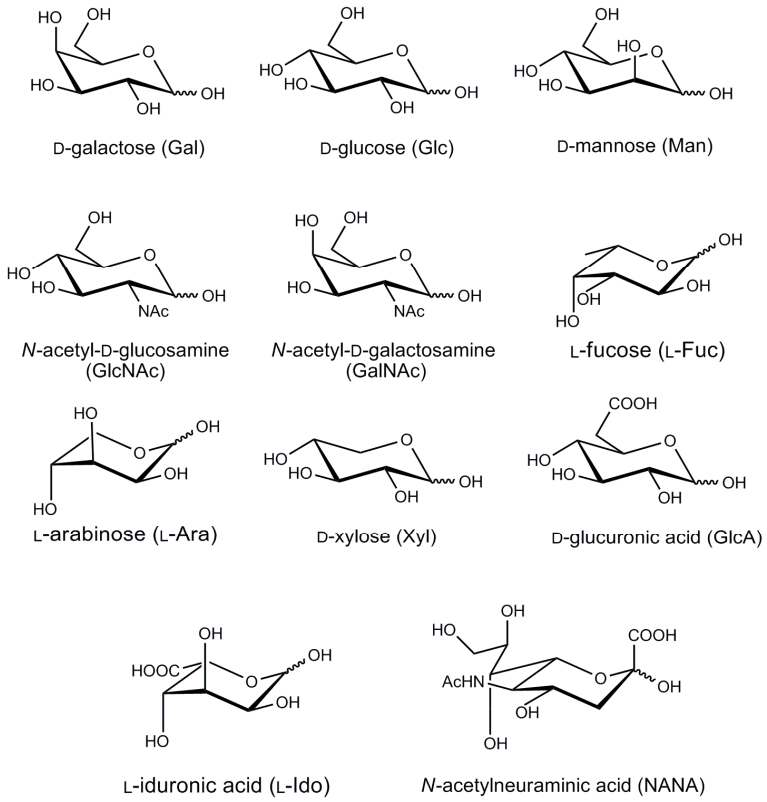

Figure 6: The monosaccharides D-galctose, D-glucose, D-mannose, *N*-acetyl-D-galactosamine, *N*-acetyl-D-glucosamine, L-fucose, L-arabinose, D-xylose, D-glucuronic acid, L-iduronic acid and *N*-acetylneuraminic acid as building blocks for glycan composition. Adapted from references [3] and [11].

However, it has to be noted that nowadays more than twenty other monosaccharides, such as 3-*O*-methyl-D-galctose, D-mannose-6-sulfate or 6-deoxyaltrose, are known to complement the set of the "classical" monosaccharides.

The glycans core structure composition depends on the type of glycosidic linkage between the protein and the carbohydrate, and is determined through the corresponding biosynthetic pathway.[14] For example, in the case of *N*-glycans there are four common types

[14] Williams, S.J. in Enceclopedia of Chemical Biology Vol. 2. T. P. Begley. Ed., John Wiley & Sons Inc., New Jersey. **2009**, 151-163.

of core pentasaccharides and further diversity of the glycan is provided by the attachment of up to five different carbohydrate chains (antennae) to the core saccharide. For *O*-glycans eight different core structures are known and again the diversity of the *O*-glycans is achieved by the attachment of different carbohydrates to these core saccharides.[12] An example for such a glycan composition is shown in Figure 7 for an *N*-glycan.

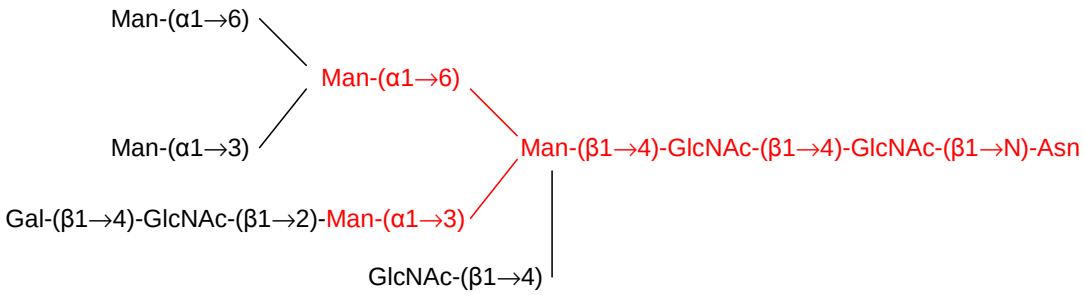

Figure 7: Example of an *N*-glycan linked to a protein via an *N*-glycosidic bond to asparagine. The core pentasaccharide is depicted in red. Adapted from reference [12].

The functional variety of glycoproteins is as broad as their structural diversity. They are involved in the identification of different cell types, cell to cell recognition, cell development and differentiation, intracellular communication, cell adhesion, microbial virulence as well as host immune responses. The glycans attached to glycoproteins have crucial impact on their overall properties and there is no unifying function for the glycans.[1] They influence the correct expression and folding, increase thermal and proteolytic stability and modulate solubility as well as *in vivo* half life.[15]

A well known example illustrating the influence of glycans on the differentiation between cell phenotypes is the determination of the human blood groups by *O*-glycans. These *O*-glycans are attached to proteins and lipids on the surface of the red blood cells. The glycoproteins of the erythrocytes all share a branched nonasaccharide core linked via an *O*-glycosidic bond to L-serine or L-threonine and the blood groups are distinguished by the attachment of different monosaccharide units to the core saccharide (Figure 8).[3] The blank core saccharide without any additional monosaccharides attached resembles 0-type human blood, attachment of *N*-acetyl-D-galactosamine or D-galactose resembles A- and B-type human blood, respectively and a mixture of both *N*-acetyl-D-galactosamine and D-galactose attached resembles AB-type human blood.

[15] Davis, B.G. Synthesis of glycoproteins. *Chem. Rev*. **2002**, *102*, 579-601.

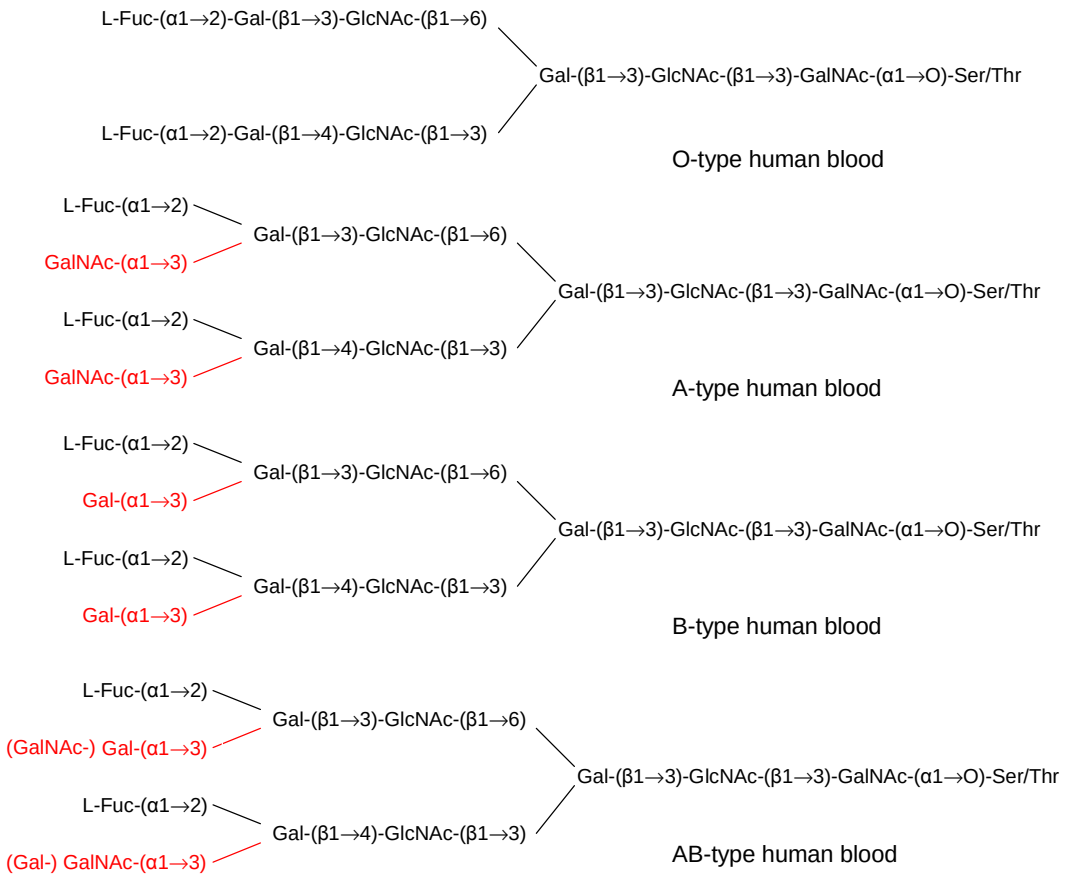

Figure 8: The glycans attached to proteins and lipids on the surface of the human blood cells. The core saccharide, which is the same for all four blood groups, is shown in black. The blood group determining monosaccharides are depicted in red. Adapted from reference [3].

In order to gain thorough understanding of the processes where glycoproteins are involved, the study of the glycans influence on the overall chemical, physical and biological properties is of fundamental importance. To probe these influences in biological studies, access to glycoproteins is required in large-scale quantities. Since glycoproteins occur in a complex and heterogeneous biological matrix, isolation techniques are often tedious, require considerable efforts and yield only small quantities of the desired compound.[11] Therefore, the chemical synthesis of glycoproteins has become an important target in the field of synthetic chemistry. Another aspect that triggers research efforts towards glycoconjugate synthesis is that carbohydrate modification can influence the physiological behaviour of therapeutic compounds. For example, it has been found that modification of insulin with sugar residues improves its intestinal adsorption as well as its stability against enzymatic degradation.[16]

[16] Haga, M.; Hashimoto, T.; Hayashi, M.; Komatsu, K.; Nomoto, M. Improvement of intestinal absorption of peptides: adsorption of B1-Phe monoglucosylated insulin to rat intestinal brush-border membrane vesicles. *Eur. J. Pharm. Biopharm*. **2000**, *50*, 197-204.

Due to the fact, that the majority of glycoproteins belong to the group of *N*- and *O*-glycosides numerous synthetic protocols towards such glycoproteins have been developed and many potential applications for those glycoproteins are being explored.[10, 11, 15, 17]

However, one drawback of *N*- and *O*-glycosides is the sensitivity of the glycosidic linkage towards chemical and enzymatic hydrolysis. This issue is of particular interest for the design of potential pharmaceutical drugs because *in vivo* degradation may affect the drugs overall properties, such as bioavailability, half life and transport properties. In order to enhance the glycoproteins stability towards acids, bases and enzymes the *N*- and *O*-glycosidic bonds can be replaced by a *C*-glycosyltype glycosidic bond.[18] Since the *C*-glycosyltype glycosidic linkage is more stable towards chemical and enzymatic hydrolysis, glycoconjugates with this feature are ideal candidates for studies on the biological role of glycoconjugates as well as for the development of new pharmaceutical drugs.[13] As a consequence, several synthetic methodologies for the synthesis of *C*-glycosyltype glycoconjugates have been reported.[13, 19] However, most of these syntheses often require long protection-deprotection sequences of both the sugars and the amino acids and therefore, give low yields. An alternative to the conventional syntheses is provided by the Amadori rearrangement. This reaction allows for simple introduction of an amine onto position C-1 of a carbohydrate and the concomitant rearrangement introduces a *C*-glycosyl type glycosidic bond, without requiring protecting group manipulations.[20]

1.1.4 The Amadori Rearrangement

The Amadori rearrangement is a reaction between α-hydroxy aldehydes and suitable amines, i. e. primary as well as secondary amines, leading to α-amino ketones. Applied on aldose **1** it leads to the introduction of an amine moiety at the anomeric carbon and subsequent isomerisation gives the corresponding 1-amino-1-deoxyketose **2** (Figure 9).[21]

[17] (a) Schachter, H. Glycoproteins: Their structure, biosynthesis, and possible clinical implications. *Clin. Biochem.* **1984**, *17*, 3-14; (b) Davis, B.G.; Doores, K.J.; Gamblin, D.P. Exploring and exploiting the therapeutic potential of glycoconjugates. *Chem. Eur. J*. **2006**, *12*, 656-665; (c) Schmidt, R.R.; Zhu, X. New priciples for glycoside bond formation. *Angew. Chem. Int. Ed*. **2009**, *48*, 1900-1934; (d) Bernardes, G.J.L.; Castagner, B.; Seeberger, P.H. Combined approaches to the synthesis and study of glycoproteins. *Chem. Biol.* **2009**, *4*, 703-713; (e) Davis, B.G.; Gamblin, D.P.; Scanlan E.M. Glycoprotein synthesis: An update. *Chem Rev*. **2009**, *109*, 131-163.

[18] Burkhart, F.; Hoffmann, M.; Kessler, H. Stereoselektive Synthese eines *C*-glycosidischen Analogons des *N*-Glucoasparagins. *Angew. Chem*. **1997**, *109*, 1240-1241.

[19] (a) Gyepesova, D.; Koos, B.; Langer, V.; Micova, J.; Steiner, M. Synthesis and structure determination of some nonanomerically C-C-linked serine glycoconjugates structurally related to mannojirimycin. *Carbohydr. Res*. **2004**, *339*, 2187-2195; (b) Leeuwenburgh, M.A.; van der Marel, G.A.; Overkleeft, H.S. Olefin metathesis in glycobiology: new routes towards diverse neoglycoconjugates. *Curr. Opin. Chem. Biol.* **2003**, *7*, 757-765; (c) Franck, R.W.; McAllister, G.D.; Talyor, R.J.K. The Ramberg-Bäcklund reaction for the synthesis of *C*-glycosides, *C*-linked disaccharides and related compound. *Carbohydr. Res*. **2006**, *341*, 1298-1311.

[20] Illaszewicz, C.; Kartusch, C.; Wrodnigg, T.M. The Amadori rearrangement as key reaction for the synthesis of neoglycoconjugates. *Carbohydr. Res*. **2008**, *343*, 2057-2066.

[21] Eder, B.; Wrodnigg, T.M. in Topics in Current Chemistry 215. Stütz, A.E. ed., Springer: Berlin, Heidelberg, New York, **2001**, 115-152.

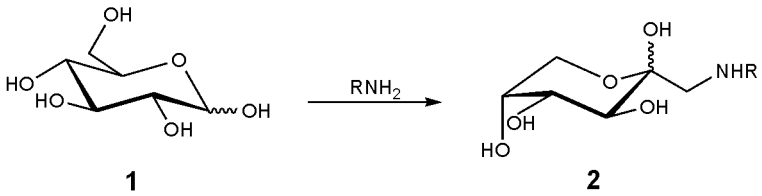

Figure 9: The Amadori rearrangement between D-glucose and a primary amine.

Together with the Heyns rearrangement (the alike reaction, applied on ketoses as starting materials, leading to the corresponding 2-amino-2-deoxyaldoses) the Amadori rearrangement is the initial step of the Maillard reaction cascade,[22] the non enzymatic browning of food. This reaction cascade takes place between reducing sugars and free amino groups of amino acids as well as proteins during cooking, baking and food preservation processes. During the reaction various complex degradation products are formed, which influence the aroma as well as the colour of food. Furthermore, some of the degradation products are believed to be involved in mutagenesis.[23] Besides its relevance for food processing and technology the Maillard reaction also takes place *in vivo*, where advanced end products of the cascade are involved in the pathology of Alzheimer's disease[24] and in the formation of diabetic cataracts.[25] Moreover, the Amadori rearrangement is involved in the synthesis of precursor molecules for the biosynthesis of folic acids[26] as well as for the biosynthesis of tryptophans.[27]

The products of the Amadori rearrangements were first reported by Mario Amadori between 1925 and 1931.[28] He investigated the reaction of D-glucose with *p*-phenetidine, *p*-anisidine and *p*-toluidine. Depending on the reaction conditions, he observed α,β-mixtures of two different products. When carried out in alcoholic media at the boiling point of the solvent the reaction afforded labile compounds, whereas the reaction gave more stable compounds when carried out "in substantia" under heating or prolonged reaction time in alcoholic media. Amadori suggested that the labile compounds are the corresponding *N*-glycosides and that

[22] (a) Maillard, M.L.-C. Formation d'humus et des combustibles mineraux sans intervention de l'oxygene atmosperique, des microorganismes, des hautes temperatures, ou des fortes pressions. *C.R. Acad. Sci*. **1912**, *2*,1554-1556; (b) Maillard, M.L.-C. Action des acides amines sur les sucres; formation des melanoidines par voie methodique. *C.R. Acad. Sci*. **1912**, *2*, 66-68.

[23] (a) Hodge, J.E.J. Dehydrated Foods: Chemistry of browning reactions in model systems. *J. Agric. Food Chem*. **1953**, *1*, 928-943; (b) Friedman, M. Food browning and its prevention: an overview. *J. Agric. Food Chem*. **1996**, *44*, 631-653.

[24] Smith, M.A. Advanced Maillard reaction end products are associated with Alzheimer disease pathology. *Proc. Natl. Acad. Sci. USA*, **1994**, *91*, 5710-5714.

[25] Cerami, A.; Monnier, V.M.; Rouzer, C.A.; Stevens, V.J. Diabetic cataract formation: Potential role of glycosylation of lens crystallins. *Proc. Natl. Acad. Sci. USA*, **1978**, *75*, 2918-2922.

[26] (a) Weygand, F. *et al.* Pterine aus 2.4.5-Triamino-6-hydroxy-pyrimidin und Zuckern. *Chem. Ber*. **1964**, *97*, 1002-1023; (b) Weygand, F. *et al.* Über die Biogenese des Leucopterins. *Angew. Chem*. **1961**, *73*, 402-407.

[27] Lignes, F.; Schraven, E. Synthesen von Amadori-Verbindungen der Anthranilsäure. *Liebigs Ann*. **1962**, *655*, 167-172.

[28] (a) Amadori, M. Proditti di condensazione tra glucosio e *p*-fenetidina. Notta I. *Atti Real. Accad. Naz. Lincei* **1925**, *2*, 337-342; (b) Amadori, M. Proditti di condensazione tra glucosio e *p*-fenetidina. Notta II. *Atti Real. Accad. Naz. Lincei* **1929**, *9*, 68-73; (c) Amadori, M. Proditti di condensazione tra glucosio e *p*-anisidina. *Atti Real. Accad. Naz. Lincei* **1929**, *8*, 226-230; (d) Amadori, M. Proditti di condensazione tra glucosio e *p*-toluidina. *Atti Real. Accad. Naz. Lincei* **1931**, *13*, 72-77.

the stable compounds are the corresponding imines. Kuhn and Dansi[29] further investigated Amadoris findings and proved that the labile compounds are indeed *N*-glycosides but they were not able to prove the formation of imines as well. Instead, they concluded that the presumed imines are the outcome of a new rearrangement process. Based on this work Kuhn and Weygand proposed a mechanism for this reaction, which, until nowadays, remained the accepted mechanism (Figure 10).[30]

The initial step in the Amadori rearrangement is the formation of the glycosyl amine **3** between aldose **1** and an amino group. Protonation at the nitrogen of **3** and ring opening forms the cationic imine **5**, which is in equilibrium with the enol **6** (enamine-aldimine tautomerism). The enol **6** is stabilized by the formation of the 1-deoxy-1-aminoketohexose **2**, which undergoes ring closure to the corresponding hemiketal. Another important contribution of Weygand to the understanding of the Amadori rearrangement was his realisation that the yields as well as the purity of the Amadori products increased significantly when the reaction was performed under acidic conditions.[31]

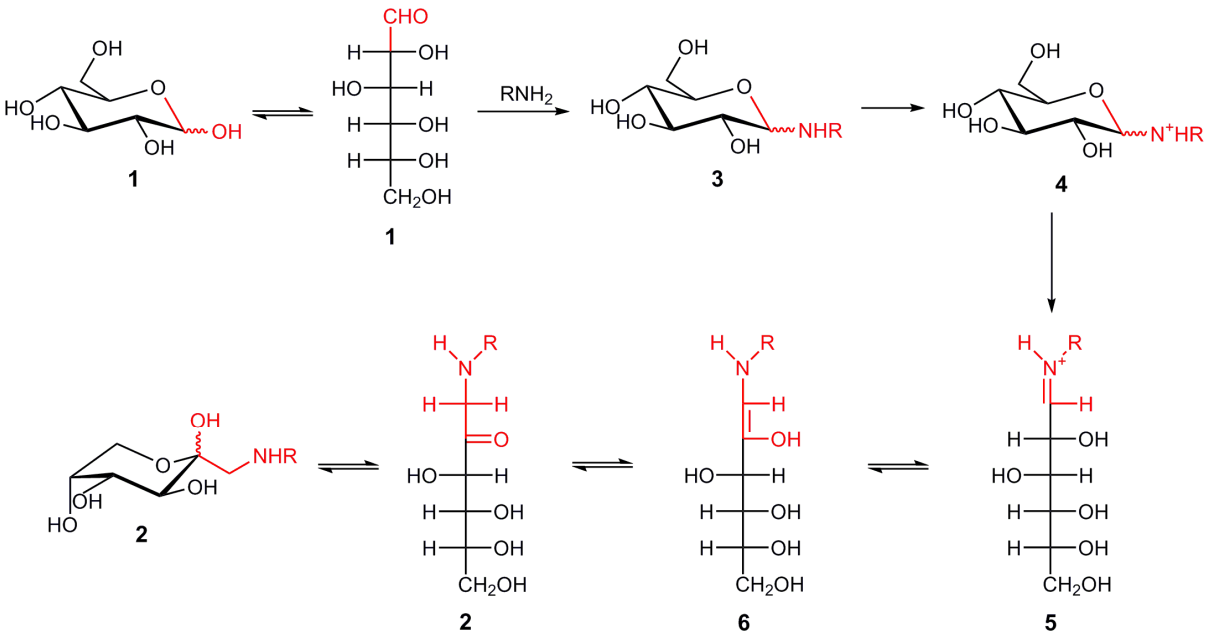

Figure 10: The mechanism of the Amadori rearrangement as suggested by Kuhn and Weygand.[30]

After the discovery of the Amadori rearrangement, which was mainly driven by investigation on the reactions between aldoses and aryl amines, the scope of the reaction was further probed with combinations of other carbohydrates as well as other amines, for

[29] Dansi, A.; Kuhn, R. Über eine molekulare Umlagerung von *N*-Glucosiden. *Ber*. **1936**, *69*, 1745-1754.
[30] Kuhn, R.; Weygand, F. Die Amadori-Umlagerung. *Ber*. **1937**, *70*, 769-772.
[31] Weygand, F. Über *N*-Glykoside, II Mitteil.: Amadori-Umlagerungen. *Ber*. **1940**, *73*, 1259-1278.

example D-glucuronic acid,[32] fructose,[33] primary and secondary aliphatic amines,[32] amino acids,[34] amino-sulfonic acids[35] as well as iminosugars.[36]

With the increasing knowledge about the Amadori rearrangement, i.e. the conditions necessary and its scope and limitations, useful synthetic applications have been found. One early application was the first synthesis of lactulose,[37] which did not employ the Lobry de Bruyn-Alberda van Ekenstein rearrangement.[38] Lactulose is a synthetic carbohydrate, which is used for the treatment of constipation and hepatic encephalopathy. Another application of the Amadori rearrangement is the synthesis of endopeptidase inhibitors.[39] Endopeptidase hydrolyses neuropetides and endogenous ligands of opiate receptors, which are important for physiological pain suppression.

In the synthesis of the powerful D-glucosidase and invertase inhibitors 2,5-dideoxy-2,5-imino-D-mannitol and derivatives thereof the Amadori rearrangement was employed for the synthesis of precursors of the actual inhibitors.[40]

More recently, Maugard *et al.* have applied the Amadori rearrangement on D-lactose **7** and *p*-amino-DL-phenylalanine **8** and afforded the corresponding *N*-[β-D-galactosyl-1-4-(1-deoxyfructos-1-yl]-*p*-amino-DL-phenylalanine rearrangement product **9** as a potential structural and functional mimic of *O*-glycoconjugates (Figure 11).[41]

[32] Heyns, K.; Schulz, W. 1-*N*-Aminosäure-1-desoxy-fructuronsäuren („Fructuron-Aminosäuren“) aus Glycin, Alanin und D-Glucuronsäure. *Chem. Ber*. **1960**, *93*, 128-132.
[33] Gottschalk, A.; Partridge, S.M. Interaction between simple sugars and amino-acids. *Nature*, **1950**, *165*, 684-685.
[34] Frowein, A.; Micheel, F. Synthese von Amadori-Derivaten der Aminosäuren. *Chem. Ber.* **1959**, *92*, 304-309.
[35] Behre, H.; Heyns, K.; Paulson, H. Darstellung von 1-Desoxy-1-(2-sulfoäthylamino)-D-fructose. *Carbohydr. Res*. **1967**, *5*, 225-228.
[36] Frowein, A.; Heinemann, K.H.; Micheel, F.; Schwieger, K.H. Amadori-Umlagerung; Synthese eines neuen *N*-Disaccharid-Typs. *Tetrahedron Lett*. **1965**, *42*, 3769-3771.
[37] Krüger, G.; Kuhn, R.; Seelinger, A. Kupplung von Amadori-Verbindungen mit Diazoniumsalzen. *Ann. Chem*. **1959**, *628*, 240-255.
[38] Angyal, S.J. in Topics in Current Chemistry 215. Stütz, A.E. ed., Springer: Berlin, Heidelberg, New York, **2001**, 1-14.
[39] Fehlhaber, H.-W.; Kogler, H.; Schindler, P.W.; Vértesy, L. Enkastines: Amadori products with a specific inhibiting action against endopeptidase-24.11-from streptomyces albus and by synthesis. *Liebigs Ann*. **1996**, 121-126.
[40] (a) Stütz, A.E. *et al*. 2,5-Dideoxy-2,5-imino-D-mannitol and -D-glucitol. Two-step bio-organic syntheses from 5-azido-5-deoxy-D-glucofuranose and -D-idofuranose; evaluation as glucosidase inhibitors and application in affinity purification and characterisation of invertase from yeast. Carbohydr. Res. 1993, 250, 67-77; (b) Stütz, A.E.; Withers, S.G.; Wrodnigg, T.M. Synthesis of 1-amino-1,2,5-trideoxy-2,5-imino-D-mannitol, a novel analogue of the powerful glucosidase inhibitor 2,5-dideoxy-2,5-imino-D-mannitol, *via* an Amadori rearrangement of 5-azido-5-deoxy-D-glucofuranose. *Tetrahedron Lett*. **1997**, *38*, 5463-5466.
[41] Bridiau, N.; Cabanel, S.; Maugard, T. Facile synthesis of pseudo-*C*-glycosyl *p*-amino-DL-phenylalanine building blocks via Amadori rearrangement. *Tetrahedron* **2009**, *65*, 531-535.

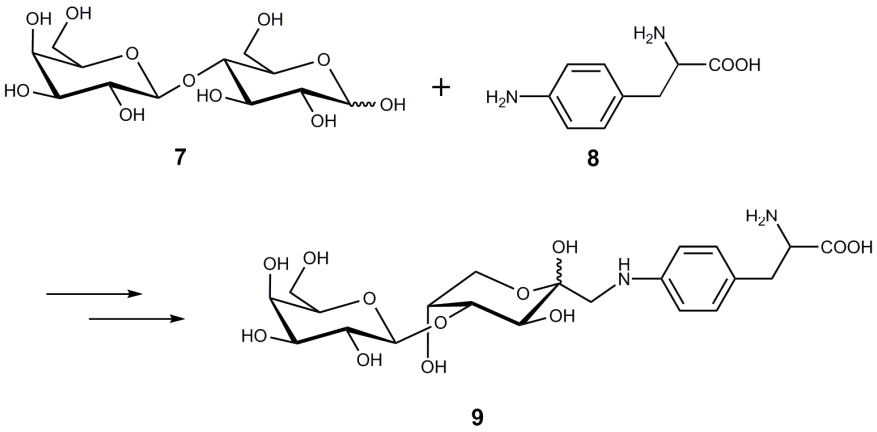

Figure 11: Amadori rearrangement between D-lactose **7** and *p*-amino-DL-phenylalanine **8** to the corresponding Amadori product *N*-[β-D-galactosyl-1-4-(1-deoxyfructos-1-yl]-*p*-amino-DL-phenylalanine **9** as potential structural and functional mimic of O-glycoconjugates. Adapted from reference [41].

Although these examples illustrate the preparative value of the Amadori rearrangement it suffers also from several preparative drawbacks. For example, depending on the acidic catalyst employed, the initial glycosylamine can either undergo the rearrangement or hydrolysis back to the starting material. In addition, the stability of the rearrangement products under the reaction conditions is limited. With prolonged reaction time and with increasing acidity of the employed catalyst more unwanted side products emerge. The basicity of the employed amine also exerts an important influence on the outcome of the reaction. The more basic the amine, the higher the possibility for inducing the formation of side products via the Lobry de Bruyn-Alberda van Ekenstein rearrangement. Taking all these side reactions into consideration it is not astonishing that the purification of the Amadori product is a difficult task and that the isolated yields usually vary between 30%-70%.[21]

Nevertheless, by thorough adjustment of the overall reaction conditions the Amadori rearrangement provides a simple and short method for the synthesis of 1-amino-1-deoxyketoses that can serve as an alternative, more stable linkage between carbohydrates and other biomolecules in glycoconjugates. Therefore, the Amadori rearrangement broadens the synthetic tools for the intentional synthesis of glycoconjugates, which can be used as probes for the study of the functions of naturally occurring glycoconjugates as well as for new therapeutic applications.

1.2 Objectives and Synthetic Plan

The objective of the presented work was to probe the general applicability of the Amadori rearrangement on disaccharides under reaction conditions previously established by our group.[20] Particular emphasis was laid on retaining the original constitution of the employed disaccharides reducing end in order to synthesise *C*-glycosyl type glycoconjugates that closely resemble the structure of naturally occurring glycoconjugates. Therefore, chain elongation of the disaccharides at the reducing end to the corresponding heptose was necessary prior to the Amadori rearrangement. Furthermore, the formation of a 1-*N*,2-*O*-cyclic carbamate between the amine function at position C-1 and the anomeric hydroxyl function at position C-2 of the rearrangement product should be investigated (Figure 12).

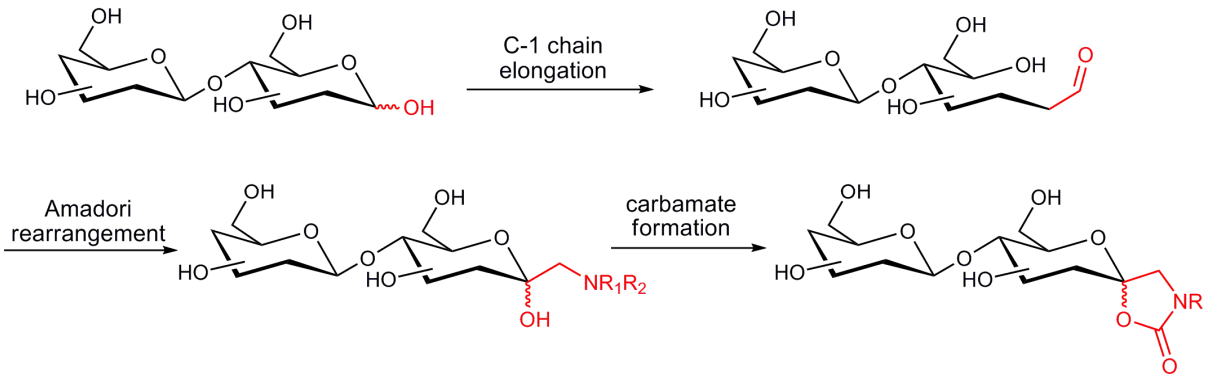

Figure 12: Schematic representation of the planned synthesis.

The disaccharides chosen were lactose **7**, cellobiose **10**, *N*-[1,3-dimethyl-2,4,6 (1H,3H,5H)-trioxopyrimidine-5-ylidene]methyl-2-amino-2-deoxy-lactose (*N*-DTPM-2-amino-2-deoxy-lactose) **11** and maltose **12**, since they consist of carbohydrate moieties, which frequently occur in natural glycoconjugates (Figure 13).[3, 11]

As amine compound dibenzyl amine **13** for carbohydrates **7**, **10** and **11** and methyl-6-aminohexanoate hydrochloride **14** for maltose **12** was chosen (Figure 13). Dibenzyl amine **13** was found to easily induce the Amadori rearrangement and furthermore it eases the purification process by column chromatography due to its low polarity. Additionally its UV-activity allows for better tracing of reaction products on TLC. Maltose **12** was reacted with methyl-6-aminohexanoate hydrochloride **14** in order to decrease the acidity of the reaction mixture, which could facilitate the cleavage of the disaccharides fragile α-glycosidic bond. Moreover, the formation of a secondary amine at position C-1 of the Amadori product in this case enabled to probe the formation of a 1-*N*,2-*O*-cyclic carbamate, in order to further stabilize the *C*-glycosyl type bond.[20]

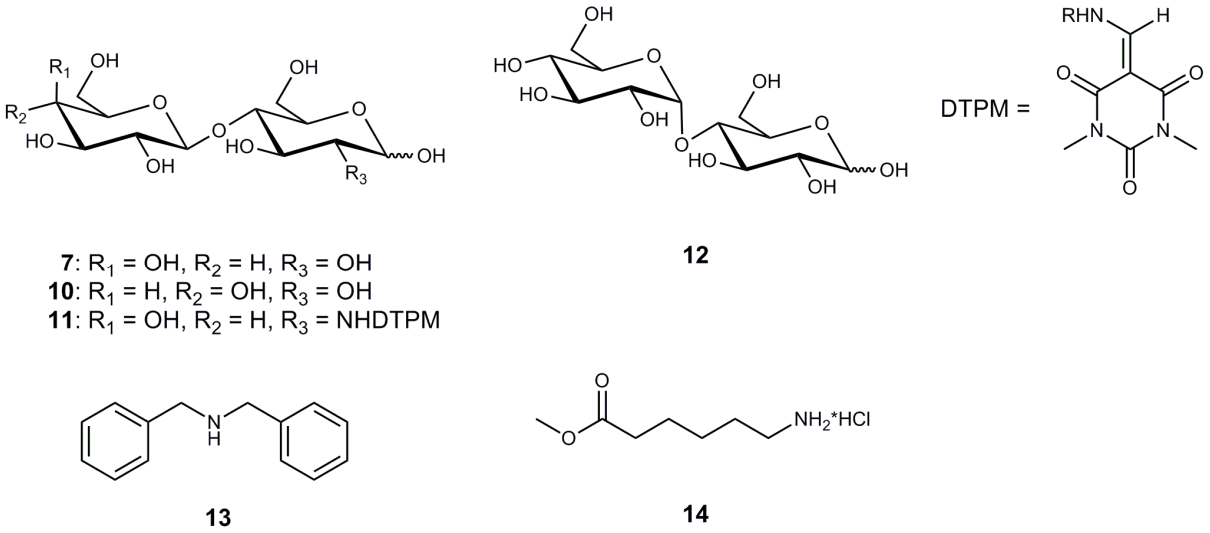

7: R_1 = OH, R_2 = H, R_3 = OH
10: R_1 = H, R_2 = OH, R_3 = OH
11: R_1 = OH, R_2 = H, R_3 = NHDTPM

12

13

14

Figure 13: Disaccharides and amines employed for the Amadori rearrangement: lactose **7**, cellobiose **10**, *N*-DTPM-2-amino-2-deoxy-lactose **11**, maltose **12,** dibenzyl amine **13** and methyl-6-aminohexanoate hydrochloride **14**.

1.3 Results and Discussion

1.3.1 Preliminary Studies with 4',6'-*O*-benzylidene protected Lactose 15

In order to probe the applicability of the Amadori rearrangement on disaccharides with heptoses as the reducing part of the disaccharide, 4',6'-*O*-benzylidene protected lactose **15** was chosen (Scheme 1).

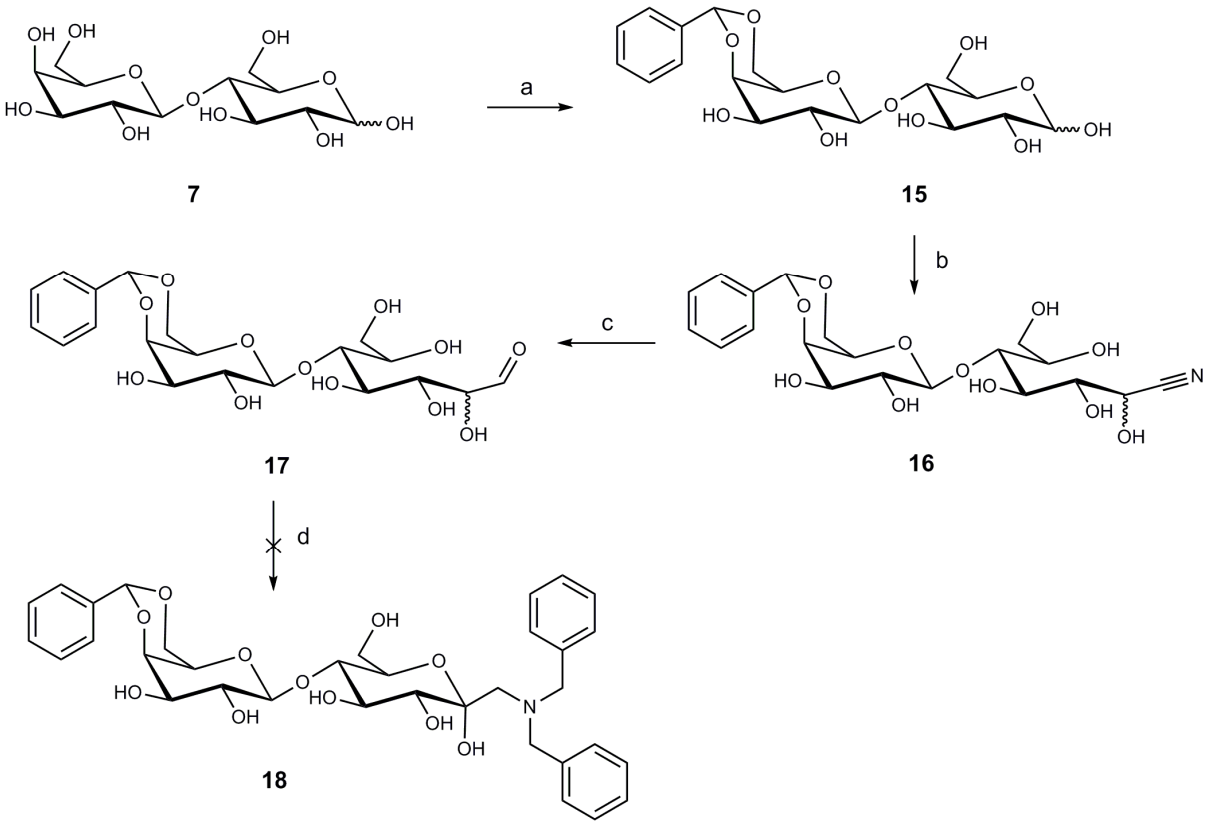

Scheme 1: (a) Benzaldehyde dimethyl acetal, *p*-TSA, DMF, 50℃, 96h; (b) HCN, Et_3N, pyridine, rt, 96h; (c) Pd/$BaSO_4$, acetic acid, H_2O, H_2, rt, 16h; (d) dibenzyl amine, acetic acid, EtOH, 40℃, 12h → 80℃, 48h.

Since it is known that the use of column chromatography as the purification protocol is very difficult with unprotected carbohydrates,[20] we believed that the use of a partially protected disaccharide would ease the purification process. Lactose derivative **15** was synthesised by a procedure of Lassaletta and Schmidt[42] and further processed to the corresponding glycosylated aldoheptose **17** via aldononitrile **16** according to a method reported by Baschang and Kuhn[43] (see sections 1.3.2 and 1.3.3 for a further discussion of this reaction sequence). The Amadori rearrangement of heptose **17** with dibenzyl amine **13**

[42] Lassaletta, J.M.; Schmidt, R.R. 1,2-*O*-Silyl group rearrangements in carbohydrates. Convenient synthesis of important lactose building blocks. *Synlett*, **1995**, *9*, 925-927.
[43] Baschang, G.; Kuhn, R. Überführung von 2-Amino-2-desoxy-hexosen in 3-Amino-3-desoxy-hexosen und –pentosen. *Liebigs Ann. Chem*. **1960**, *636*, 164-173.

afforded a complex mixture of the desired product **18** and an unwanted side product. NMR-Data indicated that the side product is the Amadori product as well but that its benzylidene group had been cleaved off during the rearrangement and/or the work up procedure. This finding was not unexpected, since the Amadori rearrangement required increased temperature in acidic media and under such conditions the benzylidene acetal can undergo hydrolysis.[44]

Therefore, we decided to perform the chain elongation of disaccharides and the subsequent Amadori rearrangement without protecting any hydroxyl groups of the employed disaccharides.

1.3.2 Chain Elongation of Lactose 7, Cellobiose 10, and *N*-DTPM-2-Amino-2-deoxy-lactose 11

The chain elongation of compounds **7**, **10** and **11** was carried out by adding conc. hydrogen cyanide (HCN) to a suspension of the α,β-mixture of the corresponding disaccharide in pyridine and triethylamine at room temperature. This procedure is a modified version of the Kiliani-Fischer reaction,[45] which was reported by Baschang and Kuhn (Scheme 2).[43]

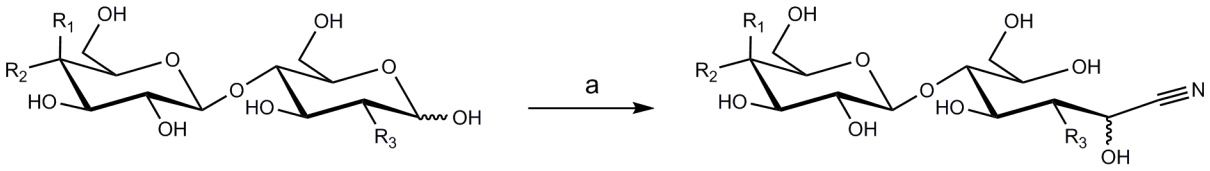

7: R_1 = OH, R_2 = H, R_3 = OH
10: R_1 = H, R_2 = OH, R_3 = OH
11: R_1 = OH, R_2 = H, R_3 = NHDTPM

19: R_1 = OH, R_2 = H, R_3 = OH
20: R_1 = H, R_2 = OH, R_3 = OH
21: R_1 = OH, R_2 = H, R_3 = NHDTPM

Scheme 2: (a) HCN, Et_3N, pyridine, rt, 96h.

The employed protocol differs from the original Kiliani-Fischer procedure by using pyridine instead of water as solvent. Moreover, the reaction time is shortened significantly, i. e. from 10-15 days to 1-3 days, by increasing the temperature and/or by using Et_3N as catalyst.[46]

In order to follow the reaction progress by TLC analysis, treatment of small reaction samples with acetic acid anhydride in pyridine was necessary, to decrease the reactants polarity. Otherwise the reactants would have been retained too strong by the stationary silica gel phase and no separation of the starting material and the product would have been

[44] Diehl, H.W.; Hann, R.M.; Hudson, C.S.; Richtmeyer, N.K. 1,3-Anhydro-2,4-metyhlene-D,L-xylitol and related compounds. *J. Am. Chem. Soc*. **1950**, *72*, 561-566.
[45] (a) Killiani, H. Über Arabinose. *Chem. Ber.* **1886**, *19*, 3029-3036; (b) Fischer, E. Reduction von Säuren der Zuckergruppe. *Chem. Ber*. **1889**, *22*, 2204-2205.
[46] Klesse, P.; Kuhn, R. Darstellung von L-Glucuse und L-Mannose. *Chem. Ber*. **1958**, *91*, 1989-1991.

observed. Furthermore, it was necessary to protect the free hydroxyl group at position C-2 of the aldononitril to avoid possible hydrolysis of the cyanohydrin on the slightly acidic TLC surface.

As suggested by Kuhn and Baschang[43] the products were used in the next step as soon as possible without further purification after they were received by crystallisation from ethanol. The reason for the proposed fast further processing of the generated aldononitriles is not given in the literature, but it might have been observed that the described aldononitriles are not stable against air and moisture over extended periods of time. Compounds **19**, **20**, and **21** have been treated with respect to this advice, but in the case of lactose **7** it was found that the corresponding aldononitril **19** seems to be very stable against water in acidic media. This was observed during the reductive hydrolysis of the nitrile **19** to the corresponding aldoheptose **22** with acetic acid and palladium on barium sulfate in water under hydrogen atmosphere and ambient pressure. The reaction mixture was stirred for 16h at rt and although TLC analysis suggested satisfying completion of the reaction, ^{13}C-NMR data indicated that a nitrile functional group was still present (Figure 14).

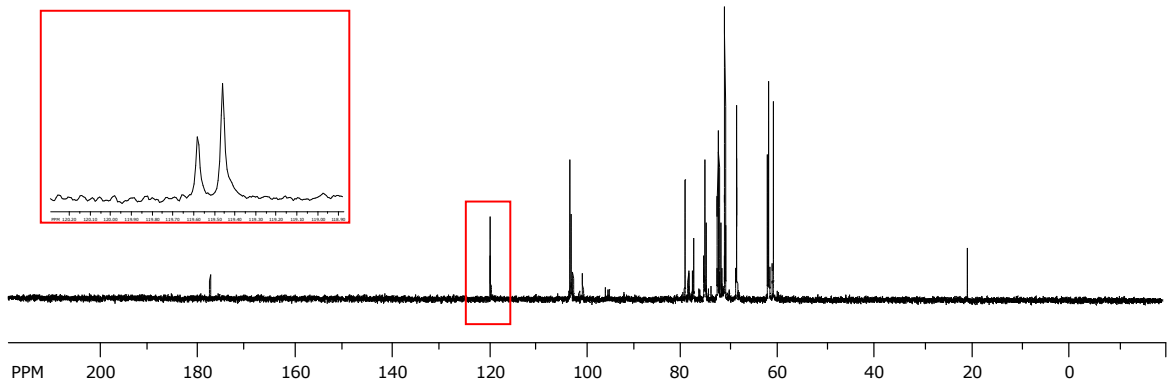

Figure 14: The ^{13}C-NMR spectrum of the reaction mixture from the reductive hydrolysis of compound **19** after 16h. The nitrile signal is indicated by the red box at 120ppm. The enlargement of the signal shows two distinctive peaks, accounting for the two epimers, which are defined by the spatial alignment of the hydroxyl group at position C-2.

The finding that some aldononitriles seem to be stable in aqueous acidic media is also supported by a work of Barker *et al.* who found that some aldononitriles, from for example D-arabinose or D-ribose are relatively stable in aqueous solution at pH 4.3 and can be stored at -15℃ over extended periods of time.[47] Why in this particular case the lactose nitrile **19** was more stable against the reduction conditions, than the corresponding nitriles of cellobiose **20** and *N*-DTPM-2-amino-2-deoxy-lactose **21**, was not further investigated, due to time restrictions.

[47] Barker, R.; Nunez, H.A.; Serianni, A.S. Carbon-13-enriched carbohydrates. Preparation of aldononitriles and their reduction with a palladium catalyst. *Carbohydr. Res.* **1979**, *72*, 71-18.

1.3.3 Reductive Hydrolysis of Aldononitriles 19, 20 and 21

The reductive hydrolysis was also carried out according to the method published by Baschang and Kuhn.[43] The crude aldononitriles **19**, **20** and **21** were reacted with palladium on barium sulfate and acetic acid in water under hydrogen atmosphere at room temperature and ambient pressure to afford the corresponding aldoheptoses **22**, **23** and **24** (Scheme 3).

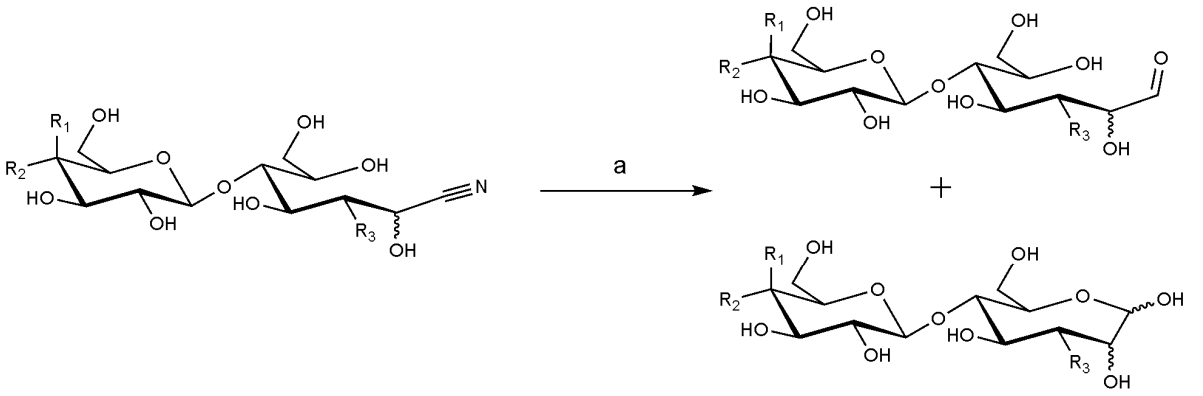

19: R_1 = OH, R_2 = H, R_3 = OH
20: R_1 = H, R_2 = OH, R_3 = OH
21: R_1 = OH, R_2 = H, R_3 = NHDTPM

22: R_1 = OH, R_2 = H, R_3 = OH
23: R_1 = H, R_2 = OH, R_3 = OH
24: R_1 = OH, R_2 = H, R_3 = NHDTPM

Scheme 3: (a) $Pd/BaSO_4$, acetic acid, H_2O, H_2, rt.

Again peracetylation of reaction samples in order to get amenable polarity for TLC analysis was necessary in this reaction step. Thus, the solvent of small samples of the reaction mixture was removed under reduced pressure and the residue was treated with acetic acid anhydride in pyridine to afford the peracetylated reactants. However, it has to be mentioned that the peracetylated reactants, thus the aldononitril and its corresponding aldoheptose, do not show distinctive differences in their rf-values. Hence, it was difficult to dinguish whether the reaction is complete or not by TLC and the completion of the reaction was finally examined by NMR-data.

As indicated in Scheme 3 the reductive hydrolysis of the aldononitriles **19**, **20** and **21** afforded the corresponding aldoheptoses **22**, **23** and **24** as a complex mixture of at least six isomers, with respect to their configuration at position C-2 as well as tautomeric forms. The configuration at position C-2 results as a consequence of the unspecific reaction of the CN-nucleophile and the respective aldehyde in the starting aldose. Additionally, the product can exist in two tautomeric forms, the open chain form and the 7-membered ring form. For the open chain form there are two epimers, distinguished by the spatial alignment of the hydroxyl-group at position C-2. The 7-membered ring additionally forms an α,β-mixture at the anomeric position.

Theoretically there is also the possibility of the formation of a 5-memberd ring, increasing the number of total isomers to ten, but in our case this was not observed. If the 5-membered ring had been formed, distinctive signals above 80ppm should have been found in the ^{13}C-NMR spectra, which was not the case.

However, given that the starting material of the previous step (the α,β-mixture of the corresponding disaccharide **7**, **10** and **11**) was still present, as indicated by ^{13}C-NMR data, a mixture of eight compounds was isolated after the completion of the reaction. The ^{13}C-NMR spectra are given in Figure 15. Due to the complexity of these spectra the reaction was regarded as finished if no more distinctive nitrile-signals around 120ppm (compare Figure 14) could be detectable in the spectra.

Regardless its configuration or constitution, the product of the reaction has at least seven free hydroxyl groups, which cause its strong polarity and hence make purification by conventional silica gel chromatography a difficult task. Therefore, it was decided to use the obtained material without any further purification in the following step, the Amadori rearrangement.

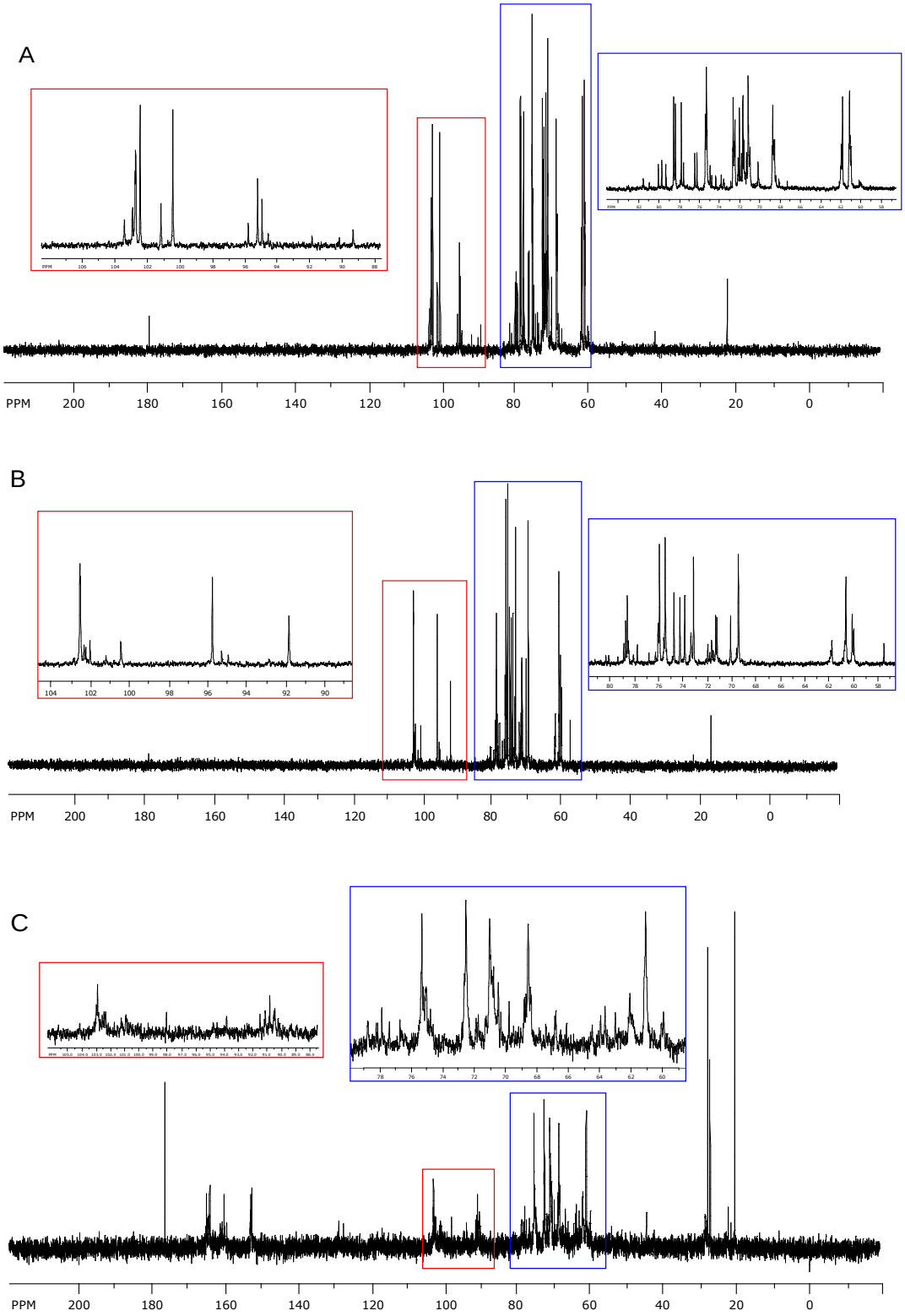

Figure 15: The ^{13}C-NMR spectra of compounds **22** (panel A), **23** (panel B), and **24** (panel C) after the completion of the reductive hydrolysis. For each spectrum the characteristic regions for the carbohydrate signals are indicated by a coloured box. The red box shows the region for the α,β-carbon atoms. The blue box shows the region for all other secondary and tertiary carbon atoms.

1.3.4 Amadori Rearrangement of the Aldoheptoses 22, 23 and 24 with Dibenzyl amine

The Amadori rearrangement between aldoheptoses **22**, **23** and **24** and dibenzyl amine was carried out in ethanol with acetic acid as catalyst (Scheme 4).[20]

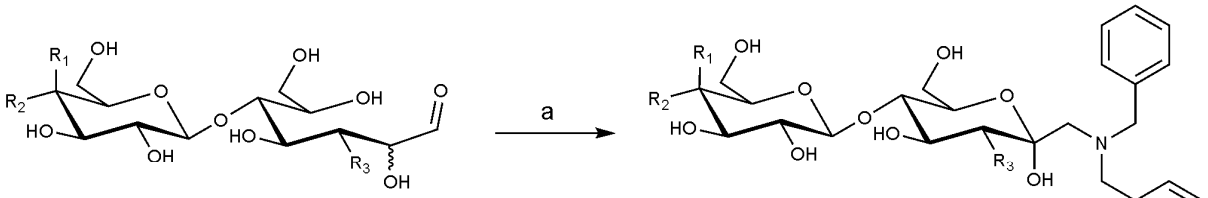

22: R_1 = OH, R_2 = H, R_3 = OH
23: R_1 = H, R_2 = OH, R_3 = OH
24: R_1 = OH, R_2 = H, R_3 = NHDTPM

25: R_1 = OH, R_2 = H, R_3 = OH
26: R_1 = H, R_2 = OH, R_3 = OH
27: R_1 = OH, R_2 = H, R_3 = NHDTPM

Scheme 4: (a) Dibenzyl amine **13**, acetic acid, EtOH, H_2O.

The reaction mixture was stirred for several days and the reaction progress was followed by TLC-analysis. Since the introduction of the nonpolar dibenzyl amine moiety on the disaccharide decreased its polarity, no more derivatization with acetic acid anhydride was necessary to get a good separation of the reactants. Nonetheless, still very polar solvent systems, such as mixtures of chloroform, methanol and aqueous ammonia, had to be applied, to get a good separation of the reaction products and the starting materials.

The reaction temperature was regulated for every reaction individually depending on the progress of the reaction as indicated by TLC analysis. The starting temperature of 40℃ was raised to 80℃ if no reaction progress was obse rved after several hours at 40℃. The period of keeping the reaction at elevated temperature was kept as short as possible to prevent the formation of side as well as degradation products by entering the Maillard reaction cascade. Actually, the reaction was stopped at satisfying formation of the desired product even if the starting material was not completely consumed.

To stop the reaction the solvents were removed under diminished pressure and the crude reaction product was purified by column chromatography. As already outlined in this section, the purification of the formed Amadori products **25**, **26** and **27** by column chromatography using silica gel turned out to be difficult and has to be performed very carefully. The major problem was the retention of the reactions products on the stationary phase, due to their strong polarity. Therefore, very polar solvent systems needed to be applied to elute the reaction products from the silica gel and still the purification time turned out to be quite long, i.e. 2-4h. The solvent systems applied consisted of chloroform, methanol and aqueous concentrated ammonia. Unfortunately, the use of such solvent systems is accompanied by some drawbacks. One major problem is that the miscibility of chloroform and methanol with each other is not unlimited and thus, not all mixtures are accessible. Applying pressure on the column to speed up the purification is also not possible because it

may lead to a phase separation of the solvents on the column, thus ruining the chromatographical separation. Furthermore, both chloroform and methanol are relatively toxic and need to be applied in high amounts.

Another problem with the purification of the Amadori compounds **25**, **26** and **27** was that even with the respective solvent systems only limited separation between the desired products and the unwanted side products was obtained. The rf-values for the separation were usually found between 0.2 and 0.3.

Nonetheless all three Amadori compounds have been purified by silica gel chromatography with the solvent systems indicated in the experimental section. The Amadori product **26** of cellobiose **10** was afforded as dark yellow oil after the column chromatography and was crystallized from water as a white solid, in a yield of 7.0% over three steps. The Amadori product **25** of lactose **7** was obtained as off white solid right after the column chromatography, in a yield of 9.5% over three steps. In the case of this compound crystallisation from water was not possible. The Amadori product **27** of *N*-DTPM-2-Amino-2-deoxy-lactose **11** was obtained as brown oil, in a yield of 0.9% over three steps. As indicated in Scheme 4, all three Amadori products **25**, **26** and **27** were isolated in the α-form exclusively. The reason for this finding is thought to be that the bulky dibenzyl amine residue at position C-1 prefers the sterically more convenient equatorial position.[20]

1.3.5 Chain Elongation and Amadori Rearrangement of Maltose 12

The chain elongation and the reductive hydrolysis of maltose **12** to afford the aldononitril **28** and the aldoheptose **29** respectively were carried out following the same procedures[43] as already described for the β-glycosidic linked bioses **7**, **10** and **11** (Scheme 5). Again purification was not performed until compound **29** was reacted with an amine in an Amadori rearrangement.

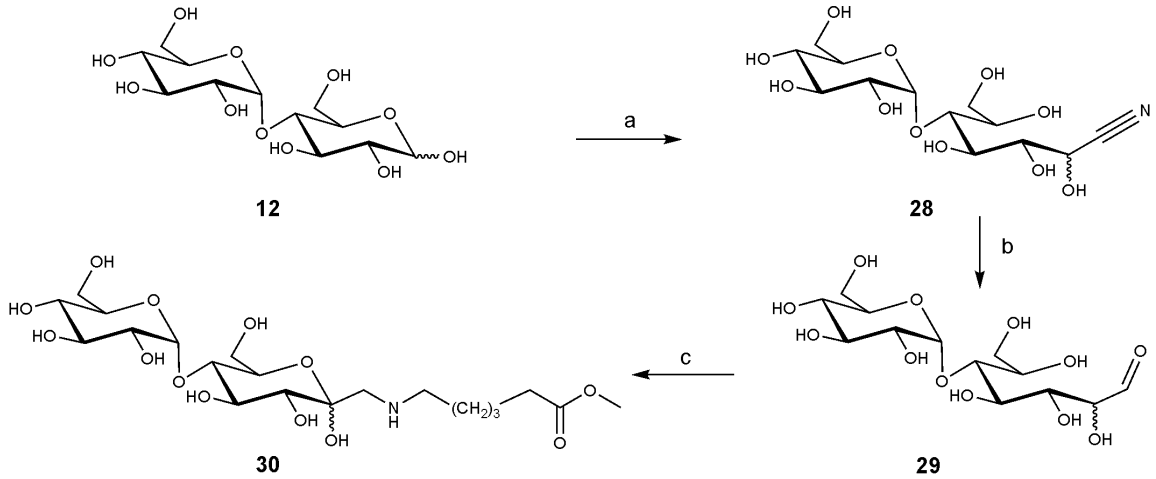

Scheme 5: (a) HCN, Et_3N, pyridine, rt, 96h; (b) $Pd/BaSO_4$, H_2, acetic acid, H_2O, rt, 84h; (c) methyl-6-aminohexanoate hydrochloride **14**, Et_3N, EtOH, rt, 24h → 70℃, 6h.

As indicated by ^{13}C-NMR data the reductive hydrolysis of the nitril **28** afforded a complex mixture containing the open chain heptose as well as the corresponding 7-membered ring heptose (Figure 16).

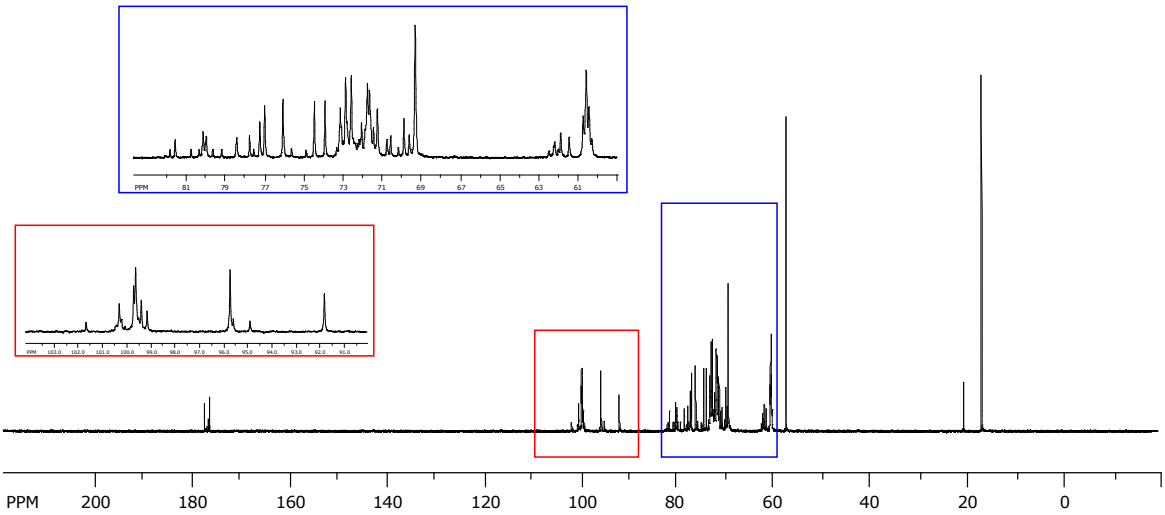

Figure 16: The ^{13}C-NMR spectrum of compound **29**. The anomeric region is marked by the red box. The region for all other secondary and tertiary C-atoms is indicated by the blue box. Both regions are shown in an enlarged box.

Since it is known that the α-glycosidic bond of maltose is labile under acidic conditions and increased temperature,[48] the Amadori rearrangement of compound **29** was not carried out with dibenzyl amine because this would have required the presence of acetic acid and presumably increased temperature. Therefore, methyl-6-aminohexanoate hydrochloride **14** was taken instead, as this reaction does not require the addition of acetic acid.[20] The methyl-6-aminohexanoate was released from its hydrochloride by addition of triethylamine and subsequently added to a solution of heptose **29** in ethanol. After completion of the reaction the crude material was purified by column chromatography. Unfortunately the product **30** was isolated together with remaining starting material **29**. In order to avoid further loss of material by repeating the same purification protocol, the crude mixture of compound **30** was converted to the corresponding 1-*N*,2-*O*-cyclic carbamate[20] with triphosgene and sodium carbonate in water. The resulting material was treated with acetic acid anhydride in pyridine to afford the peracetylated compound **31** (Scheme 6). This conversion should allow for easier purification and additionally, should investigate the possibility of formation of the cyclic carbamate on Amadori products with secondary amines and disaccharides as the carbohydrate moiety.

[48] Capon, B. Mechanism in Carbohydrate Chemistry. *Chem. Rev*. **1969**, *69*, 407-498.

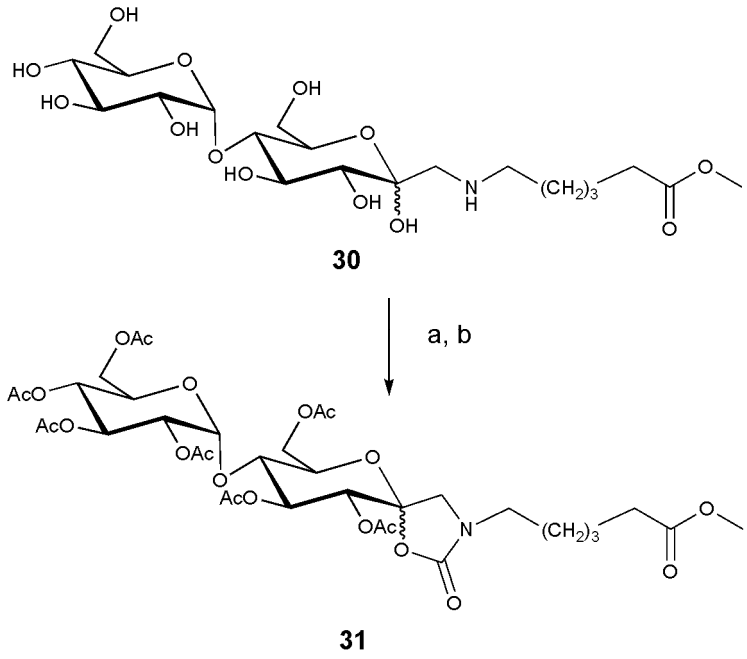

Scheme 6: (a) Triphosgene, Na_2CO_3, H_2O, 0℃, 20min $\rightarrow$ rt, 16h; (b) acetic acid anhydride, DMAP, pyridine 0℃ $\rightarrow$ rt, 72h.

Purification by column chromatography afforded compound **31** reasonably clean by NMR–spectroscopy in a yield of 8.8% over two steps.

In contrast to compound **25**, **26** and **27** compound **31** was isolated as α,β-anomeric mixture in a ration of 3 : 2. The formation of a α,β-anomeric mixture is presumeably caused, because the sterically less demanding primary amine is employed in the Amadori rearrangement.

1.4 Conclusions and Outlook

In conclusion, the general applicability of the Amadori rearrangement onto disaccharides (lactose **7**, cellobiose **10**, *N*-DTPM-2-amino-2-deoxy-lactose **11** and maltose **12**) and model amines (dibenzyl amine **13** and methyl-6-aminohexanoate hydrochloride **14**) for the synthesis of glycosylated *C*-glycosyl type glycoconjugates has been demonstrated. In order to closely mimic the structure of naturally occurring glycoconjugates the disaccharides have been converted to the corresponding aldoheptoses, in a two-step-procedure, prior to the Amadori rearrangement.

Although the Amadori rearrangement afforded the desired products in all cases the obtained yields are rather low, i.e. < 10% over three steps. In order to improve the outcome of the presented synthetic method the reaction conditions for the Amadori rearrangement as well as the purification protocol for the rearrangement products need optimization.

One major reason for the loss of material during the reaction sequence was the employed purification protocol, i. e. conventional silica gel column chromatography, for the final Amadori compound. Therefore, alternative purification techniques need to be considered. These could either be the development of a suitable preparative HPLC method, or the use of protecting groups for the disaccharides hydroxyl functions. These protecting groups are required to be stable towards the reaction conditions throughout the whole synthetic sequence and should decrease the reactants polarity in order to allow silica gel column chromatography. Furthermore, a suitable purification method would also allow for the purification of the aldoheptoses prior to the Amadori rearrangement, which would probably result in the formation of less side products during the rearrangement reaction. Purification by reversed phase chromatography could also be considered.

With regard to the optimization of the Amadori rearrangement conditions, several factors, such as the solvent, the reaction temperature as well as the acidic catalyst, need to be considered. For instance, the use of water instead of ethanol as the solvent could facilitate the solvation of the starting material as well as the formation of the positively charged imine from the glycosyl amine. Considering the reaction temperature, it should be investigated if the formation of the Amadori product reaches a maximum at a certain temperature and which temperature should not be exceeded, in order to avoid the entering of the Amadori product into the Maillard reaction cascade. Concerning the reaction time, similar investigations as for the reaction temperature can be made. Additionally the influence of different acidic catalysts, such as oxalic acid or ammonium acetate, could be investigated. To perform the proposed optimizations it is also necessary to develop an analytical HPLC method that allows for accurate determination of the reaction progress.

Once a suitable purification protocol is worked out and the reaction conditions are optimized, the presented method should allow for a convenient, efficient as well as short synthesis, of glycosylated *C*-glycosyl type glycoconjugates with amino acids or smaller peptides, in order to generate mimics of naturally occurring glycoconjugates.

1.5 Experimental

1.5.1 Materials and Methods

Unless otherwise stated all chemicals were obtained commercially and were used as received.

The required amount of HCN was freshly prepared prior to the chain elongation reactions by adding saturated NaCN solution dropwise to aqueous sulphuric acid (60%) at 80℃. The generated gaseous HCN was transferred thr ough a $CaCl_2$-drying column by a nitrogen stream and condensed in a cooling trap at -12℃. All reaction equipment involved in HCN generation or chain elongation reactions was exclusively used in a fume hood specialized for this purpose. Continuous warning about HCN concentration in the fume hood was provided by an electrochemical sensor for HCN detection. All HCN or cyanide contaminated waste material was treated with aqueous sodium hypochlorite solution (10%) and subsequently the pH of the waste solutions was adjusted to 7.0 with aqueous sulphuric acid.[49]

Analytical thin layer chromatography was performed on silica gel 60 F_{254} aluminium sheets (Merck) and visualized by UV light and/or with ceric ammonium molybdate (100g ammonium molybdate and 8g ceric sulfate in 1L 10% H_2SO_4) and subsequent heating. Column chromatography was carried out using silica gel 60 (230-400 mesh, Merck).

^{1}H-NMR and ^{13}C-NMR spectra were recorded on a Brucker Ultrashield 300MHz spectrometer at 300.36MHz and 75.53MHz respectively. For ^{1}H-NMR spectra chemical shifts are reported in ppm from tetramethylsilane with the solvent signal, resulting from incomplete deuteration, as internal standard. For ^{13}C-NMR spectra chemical shifts are reported with the ^{13}C resonance of the deuterated solvent as internal standard. The data is reported as follows: chemical shift, integration, multiplicity (s = singlet, d = doublet, t = triplet, dd = doublet-doublet, m = multiplett), coupling constants (if appropriate) and assignment.

Optical rotations were obtained on a Perkin Elmer 341 polarimeter at the wavelength of 589nm using a cell path length of 1dm and are given in 10^{-1}deg cm^2 g^{-1}.

Mass spectra were recorded on an Agilent Systems 6120 quadrupole LC-MS using APCI in positive mode.

Melting points (mp) were determined on an Electrothermal® MEL-TEMP® apparatus and are uncorrected.

[49] Griengl, H. et al. α- and β-oxygenated aldehydes derived from Diels-Alder reactions as substrates for hydroxynitrile lyases. *Journal of Molecular Catalysis B: Enzymatic*, **2009**, *61*, 268-273.

1.5.2 Experimental Procedures

General method A (Chain elongation of disaccharides by hydrogen cyanide addition)

The respective disacharide and Et_3N (0.08 equiv.) were dissolved in dry pyridine (40 equiv.) and HCN (8.6 equiv.) was added. The mixture was stirred for 96h at rt. The excess of HCN and the solvent were removed under diminished pressure at rt. EtOH (approx 130 equiv.) was added and the solvent was again removed under reduced pressure at rt until a slurry remained. A solution of Et_2O and EtOAc (1:1 v/v) was added to the slurry the resulting suspension was kept for 1h in a fridge. Finally, the product was obtained as a solid via filtration from the suspension.

General method B (Reductive hydrolysis of aldononitriles to the corresponding aldoheptoses)

The respective aldononitrile was dissolved or suspended in water (6mL per 1g of the respective aldononitril) and acetic acid (1.2 equiv.) and palladium on bariumsulfate (5%Pd/$BaSO_4$) (33% w/w related to the corresponding starting material) were added to the mixture. The reaction was stirred under hydrogen atmosphere at rt and ambient pressure until TLC indicated satisfying conversion of the starting material to the product. The catalyst was removed by filtration and the initial pH of the remaining filtrate was adjusted to 3 by adding Amberlite IR-120+ ion exchanger resin (the resin was washed with water prior to use). The resin was washed with water and the filtrate was concentrated under reduced pressure. For withdrawal of remaining acetic acid the residue was dissolved in water and the water was removed *in vacuo*.

General method C (Amadori rearrangement of aldoheptoses with dibenzyl amine)

The respective sugar was dissolved in a small amount of H_2O and EtOH (approx 20mL per 1g aldoheptose) was added. If the starting material precipitated again upon addition of EtOH, more water was added in small portions until the starting material was dissolved again. Once a solution was obtained acetic acid (2 equiv.) and dibenzyl amine (2 equiv.) were added consecutively and the mixture was stirred at 40℃ until TLC indicated satisfying conversion of the starting material. If no progress of the reaction was observed after several hours at 40℃ by TLC, the temperature was raised to 80℃. The product was obtained after removal of the solvent *in vacuo* and purification of the residue by column chromatography employing the indicated solvent system.

β-D-Galactopyranosyl-(1→5)-D-*glycero*-D-*gulo*/D-*ido*-heptononitrile (19). Applying general procedure A on α,β-lactose **7** (2.78g, 8.1mmol), HCN (2.75mL, 69mmol), Et_3N (0.09mL, 0.7mmol) and pyridine (25mL) afforded crude compound **19** as a brown solid (3.00g, 92.7% crude).

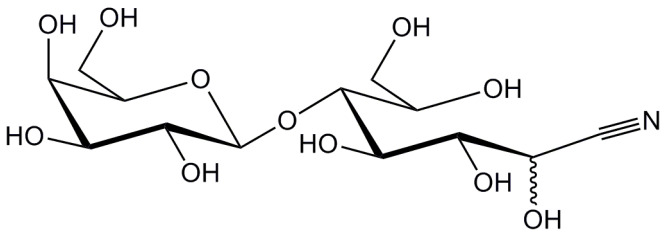

TLC-S:	CH : EtOAc = 1 : 2*
Yield:	92.7% crude
MW:	369.32g*mol^{-1}

β-D-Galactopyranosyl-(1→5)-D-*glycero*-D-*gulo*/D-*ido*-heptose (22). According to general method B compound **19** (3.00g crude) was reacted with Pd/$BaSO_4$ (0.99g) and acetic acid (0.56mL, 9.8mmol) in water (18mL) under H_2-atmosphere and ambient pressure to afford compound **22** as a brown syrup. Since ^{13}C-NMR spectra indicated that the nitrile group was still present the whole procedure was repeated using Pd/$BaSO_4$ (0.99g), acetic acid (0.56mL, 9.8mmol) and water (20mL) and heptose **22** was obtained as brown oil (2.34g, 77% crude).

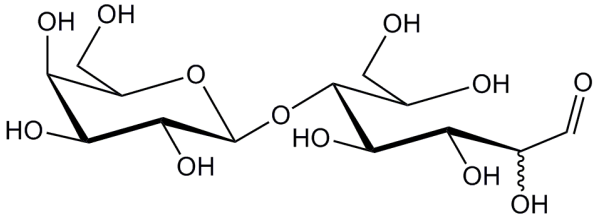

TLC-S:	CH : EtOAc = 1 : 2*
Yield:	77% crude
MW:	372.32g*mol^{-1}

β-D-Galactopyranosyl-(1→5)-1-(*N,N*-dibenzyl)amino-1-deoxy-α-D-*gluco*-hept-2-ulopyranose (25). Following general method C compound **22** (2.34g crude) was reacted with dibenzyl amine **13** (2.4mL, 12.6mmol) and acetic acid (0.7mL, 12.6mmol) in EtOH (40mL). The mixture was stirred for 24h at 80℃ and consecutively for 12h at 40℃. Column chromatography of the crude product afforded compound **25** as an off white solid (0.33g, 0.60mmol, 9.5% over 3 steps from **7**).

* For the peracetylated compound.

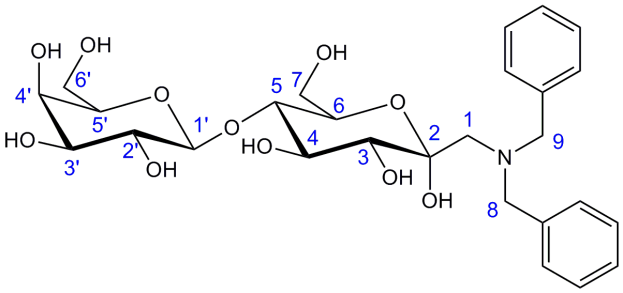

TLC-S: $CHCl_3$: MeOH = 2 : 1

CC-S: $CHCl_3$: MeOH = 5 : 1 → 3 : 1 → 1 : 1 → MeOH pure + 1% aq. NH_3

Yield: 9.5% over 3 steps from **7**

MW: 551.58g*mol^{-1}

^{1}H-NMR (300MHz, d_6-DMSO): δ = 7.32-7.21 (10H, m, H-phenyl), 4.21 (1H, d, $J_{1'2'}$ = 6.7Hz, H-1'), 3.82 (2H, d, $J_{8a, 8b \text{ or } 9a, 9b}$ = 13.8Hz, H-8 or H-9), 3.72-3.68 (1H, m, H-6), 3.62-3.42 (9H, m, H-3', H-4', H-5', H-6', H-7, H-8 or H-9), 3.36-3.16 (4H, m, H-2', H-3, H-4, H-5), 2.72 (1H, d, $J_{1a,1b}$ = 13.4Hz, H-1a), 2.63 (1H, d, H-1b). ^{13}C-NMR (75MHz, d_6-DMSO): δ = 138.8, 128.9, 128.2, 126.8 (12C, C-phenyl), 103.9 (C-1'), 97.4 (C-2), 81.5 (C-5), 75.5 (C-5'), 73.2 (C-2'), 72.3, 72.2 (C-3, C-3'), 70.6 (C-4, C-6), 68.0 (C-4'), 60.9 (C-7), 60.3 (C-6'), 58.0 (C-8, C-9), 57.7 (C-1). m/z: 552.3 (MH^+); $[\alpha]_D^{25}$ = + 38.6 (c = 1.2, DMSO); mp: decomposition above 160℃.

β-D-Glucopyranosyl-(1→5)-D-*glycero*-D-*gulo*/D-*ido*-heptononitrile (20). According to general method A α,β-cellobiose **10** (2.78g, 8.1mmol) was reacted with HCN (2.75mL, 69mmol) and Et_3N (0.09mL, 0.65mmol) in pyridine (20mL). Precipitation from a mixture of Et_2O-EtOAc (20mL) afforded compound **20** as a brown solid (2.48g, 82.7% crude).

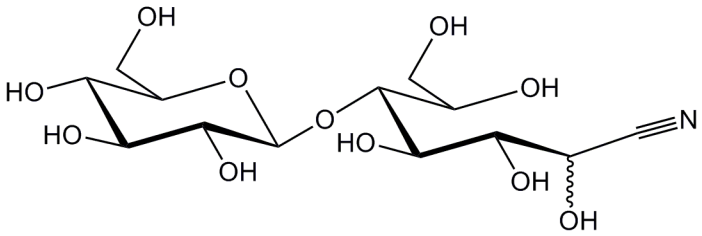

TLC-S: CH : EtOAc = 1 : 2*

Yield: 82.7% crude

MW: 369.32g*mol^{-1}

β-D-Glucopyranosyl-(1→5)-D-*glycero*-D-*gulo*/D-*ido*-heptose (23). General method B was applied to nitrile **20** (2.48g crude), Pd/$BaSO_4$ (1.5g), acetic acid (0.46mL, 8.0mmol) and water (15mL). The mixture was stirred for 84h at rt under hydrogen atmosphere and ambient pressure. The product **23** was afforded as dark brown syrup (2.06g, 82.4% crude).

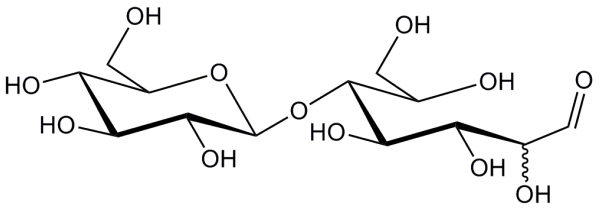

TLC-S: CH : EtOAc = 1 : 4*

Yield: 82.4% crude

MW: 372.32g*mol^{-1}

β-D-Glucopyranosyl-(1→5)-1-(*N,N*-dibenzyl)amino-1-deoxy-α-D-*gluco*-hept-2-ulopyranose (26). Following general method C compound **23** (2.06g crude), dibenzyl amine **13** (2.1mL, 11.07mmol) and acetic acid (0.63mL, 11.07mmol) were reacted in EtOH (40mL) for 6h at 80℃ and subsequently for 21h at rt. Colu mn chromatography and crystallisation from water afforded compound **26** (0.215g, 0.4mmol, 7.0% over 3 steps from **10**) as a white solid.

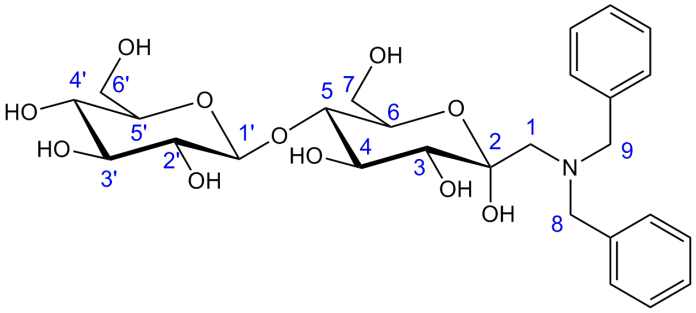

TLC-S:	$CHCl_3$: MeOH = 2 : 1
CC-S:	$CHCl_3$: MeOH = 8 : 1 → 3 : 1 → 1 : 1 → 1 : 3 + 1% aq. NH_3
Yield:	7.0% over 3 steps from **10**
MW:	551.58g*mol^{-1}

^{1}H-NMR (300MHz, DMSO-d_6): δ = 7.32-7.21 (10H, m, H-phenyl), 4.25 (1H, d, $J_{1',2'}$ = 7.8Hz, H-1'), 3.82 (2H, d, $J_{8a, 8b \text{ or } 9a, 9b}$ = 13.8Hz, H-8 or H-9), 3.72-3.373 (8H, m, H-4, H-6, H-6', H-7, H-8 or H-9), 3.34-3.27 (1H, m, H-5), 3.22-3.13 (3H, m, H-3, H-3', H-5'), 3.08-2.97 (2H, m, H-2', H-4'), 2.72 (1H, d, $J_{1a,1b}$ = 13.4Hz, H-1a), 2.63 (1H, d, H-1b). ^{13}C-NMR (75MHz, DMSO-d_6): δ = 138.9, 129.0, 128.2, 126.9 (12C, C-phenyl), 103.2 (C-1'), 97.4 (C-2), 81.2 (C-5), 76.8 (C-5'), 76.4 (C-3'), 73.3 (C-2'), 72.4, 72.3 (C-3, C-4), 70.7 (C-6), 70.0 (C-4'), 61.0 (C-6'), 60.8 (C-7), 58.0 (C-8, C-9), 57.7 (C-1). m/z: 552.6 (MH^+); $[\alpha]_D^{25}$ = + 34.3 (c = 1.0, DMSO); mp: decomposition above 164℃.

β-D-Galactopyranosyl-(1→5)-2-*N*-[1,3-dimethyl-2,4,6 (1H,3H,5H)-trioxopyrimidine-5-ylidene]methylamino-2-deoxy-D-*glycero*-D-*gulo*/D-*ido*-heptononitrile (21).
General method A was applied to compound **11** (4.12g, 8.1mmol), HCN (2.75mL, 69mmol), Et_3N (0.09mL, 0.65mmol) and pyridine (25mL). Precipitation with an Et_2O-EtOAc solution (20mL) afforded the title compound **21** as a brownish orange solid (4.20g, 96.8% crude).

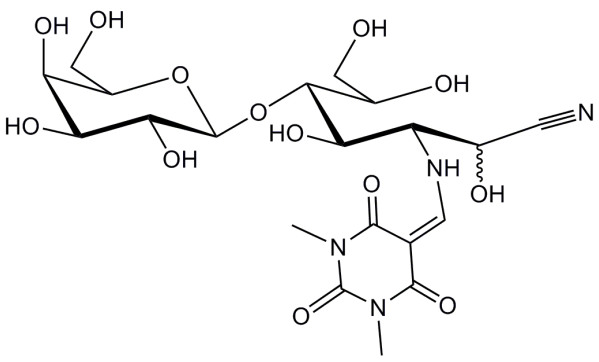

TLC-S:	CH : EtOAc = 1 : 2*
Yield:	96.8% crude
MW:	534.47g*mol^{-1}

β-D-Galactopyranosyl-(1→5)-2-*N*-[1,3-dimethyl-2,4,6 (1H,3H,5H)-trioxopyrimidine-5-ylidene]methylamino-2-deoxy-D-*glycero*-D-*gulo*/D-*ido*-heptose (24).

General method B was applied to compound **21** (4.20g crude), Pd/$BaSO_4$ (1.4g), acetic acid (0.79mL, 13.6mmol) and water (25mL). The mixture was stirred under hydrogen atmosphere and ambient pressure for 20h at rt and after the corresponding work up procedure compound **24** was obtained as a yellowish brown syrup (1.50g, 35.5% crude).

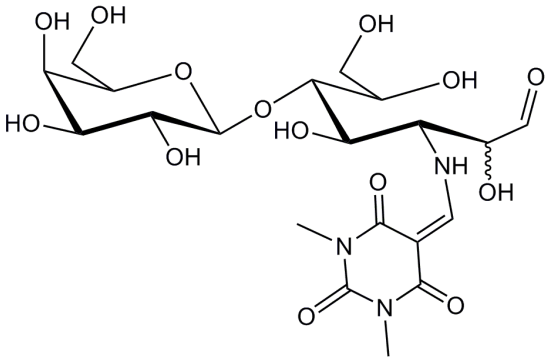

TLC-S: CH : EtOAc = 1 : 2*

Yield: 35.5% crude

MW: 537.47g*mol^{-1}

β-D-Galactopyranosyl-(1→5)-1-(*N,N*-dibenzyl)amino-1-deoxy-2-*N*-[1,3-dimethyl-2,4,6 (1H,3H,5H)-trioxopyrimidine-5-ylidene]methylamino-2-deoxy-α-D-*gluco*-hept-2-ulopyranose (27). Following general method C compound **24** (1.50g crude) was reacted with dibenzyl amine **13** (1.07mL, 5.6mmol) and acetic acid (0.32mL, 5.58mmol) in EtOH (40mL). The reaction mixture was stirred for 96h at 80℃. Column chromatography of the resulting crude product afforded the title compound **27** as brown oil (0.05g, 0.9% over 3 steps from **11**).

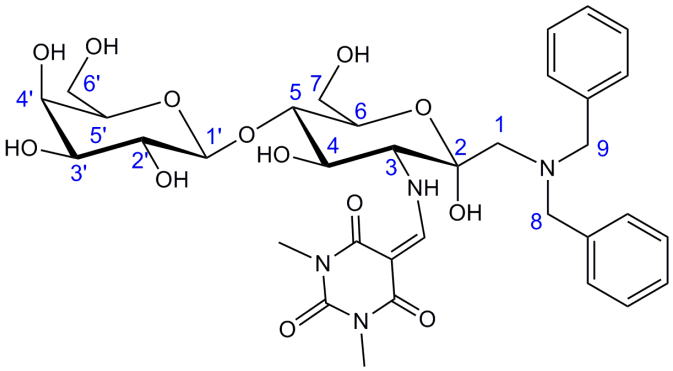

TLC-S: $CHCl_3$: MeOH = 3 : 1 : 1
1% aq. NH_3

CC-S: $CHCl_3$: MeOH = 3 : 1 : 1
1% aq. NH_3

Yield: 0.9% over 3 steps from **11**

MW: 716.73g*mol^{-1}

^{1}H-NMR (300MHz, MeOD): δ = 7.88 (1H, s, DTPM) 7.32-7.18 (8H, m, H-phenyl), 7.10-7.06 (2H, m, H-phenyl), 4.40 (1H, d, $J_{1',2'}$ = 7.1Hz, H-1'), 3.96-3.92 (1H, m, H-6), 3.90-3.68 (8H, m, H-4, H-4', H-6'a, H-6'b, H-7a, H-7b, H-8a and H-8b or H-9a and H-9b), 3.68-3.56 (4H, m, H-5, H-5', H-8a and H-8b or H-9a and H-9b), 3.56-3.45 (3H, m, H-2', H-3', H-4), 3.34-3.27 (3H, m, DTPM), 3.27-3.17 (3H, m, DTPM), 2.75 (1H, d, $J_{1a,1b}$ = 13.6Hz, H-1a), 2.62 (1H, d, H-1b).

^{13}C-NMR (75MHz, MeOD): δ = 165.5, 164.6, 161.0, 153.6 (4C, DTPMH), 140.2, 131.0, 130.2, 129.3 (12C, C-phenyl), 105.1 (C-1'), 97.5 (DTPM), 91.8 (C-2), 80.6 (C-5), 77.1 (C-5'), 74.8 (C-3'), 72.9 (C-2'), 72.8, 72.7 (C-4, C-6), 70.3 (C-3), 65.8 (C-4'), 62.6 (C-7), 62.0 (C-6'), 60.6 (C-8, C-9), 58,0 (C-1), 28.1 (DTPM), 27.4 (DTPM).

α-D-Glucopyranosyl-(1→5)-D-*glycero*-D-*gulo*/D-*ido*-heptononitrile (28). α,β-Maltose **12** was dried by co-evaporation with toluene (20mL each) 3 times. According to general method A α,β-maltose **12** (2.28g, 6.65mmol) was reacted with HCN (2.25mL, 8.6mmol) and Et_3N (0.07ml, 0.05mmol) in pyridine (20mL) to afford the title compound **28** as a brown syrup (2.60g, 105.7% crude).

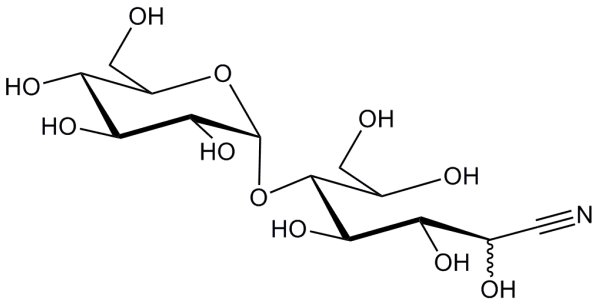

TLC-S: CH : EtOAc = 1 : 2*
Yield: 105.7% crude
MW: 369.32g*mol^{-1}

α-D-Glucopyranosyl-(1→5)-D-*glycero*-D-*gulo*/D-*ido*-heptose (29). General method B was applied to compound **28** (2.60g crude), Pd/$BaSO_4$ (1.07g), acetic acid (0.49mL, 9.8mmol) and water (18mL). The mixture was stirred under hydrogen atmosphere and ambient pressure for 84h and the product **29** was obtained as brown syrup (2.29g, 87.4% crude).

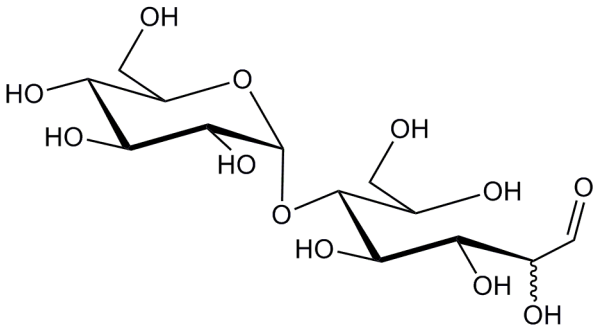

TLC-S: CH : EtOAc = 1 : 4*
Yield: 87.4% crude
MW: 372.32g*mol^{-1}

α-D-Glucopyranosyl-(1→5)-1-(*N*-methoxycarbonylpentyl)amino-1-deoxy-α,β-D-*gluco*-hept-2-ulopyranose (30). A solution of methyl-6-aminohexanoate hydrochlorid **14** (1.78g, 12.3mmol) and Et_3N (1.36mL, 12.3mmol) in EtOH (10mL) was stirred for 30min at rt. This solution was added to a stirred solution of compound **29** (2.29g crude) in EtOH (30mL) at rt.

The resulting mixture was stirred for 24h at rt and consecutively for 6h at 70℃. The solvent was removed under reduced pressure and the remaining material was purified by column chromatography to afford the title compound **30** as brown oil (0.45g, 14.6% crude).

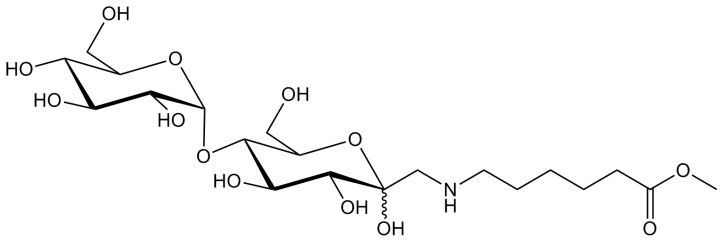

TLC-S:	$CHCl_3$: MeOH = 2 : 1
CC-S:	$CHCl_3$: MeOH = 6 : 1 → 4 : 1 → 1 : 1 → 1 : 5 + 1% aq. NH_3
Yield:	14.6% crude
MW:	499.51g*mol^{-1}

2',3',4',6'-Tetra-*O*-acetyl- α-D-glucopyranosyl-(1→5)-3,4,7-tri-*O*-acetyl- 1-(*N*-methoxycarbonylpentyl)amino-1-*N*,2-*O*-carbonyl-1-deoxy-(1→4)-α,β-D-*gluco*-hept-2-ulopyranose (31).

A mixture of compound **30** (0.18g, 0.36mmol) and Na_2CO_3 (0.23g, 2.2mmol) in water (5mL) was stirred for 20min at 0℃. Triphosgene (0.20g, 0 .40mmol) was added to the suspension at 0℃ and consecutively the reaction mixture was stir red for 16h at rt. The solvent was removed under reduced pressure and the remaining material (1g of a grey solid) was dissolved in pyridine (5mL). To the resulting solution a catalytic amount of DMAP and subsequently acetic acid anhydride (0.6mL, 6.3mmol) were added at 0℃ and the mixture was stirred for 72h at rt. The reaction mixture was poured into ice water and extracted with DCM (10mL each) twice. The combined organic layers were washed with aq. HCl (15mL), sat. aq. Na_2CO_3 (15mL) and water (15mL) and dried over Na_2SO_4. The solvent was removed under reduced pressure and the residue was purified by column chromatography to afford compound **31** as yellow oil in an α : β – ratio of 3 : 2 (0.03g, 0.03mmol, 8.8% from 0.18g of **30**).

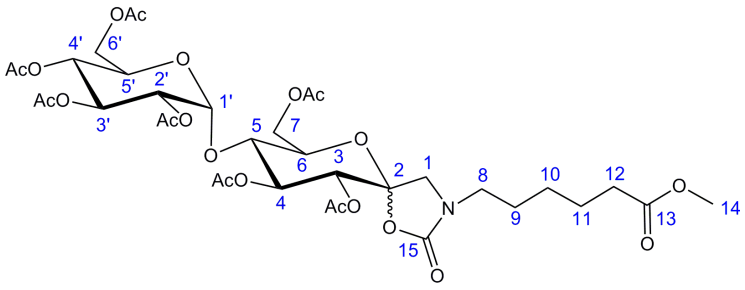

TLC-S:	$CHCl_3$: MeOH = 2 : 1
	CH : EtOAc = 2 : 1
CC-S:	CH : EtOAc = 2 : 1
Yield:	8.8% from 0.18g of **30**
MW:	819.76g*mol^{-1}

^{1}H-NMR (300MHz, $CDCl_3$) α-anomer: δ = 5.54 (1H, dd, $J_{5,4}$ = 9.6Hz, $J_{5,6}$ = 9.6Hz, H-5), 5.40 (1H, d, $J_{1',2'}$ = 3.8Hz, H-1'), 5.32 (1H, dd, $J_{3',2'}$ = 10.0Hz, $J_{3',4'}$ = 9.8Hz, H-3'), 5.31 (1H, d, $J_{3,2}$ = 10.0Hz, H-3), 5.10-4.94 (2H, m, H-4, H-4'), 4.82 (1H, dd, $J_{2',1'}$ = 4.0Hz, H-2'), 4.34-3.94 (6H, m, H-5', H-6 H-6'a, H-6'b, H-7a, H-7b), 3.65 (3H, s, H-14), 3.44-3.30 (2H, m, H-1a, H-1b), 3.30-3.17 (2H, m, H-8), 2.29 (2H, t, H-12a, H-12b), 2.05-1.92 (21H, m, H-acetyl), 1.69-1.57 (2H, m, H-11a, H-11b), 1.57-1.44 (2H, m, H-9a, H-9b), 1.39-1.19 (2H, m, H-10a, H-10b). ^{13}C-NMR (300MHz, $CDCl_3$) α-anomer: δ = 173.8 (C-13), 170.9, 170.6, 170.4, 170.3, 169.9, 169.7, 169.6 (C=O acetyl), 154.9 (C-15), 99.6 (C-1'), 95.6 (C-2), 73.4 (C-5), 71.9 (C-5'), 71.0 (C-3, C-6), 70.1 (C-4), 69.4 (C-2'), 68.6 (C-3'), 68.1 (C-4'), 62.3 (C-7), 61.5 (C-6'), 52.0 (C-1), 51.7 (C-14), 43.6 (C-8), 33.8 (C-12), 27.0, 26.0, 24.5 (C-9, C-10, C-11), 20.9, 20.8, 20.7, 20.6, 20.5 (7C, CH_3 acetyl).

Part 2

2 Synthesis of Novel Transition State Analogue Inhibitors for Human 5'-Methylthioadenosine Phosphorylase and Bacterial 5'-Methylthioadenosine Nucleosidases

2.1 Introduction

2.1.1 Enzymes, Transition State Theory and the Determination of Transition State Structures

Enzymes play an ubiquitous role as biocatalysts in all biochemical processes and pathways. The rate enhancements achieved are remarkable and are found between 10^6 and 10^{17}, thus achieving in one second what would otherwise require ten days to three billions of years.[50] Like all catalysts, enzymes lower the activation energy (E_a) barrier for chemical reactions, without altering the position of the chemical equilibrium. According to transition state theory the decrease in E_a is achieved by tight binding to the transition state. The transition state ($ES^{\ddagger}$) is formed after the Michaelis complex (ES) and is the point in the reaction coordinate where the substrate is finally converted to the product (Figure 17).

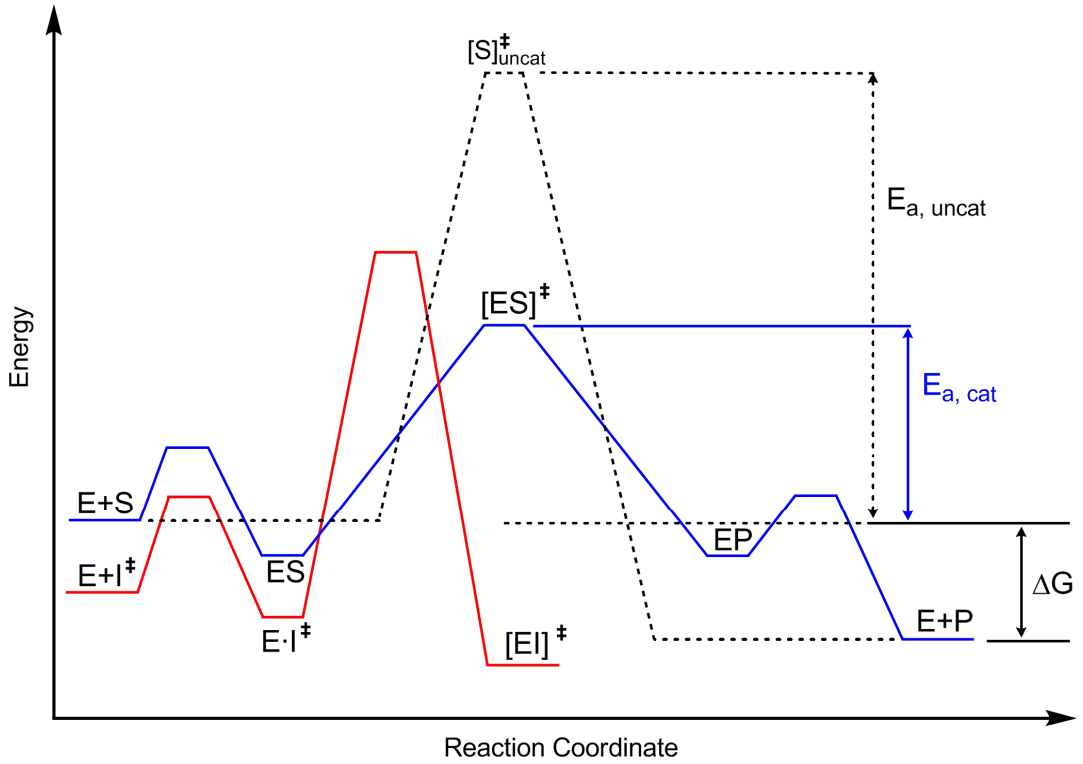

Figure 17 Reaction coordinate diagram with a comparison between a noncatalyzed (black dashed) and an enzyme catalyzed reaction (blue) with the binding of a transition state analog (red). The formation of the weak enzyme- inhibitor complex ($E^{\bullet}I^{\ddagger}$) lies similar in the reaction coordinate to the formation of the enzyme-substrate complex and is then followed by the high energy demanding (slow-onset phase) conversion to the tight bound stable complex $EI^{\ddagger}$. Adapted from reference [51].

[50] Bugg, T. D. H. in Enceclopedia of Chemical Biology Vol. 1. T. P. Begley. Ed., John Wiley & Sons Inc., New Jersey. **2009**, 653-663.

After forming the Michealis complex, structural rearrangements of the enzyme around the active site alter the electron distribution in the substrate and place the substrate in the solvent restricted catalytic site of the enzyme. These changes cause distortion of the substrate towards the transition state and increase binding interactions between the substrate and the enzyme. At the transition state binding interactions reach a maximum and strongly stabilize the transition state, which accounts for the lowering of the E_a and the accelerated reaction rate. The formation of the product alters the electron distribution again and causes repulsive forces that open the active site and release the product.[51] According to Pauling and Wolfenden, who pioneered the ideas of transition state theory in enzyme catalysis, the rate enhancements are achieved by binding more tightly to the transition state than to the Michealis complex by a factor, which resembles the rate enhancement. Furthermore, they suggested that chemically stable molecules, which closely resemble the transition state (transition state analogues), would bind much tighter than the natural substrate and, because of being nonreactive, would provide powerful enzyme inhibitors.[52]

Enzyme inhibition leads to a decrease of the enzymes activity and can be achieved by molecules, the so called enzyme inhibitors, which interact with either the enzyme or the substrate or both in a specific way and prevent the enzyme from catalyzing its usual reaction. Inhibition occurs naturally and is used for the regulation of metabolic processes wherever enzymes are involved in these processes. This regulation mechanism provides a worthwhile possibility to intervene in metabolic pathways by intentional designed inhibitors and thus many pharmaceutical drugs are enzyme inhibitors. The mechanisms of inhibition are manifold but can be divided into two main groups: irreversible and reversible inhibitors. Irreversible inhibitors usually interact covalently with the enzyme and deactivate the enzyme completely, whereas reversible inhibitors only cause temporally limited inhibition, thus the activity of the enzyme can be fully restored after displacement of the inhibitor in this case.

Inhibitors resembling transition state structures cause a special form of reversible enzyme inhibition, which is also referred to as *transition state analogue inhibition* or *slow onset tight binding inhibition*. In this type of inhibition the enzyme (E) and the inhibitor ($I^{‡}$) rapidly form an initial weak bound enzyme - inhibitor complex ($E{\cdot}I^{‡}$), which is followed by a slow, high energy demanding, transformation of the initial complex ($E{\cdot}I^{‡}$) to the tight bound stable complex $EI^{‡}$ (Figure 17).

The duration of this process arises from the fact that the enzyme is designed to recognize its natural substrate better than any designed substrate analogue. Therefore, by

[51] Schramm, V.L. Enzymatic transition states and transition state analog design. *Annu. Rev. Biochem*. **1998**, *67*, 693-720.
[52] (a) Pauling, L. Molecular architecture and biological reactions. *Chem. Eng. News* **1946**, *24*, 1375-1377; (b) Pauling, L. Chemical achievement and hope for the future. *Amer. Sci.* **1948**, *36*, 50-58; (c) Wolfenden, R. Transition state analogs for enzyme catalysis. *Nature* **1969**, *223*, 704-705; (d) Wolfenden R. Analogue approach to the structure of the transition state in enzyme reactions. *Acc. Chem. Res.* **1972**, *5*, 10-18.

forming a complex with the inhibitor, the structural changes in the enzyme are not induced as efficiently as by forming a complex with the substrate and the time to reach transition state conformation is extended.[51] This results in a time dependent inhibition with transition state analogues whereas other types of inhibitors often show instantaneous inhibition.[53]

Since the first enzymes known to interact with and to be inhibited by transition state analogues have been reported in the 1970s their number is continuously growing. The first transition state analogues were natural products but soon they were replaced by intentionally synthesized inhibitors as a result of the development of inhibitors for the AIDS protease, *β*-lactamases, metalloproteinases, cyclooxygenases and other enzymes that are pharmaceutical targets.[51]

Although transition state analogues are very powerful enzyme inhibitors, the elucidation of the transition states structure is a very demanding task and requires accurate knowledge of the enzymatic catalytic mechanism and a combination of computational chemistry and physicochemical methods.[54, 55] The most challenging problem in transition state analysis emerges from the transition states lifetime, which is found in the range of 10^{-13} s, i.e. the time of a single bond vibration. This extremely short period deprives itself from all direct physical observation in solution and an indirect method needs to be applied to reveal transition state features. The determination of kinetic isotope effects (KIE) in combination with computational chemistry is such a method.[54, 56] KIEs compare the rate of an enzymatic reaction with isotopically labeled and unlabeled substrates, utilizing the fact that labeled substrates differ in energy from their unlabeled counterparts and thus require a different amount of energy to reach the transition state. KIE analysis provides defining features of the transition state, such as bond lengths, bond angles and molecular electrostatic potential surfaces for every atomic position that is perturbed upon transformation from the substrate to the transition state. With a set of KIE data a computational model of the transition states structure that fits the experimental KIEs can be established. This computational model is approached iteratively, starting from an *ab initio* transition state model for reactants with a geometry that resembles the structure of the enzymes catalytic site.[54] If the reactant geometry at the catalytic site is not known, bond angels can be varied to predict the transition states structure.[56]

[53] Silverman, R.B. in Enceclopedia of Chemical Biology Vol. 1. T. P. Begley. Ed., John Wiley & Sons Inc., New Jersey. **2009**, 663-681.
[54] Schramm, V.L. Enzymatic transition states: thermodynamics, dynamics and analogue design. *Arch. Biochem. Biophys*. **2005**, *433*, 13-26.
[55] Bagdassarian, C.K.; Furneaux, R.H.; Miles, R.W.; Schramm, V.L.; Tyler, P.C. One-third-the-sites transition state inhibitors for purine nucleoside phosphorylase. *Biochemistry* **1998**, *37*, 8615-8621.
[56] Schramm, V.L. Enzymatic transition-state analysis and transition state analogs. *Methods Enzymol.* **1999**, *308*, 301-355.

The technique of KIE analysis was first described by Bigeleisen[57] and co-workers in the 1940 and Schramm and co-workers have used this technique together with computational methods to establish a protocol for the determination of transition state structures and their conversion to blueprints for stable analogues.[58] The steps in this protocol are:

- Selection of an enzyme where KIE analysis is possible and which is a biological target.
- Synthesis of substrates with isotopic labelling in and around the reaction centre.
- Measurement of intrinsic KIEs (isotopic effects only on the chemical steps, ignoring the influence of non chemical steps).
- Calculation of a quantum mechanical model of the transition state that accounts for the experimental KIEs.
- Conversion of the transition states electronic structure to a molecular electrostatic potential map.
- Synthesis of chemical stable analogs which resemble the transition states structure in terms of geometry and the molecular electrostatic van der Waals surface.
- Testing of these analogues against the target enzymes.

The design of transition state analogues based on the above described method was, besides some inhibitors for the ricin A-chain, mostly developed with *N*-ribosyltransferases such as inosine-uridine nucleoside hydrolase (IU-NH), inosine-adenosine-guanosine nucleoside hydrolase (IAG-NH), bovine and human purine nucleoside phosphorylases (PNPs) and 5′-methylthioadenosine nucleosidases (MTANs) and phosphorylases (MTAPs).[58]

In the case of PNP thorough transition state analysis for both, the human and the bovine enzyme, has led to the development of a series of inhibitors and two of them, namely Immucillin-H and DADMe-Immucillin-H (Figure 18), have entered human clinical trials.[59] Immucillin-H is in trials for T-cell leukemia under the name of Fodosine™ and DADMe-

[57] Bigeleisen, J.; Mayer, M.G. Calculation of equillibrium constants for isotopic exchange reactions. *J. Chem. Phys*. **1947**, *15*, 261-267.

[58] Schramm, V.L.; Tyler, P.C. in Iminosugars. From synthesis to therapeutic application. Compain, P.; Martin, O.R. eds., John Wiley & Sons, Ltd. Chichester, **2007**, 177-208.

[59] (a) Kline, P.C.; Schramm, V.L. Purine nucleoside phosphorylase. Catalytic mechanism and transition state analysis of the arsenolysis reaction. *Biochemistry* **1993**, *32*, 13212-13219; (b) Lewandowicz, A.; Schram, V.L. Transition state analysis for human and *Plasmodium falciparum* purine nucleoside phosphorylases. *Biochemistry* **2004**, *43*, 1458-1468; (c) Evans, G.B.; Furneaux, R.H.; Gainsford, G.J.; Schramm, V.L.; Tyler, P.C. Synthesis of transition state analogue inhibitors for purine nucleoside phosphorylase and *N*-riboside hydrolases. *Tetrahedron* **2000**, *56*, 3053-3062; (d) Evans, G.B.; Furneaux, R.H.; Lewandowicz, A.; Schramm, V.L.; Tyler, P.C. Synthesis of second-generation transition state, analogues of human purine nucleoside phosphorylase. *J. Med. Chem*. **2003**, *46*, 5271-5276.

Immucillin-H is in trials for T-cell autoimmune disorders under the name of BCX-4208.[60] These results demonstrate the potential of transition state analysis for the development of pharmaceutical drugs on the basis of enzyme inhibitors.

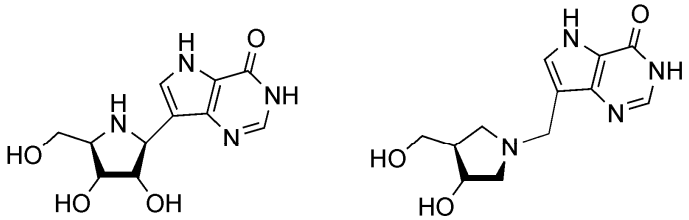

Figure 18 The structures of the transition state analogs Immucillin-H (left) and DADMe-Immucillin-H (right) for human and bovine PNP. Both inhibitors have entered clinical trials against T-cell malignancies and T-cell autoimmune disorders.

2.1.2 The Biological Function of 5′-Methylthioadenosine Phosphorylase (MTAP) and 5′-Methylthioadenosine/S-adenosylhomocysteine Nucleosidase (MTAN)

5′-Methylthioadenosine phosphorylase (MTAP) is involved in the polyamine biosynthesis in prokaryotes and eukaryotes (Figure 19). In this pathway decarboxylated S-adenosylmethionone (decarboxy-SAM) is used by both spermidine and spermine synthase to transfer propylamine groups to putrescine and spermidine, respectively. Thereby, the decarboxylated S-adenosylmethionone is degraded to 5′-methylthioadenosine (MTA) which is further metabolized to methylthioribose-1-phosphate and adenine by MTAP. The adenine is returned to the adenylate pool by conversion to adenosine monophosphate (AMP) by adenine phophoribosyltransferase and the methylthioribose is further converted to methionine which regenerates S-adenosylmethionine (SAM) upon conversion with ATP. Therefore, the polyamine pathway recycles both products of MTAP back to SAM, one of the precursor compounds for polyamine biosynthesis.

The polyamines putrescine, spermidine and spermine, which are generated in the pathway described above, are important compounds in all mammalian cells, protozoa, bacteria and fungi. They are required in replication, transcription and translation and thus play an important role in growth related processes. Cellular proliferation comes along with elevated polyamine levels and it has been recognized, that rapidly dividing cells have increased polyamine concentrations. Thus, the polyamine pathway has become a promising target for the treatment of proliferative diseases, such as cancer and parasitic infections.[61]

[60] *http://www.biocryst.com/clinical_pipeline*; 30 Jan 2010
[61] Evans, G.B.; Furneaux, R.H.; Schramm, V.L.; Singh, V.; Tyler, P.C. Targeting the polyamine pathway with transition state analogue inhibitors of 5′-methylthioadenosine phosphorylase. *J. Med. Chem.* **2004**, *47*, 3275-3281.

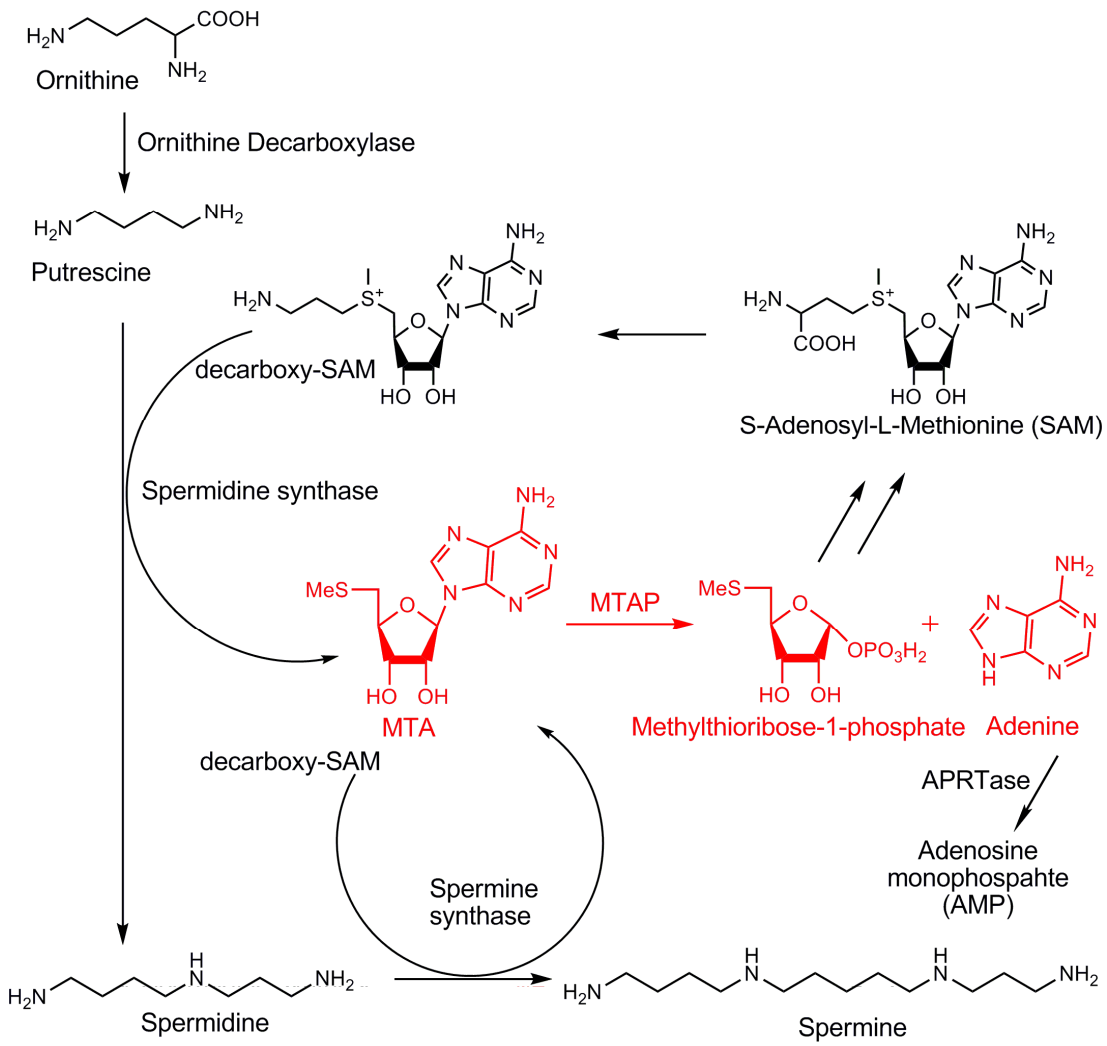

Figure 19 The pathway of the polyamine biosynthesis. The reaction of MTA to methylthioribose-1-phosphate and adenine, catalyzed by MTAP is shown in red. Adapted from references [58] and [62].

Since MTAP is the only enzyme in humans which processes MTA and genomic studies indicate that there is only one gene locus for the enzyme, it is proposed that inhibition of MTAP might raise the concentration of MTA. This would achieve feedback inhibition of the polyamine biosynthesis, which might have anitproliferative activity.[62] Evidence for this proposal was provided in 2007, when Schramm and co-workers found that inhibition of MTAP by a transition state analogue induces apoptosis in certain head and neck cancer cell lines.[63]

In bacteria 5′-methylthioadenosine/S-adenosylhomocysteine nucleosidase (MTAN) is, like MTAP, involved in the polyamine biosynthesis but also acts in the activated methyl cycle,

[62] Evans, G.B.; Furneaux, R.H.; Lenz, D.H.; Painter, G.F.; Schramm, V.L.; Singh, V.; Tyler, P.C. Second generation transition state analogue inhibitiors of human 5′-methylthioadenosine phosphorylase. *J. Med. Chem.* **2005**, *48*, 4679-4689.
[63] Basu, I.; Belbin, T.J.; Cordovano, G.; Das, I.; Guha, C.; Schramm, V.L. A transition state analog of 5'-methylthioadenosin phosphorylase induces apoptosis in head and neck cancers. *J. Biol. Chem.* **2007**, *282*, 21477-21486.

where S-adenosylhomocysteine (SAH) is used as substrate (Figure 20). In this pathway SAH is formed by SAM-dependent transmethylases from SAM and is further converted to adenine and S-ribosyl-homocysteine (SRH). The SRH cleavage enzyme LuxS converts SRH to homocysteine and 4,5-dihydroxy-2,3-pentadione, which is a precursor in the synthesis of autoinducer-2 (AI-2).[64] Furthermore, the amino-acid moiety of SAM is transferred to an acyl acceptor by AHL synthase to produce homoserine lactones which are used in the synthesis of autoinducer-1 (AI-1).[65]

Both autoinducers AI-1 and AI-2 are used as signalling molecules in intra- and interspecies communication between bacteria, commonly referred to as quorum sensing. Quorum sensing is induced, when bacterial populations reach a certain size and it is used to coordinate cooperative multicellular behaviour, which is beneficial to the microbial community. Examples for such cooperative behaviour are the feeding and sporulation of myxobacteria or the swarming motility of *Vibrio parahaemolyticus*.[66] The virulence of some pathogen bacteria is also linked to quorum sensing and thus this process provides an ideal target for the design of antibiotics. The finding, that a quorum sensing deficient *Neisseria meningitides* strain in infant rats is unable to produce viable bacteria in the blood, or that quorum sensing disabled *Streptococcus pneumoniae* infections in mice are less effective in spreading, support this approach.[67, 68]

Since MTANs are directly involved in the biosynthesis of autoinducers, it has been proposed that the inhibition of MTANs could be a possible way to disrupt quorum sensing. Given that the inhibition of MTAN is not lethal to bacteria, it is also believed that the potential of bacteria to develop resistance to these enzyme inhibitors is less likely compared to traditional antibiotics. [65]

[64] Hardie, K.R.; Williams, P.; Winzer, K. LuxS and autoinducer-2: Their contribution to quorum sensing and metabolism in bacteria. *Advances in applied microbiology* **2003**, *53*, 291-396.
[65] Gutierrez, J. A.; Crowder, T.; Rinaldo-Matthis, A.; Ho, M. C.; Almo, S. C.; Schramm, L. V. Transition state analogues of 5′-methylthioadenosine nucleosidase disrupt quorum sensing. *Nature Chemical Biololgy* **2009**, 5, 251-257.
[66] Fuqua, W.C.; Greenberg, E.P.; Winans, S.C. Quorum sensing in bacteria: the luxR-luxI family of cell density-responsive transcriptional regulators. *J. Bacteriol*. **1994**, *176*, 269-275.
[67] Baldwin, T.J.; Blackley, D.; Delory, M.; Green, A.; Hardie, K.R.; Sun, Y.; Tang, C.M.; Winzer, K. Role of *Neisseria meningitides* luxS in cell-to-cell signalling and bacteremic infection. *Infect. Immun*. **2002**, *70*, 2245-2248.
[68] Ogunniyi, A.D.; Paton, J.C.; Paton, U.H.; Stroeher, U.H. Mutation of luxS of *Streptococcus pneumoniae* affects virulence in a mouse model. *Infect. Immun*. **2003**, *71*, 3206-3212.

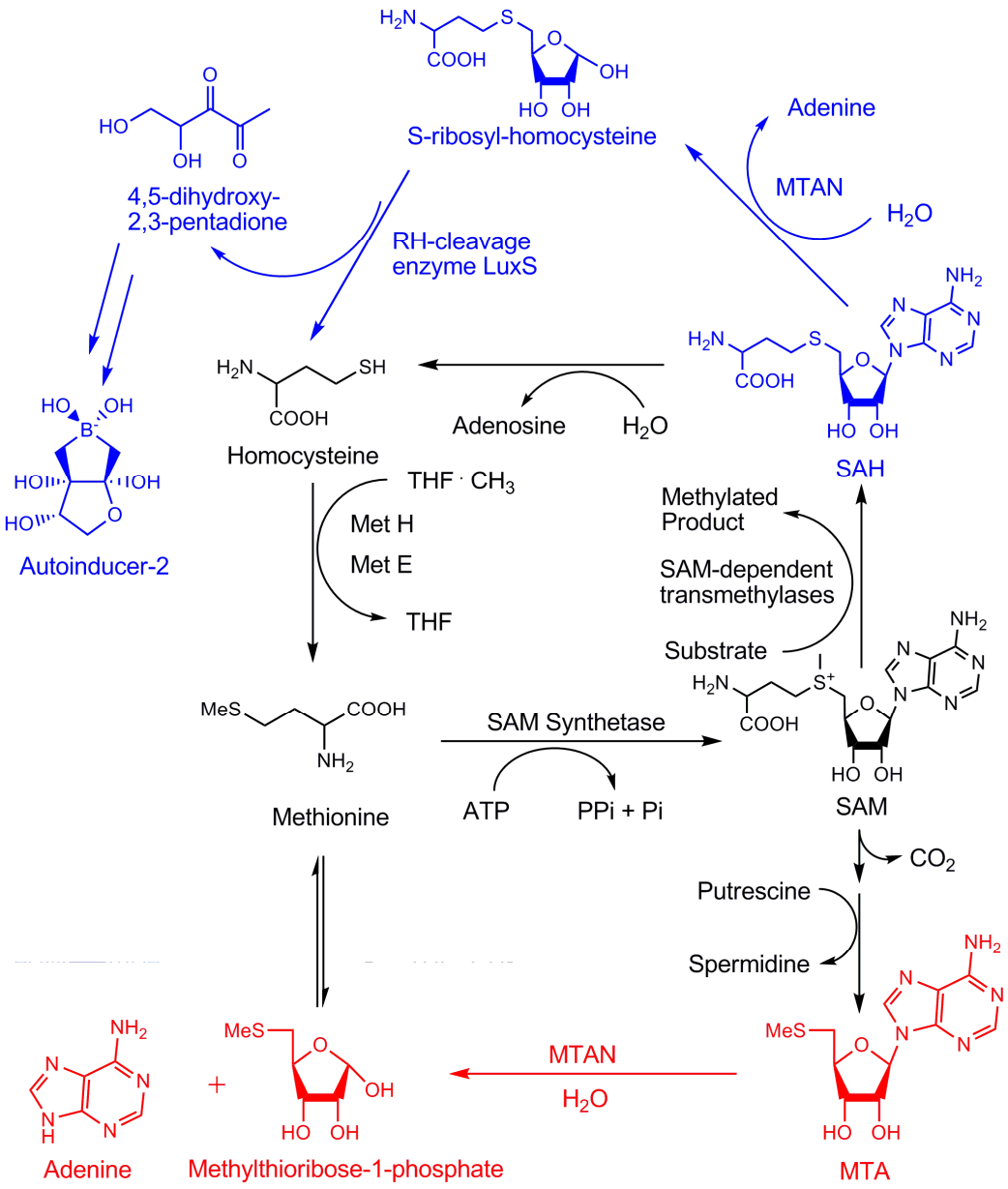

Figure 20 The biosynthetic pathway for the synthesis of autoinducer-2 signalling molecules in bacteria. The reactions catalyzed by MTAN are shown in red and blue. Red: the deadenylation of MTA in the polyamine-biosynthesis. Blue: the deadenylation of SAH to SRH, which is further converted to homocysteine and 4,5-dihydroxy-2,3-pentadione, the precursor in the synthesis of AI-2. Adapted from references [58] and [64].

2.1.3 Transition State Structures and Analogues of MTAP and MTAN

The transition states of MTA and SAH metabolizing human and bacterial enzymes have been revealed by KIE analysis and are either early or late dissociative S_N1 transition states. Whether the transition state is early or late is determined by the distances between the ribosyl anomeric carbon (C1') and the N9 in the adenine leaving group. The C1'-N9 distance of early transition states is 2.0Å or less and for late transition states it is 3.0Å or more (Figure 21).

Human MTAP, *E. coli* as well as *S. pneumoniae* MTANs show late dissociative transition states with extensive cleavage of the bond between the adenine and the ribosyl moiety. In

MTAP the attacking nucleophile is involved in the transition state whereas in *E. Coli* and *S. pneumoniae* MTANs significant participation of the nucleophile in the transition state is not observed.[69, 70, 71]

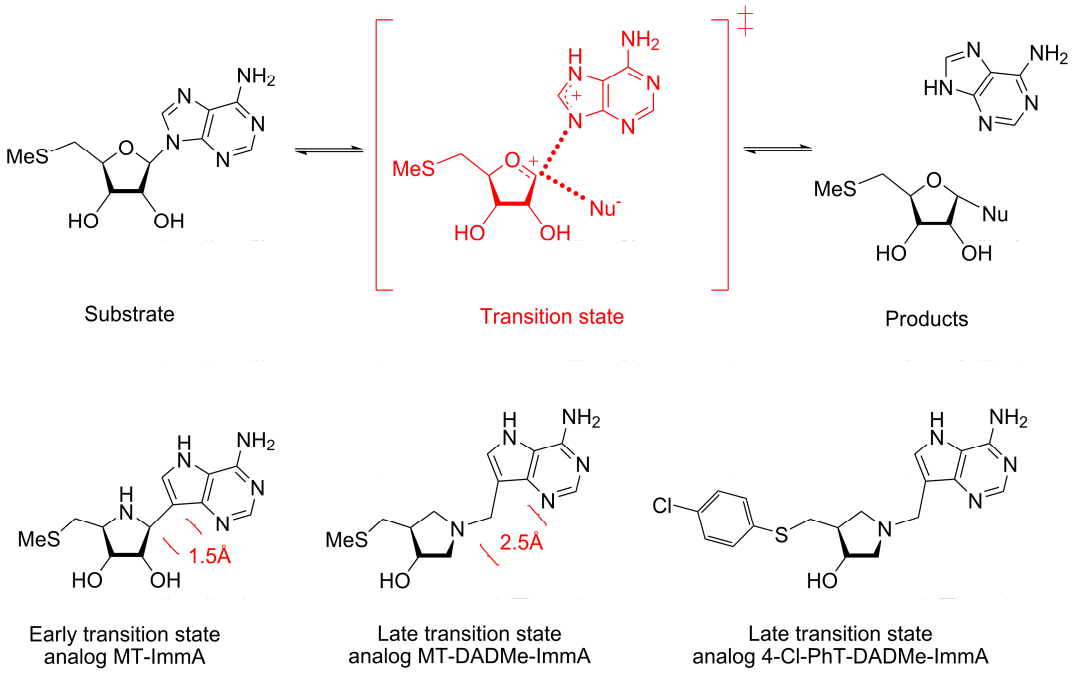

Figure 21 Top, the reaction catalyzed by MTAP and MTANs with MTA as substrate with the transition state shown in red. In the case of MTAP the attacking nucleophile (Nu^-) is phosphate whereas in MTANs it is water. Bottom, early and late transition sate analogues MT-ImmA and MT-DADMe-ImmA showing the distances between the ribosyl and the adenine mimics and the powerful late transition state analog 4-Cl-PhT-DADMe-ImmA. Adapted from reference [65].

The transition state of *N. meningitides* MTAN is an early S_N1 transition state where the bond between adenine and the anomeric carbon of the ribosyl is not fully broken.[72]

To account for the differences in the transition state structures two types of transition state analogues have been designed. 5′-Methylthio-Immucillin-A (MT-ImmA) resembles early dissociative transition states whereas 5′-Methylthio-DADMe-Immucillin-A (MT-DADMe-ImmA) accounts for late dissociative transition states (Figure 21).

Previously MT-ImmA, MT-DADMe-ImmA and derivatives thereof have been designed, synthesised and tested[58] against the enzymes described in section 2.1.2 and they have proven to be the most powerful inhibitors for these enzymes known so far. For example, the 4'-(4-chlorophenyl)thio-derivative of MT-DADMe-ImmA (4-Cl-PhT-DADMe-ImmA) binds $5*10^5$ times more tightly to MTAP than its natural substrate MTA and $9.1*10^7$

[69] Singh, V.; Schramm, V. L. Transition state structure of human 5′-methylthioadenosine phosphorylase. *J. Am. Chem. Soc*. **2006**, *128*, 14691-14696.
[70] Singh, V.; Lee, J. E.; Nunez, S.; Howell, P. L.; Schramm, V. L. Transition state structure of 5′-methylthioadenosine/S-adenosylhomocysteine nucleosidase from Escherichia Coli and its similarity to transition state analogues. *Biochem.* **2005**, *44*, 11647-11659.
[71] Singh, V.; Schramm, V. L. Transition state analysis of S-pneumoniae 5′-methylthioadenosine nucleosidase. *J. Am. Chem. Soc.* **2007**, *129*, 2783-2795.
[72] Singh, V.; Luo, M.; Brown, R. L.; Norris, G. E.; Schramm, V. L. Transition state structure of Neisseria meningitides 5′-methylthioadenosine/S-adenosylhomocysteine nucleosidase. *J. Am. Chem. Soc.* **2007**, *129*, 13831-13833.

more tightly to *E. coli* MTAN than the natural substrate SAH (Figure 21). This data emphasises that transition state analysis together with synthetical chemistry provides a useful methodology for the production of geometric and electrostatic transition state analogs that act as powerful enzyme inhibitors. Although the approach to enzyme inhibitors through transition state analysis is a relatively new science and is limited to the *N*-ribosyltransferase family so far, it is likely that this approach will have future impact on drug design. The clinical trials for Immucillin-H and DADMe-Immucillin-H and the results of the ongoing research in this field emphasize this prospect.

2.2 Objectives and Synthetic Plan

This work is part of a project with the objective to synthesise new derivatives of MT-DADMe-ImmA and to test them against human MTAP and MTANs from *E. coli* as well as *N. meningitides*. The particular emphasis lies on using previously reported, convenient and cheap methods for the synthesis of the Immucillins hydroxypyrrolidine core and on replacing the sulfur containing moieties in order to probe the sulfurs influence on the biological activity as well as the bioavailability and to simplify the overall chemical synthesis of the inhibitors.[73]

The new synthetic strategy for non sulfur containing derivatives of the late transition state analogue MT-DAD-ImmA (Figure 21) can retro synthetically be divided into five major steps (Figure 22). The transition state analogue **1** can be prepared by a Mannich reaction between 9-deazaadenine **2** and amine **3**.[74] Amine **3** is prepared by ring opening of the epoxide **5**[75] which could be obtained from commercially available diallyl amine **7**.[76]

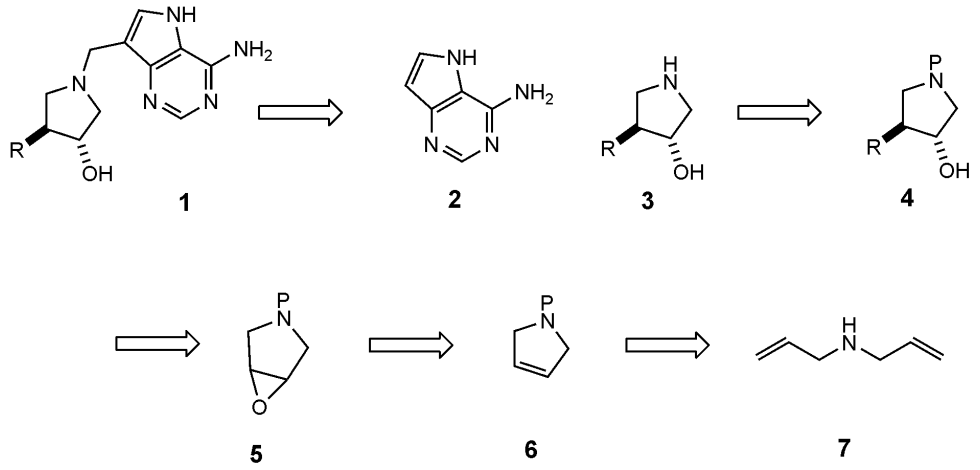

Figure 22 Retro synthetic analysis for the transition state analogues of MTAP and MTANs.

Bols and co-workers have shown that copper (I) salts assist the opening of epoxide **5** with Grignard reagents and under these conditions the trans isomer of the resulting protected amine **4** is formed predominatly.[75]

The amines **4** previously synthesised by our group are presumed to have *trans*-sterochemistry and are racemic. Since there are no crystal structures available so far, another synthetic route, which leads to amines with stereochemistry defined by their starting material was considered in order to confirm the stereochemistry of the amines obtained by the procedures according to Bols *et al*.[75]

[73] Personal communication with Vern L. Schramm.
[74] Evans, G.B.; Furneaux, R.H.; Schramm, V.L; Tyler, P.C. Synthesis of a transition state analogue inhibitor of purine nucleoside phosphorylase via the Mannich reaction. *Org. Lett*. **2003**, *5*, 3639-3640.
[75] Hansen, S.U.; Bols, M. 1-Azaribofuranoside analogues as designed inhibitors of purine nucleoside phosphorylase. Synthesis and biological evaluation. *Acta. Chem. Scand.* **1998**, *52*, 1214-1222.
[76] Kamal, A.; Shaik, A.; Sanbohr, M.; Malik, M. S.; Azeeza, S. Chemoenzymatic synthesis of (3*R*,4*S)*- and (3*S*,4*R)*-3-methoxy-4-methylaminopyrrolydine. *Tetrahedron Asymmetry* **2006**, **17**, 2876-2883.

Furthermore, the synthesis of enantiopure amines provides building blocks for the synthesis of chiral Immucillins, which are expected to show different inhibition constants (K_i-values) compared to the K_i-values of their racemic counterparts. These differences are of interest since it is known that the reaction enhancements afforded by enzymes depend on the stereochemistry of their substrates.

The research carried out during this project could be divided into three sections: first: the synthesis of hydroxypyrrolidines **8** and **9**; second: the synthesis of 9-deazaadenine **2** as a major building block for the transition state analogues of MTAN and MTAP and third: the synthesis of enantiopure transition state analogue **10** and the racemic transition state analogue **11** (Figure 23).

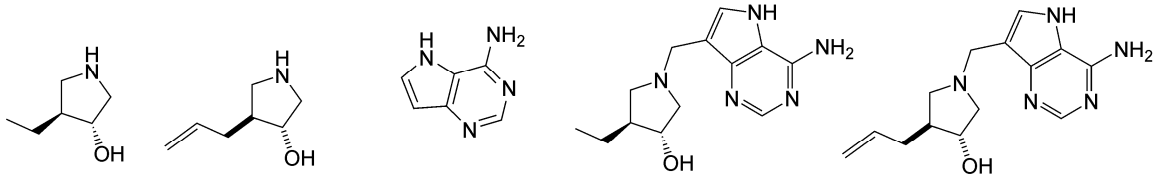

Figure 23 Racemic and enantiopure amines **8** and **9**, 9-deazaadenine **2**, enantiopure transition state analogue **10** and racemic transition state analogue **11**.

The enantiopure transition state analogue **10** and its corresponding amine **8** have been chosen as targets, because their racemic counterparts have been already synthesised and tested against human MTAP and MTANs from *E. coli* and *N. meningitides*, thus offering ideal candidates for a comparison between racemic and enantiopure transition state analogues. Hydroxypyrrolidine **9** and the corresponding Immucillin **11** are part of a new series of inhibitors, differing from each other only in the form of the alkyl moiety on position C-4 on the pyrrolidine ring.

2.3 Results and Discussion

2.3.1 Synthesis of *trans*-Amine 8 and *trans*-Transition State Analogue 10

The synthesis of the enantiopure *trans*-amine **8** started with the (3*R*,4*R*)-1-*tert*-butoxycarbonyl-3-hydroxy-4-(hydroxymethyl)pyrrolidine (**12**).[62] The primary hydroxyl group was selectivly protected as a benzoylester and the secondary hydroxyl group as a *tert*-butyldimethylsilylether to afford the fully protected pyrrolidine **14**. Removal of the benzoyl protecting group with sodium methoxide in methanol gave alcohol **15** which was oxidised either under Swern (Method A) or Dess-Martin (Method B) conditions to afford aldehyde **16**. The Dess-Martin oxidation proved to be the method-of-choice for this case, because it increased the yield from 60% to 88% and was much easier to handle.

The aldehyde **16** was subjected to a Wittig olefination with methyltriphenylphosphonium bromide and n-BuLi in THF to afford methenylated pyrrolidine **17**. Although this transformation has already been reported with ethyltriphenylphosphonium bromide and benzyltriphenylphosphonium bromide on the same system with moderate yields,[62] in this particular case the alkene **17** could either not be isolated at all, or only in very poor yields. Driven by this drawback several alternative routes to compound **17** have been considered, for example the Tebbe, Petasis and Nysted reagents, since all of them have been reported to be useful as methylenation reagents.[77] The use of Nysted reagent in THF with BF_3*Et_2O as catalyst was investigated first because it was readily available, but only decomposition of the starting material **16** was observed. However, finally the yield of the Wittig reaction was increased from 30% to 89%, by the use of newly purchased chemicals exclusively and thorough drying of all these reagents.

Hydrogenation of vinyl pyrrolidine **17** afforded ethyl pyrrolidine **18** which was subsequently deprotected with pure trifluoroacetic acid (TFA) to provide the presumably enantiopure *trans*-amine **8**. The optical rotation for **8** was +5.04 (c = 1.15, MeOH) whereas it was 0 (c = 1.05, MeOH) for the previously synthesised racemic analogue of **8**. The comparison of the ^{1}H- and ^{13}C-NMR spectra of **8** and its racemic analogue did not show major changes in the chemical shifts as expected. Therefore, the enantiopure *cis*-amine needs to be synthesised which was not completed due to time restrictions.

Amine **8** was subjected to a Mannich reaction with 9-deazaadenine **2**, formaldehyde in 1,4-dioxane and water to afford the presumably enantiopure Immucillin **10** in satisfying yield (67%) and 98% purity by HPLC (Scheme 7). The optical rotation for **10** was +3.48 (c = 1.03, MeOH) whereas it was 0 (c = 1.10, MeOH) for its racemic analogue. Again no major

[77](a) Morriello, G.J. et.al. Fused bicyclic pyrrolizinones as new scaffolds for human NK_1 antagonists. *Bioorganic & Medicinal Chemistry* **2008**, *16*, 2156-2170; (b) Aïssa, C.; Riveiros, R.; Ragot, J.; Fürstner, A. Total syntheses of Amphidinolide T1, T3, T4 and T5. *J. Am. Chem. Soc*. **2003**, *125*, 15512-15520.

difference in the ^{1}H- and ^{13}C-NMR shifts between **10** and its racemic analogue were observed, as expected.

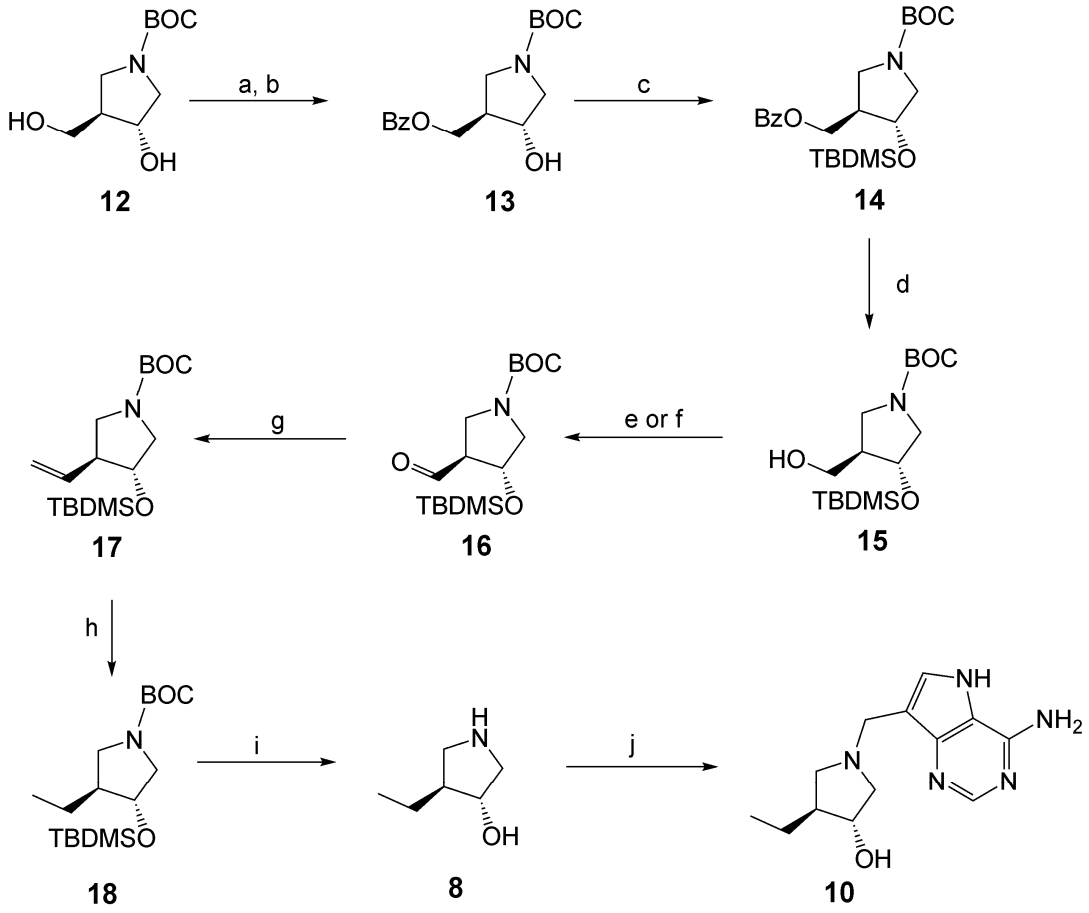

Scheme 7 (a) $(Bu)_2SnO$, toluene, reflux 1h; (b) BzCl, 5ºC → rt, 12h, 41%; (c) TBDMS-Cl, imidazole, DMF, rt, 12h; (d) NaOMe, MeOH, rt, 3h, 47%; (e) $(CF_3CO)_2O$, DMSO, Et_3N, DCM, -78ºC → -10ºC, 60%; (f) Dess-Martin periodinane, DCM, RT, 2h, 88%; (g) $(Ph)_3PCH_3Br$, n-BuLi, THF, -78ºC → rt, 3.5h, 89%; (h) 10%Pd/C, H_2 (1atm), EtOH, rt, 15h, 88%; (i) TFA, rt, 14h, 76%; (j) 9-deazaadenine, CH_2O, H_2O, 1,4-dioxane, rt, 60h.

2.3.2 Synthesis of 9-Deazaadenine 2

For the synthesis of 9-deazaadenine **2** a previously established procedure was used (Scheme 8).[78] Displacement of the ethoxy-group in acrylate **19** with aminoacetonitrile bisulfate afforded the amino-acrylate **20**, which was further converted to the carbamate **21** with methylchloroformate and triethylamine in DCM. Cyclisation of compound **21** with DBU in DCM and subsequent cleavage of the methyl ester moiety gave the pyrrole-derivative **22**, which upon a second cyclisation with formamidine acetate afforded the deaza-purine derivative **23**. Refluxing of **23** and potassium hydroxide in water removed the ethyl ester moiety and finally gave 9-deazaadenine **2**.

[78] (a) Evans, G.B. The synthesis of *N*-ribosyl transferase inhibitors based on a transition state blueprint. *Aust. J. Chem*. **2004**, *57*, 837-854; (b) Klein, R.S; Lim, M.-I. Synthesis of „9-deazaadenosine"; a new cytotoxic C-nucleoside isostere of adenosine. *Tetrahedron Lett*. **1981**, *22*, 25-28.

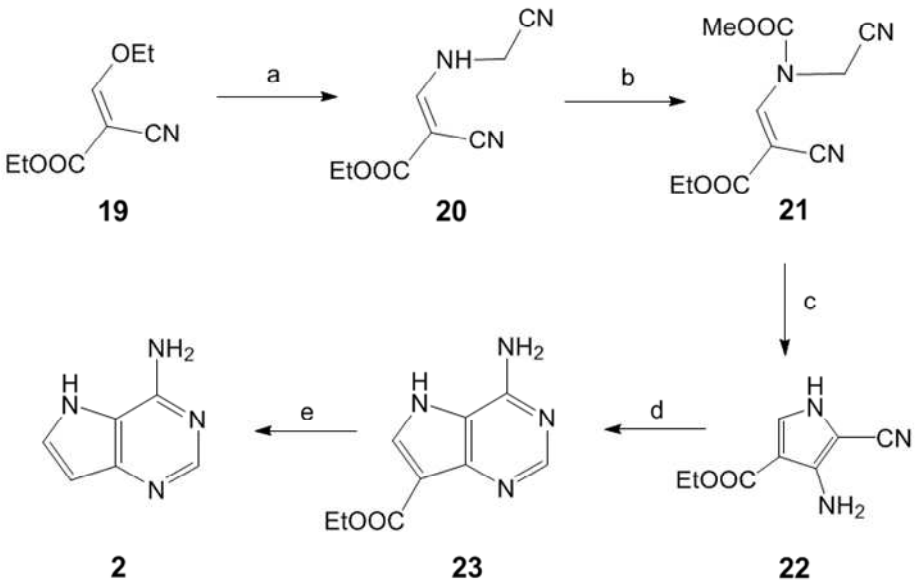

Scheme 8 (a) aminoacetonitrile bisulfate, CH_3COONa, MeOH, rt, 3.5h; (b) methylchloroformate, Et_3N, DCM, rt, 3h; (c) DBU, DCM, 3.5h rt, 12h, reflux; (d) formamidine acetate, EtOH, reflux, 21h; (e) KOH, H_2O, reflux, 48h.

This synthesis was carried out two times on a 10g scale, but the product could never be isolated with a reasonable yield. The first attempt gave 0.13g, which is an overall yield of only 1.5%, whereas the second attempt gave no desired product at all.

The reason for this problem might be traced back to the starting material **19**, which was a mixture of *Z/E*-isomers. Although this does not cause any problems with the formation of the carbamate **21**, the following cyclisation to compound **22** is solely accessible via the *E*-isomer of **21**. Thus, in case of a *Z/E*-mixture, only the *E*-isomer can react to the desired product and consequently the yield gets decreased. Furthermore, the carbanion, which is generated from **21,** may not only attack the nitrile group intramoleculary, but may also attack intermoleculary nitrile groups of other starting molecules **21**, or even the already formed product, thus forming a complex mixture of several compounds and further decreasing the yield of **22**. This suggestion is supported by the ^{1}H-NMR data for compounds **20** and **21**, which shows an excess of the corresponding *Z*-isomers, and **22**, which shows a complex mixture of several products.

Driven by this drawback, another synthetic route towards 9-deazaadenine **2** was considered (Scheme 9).

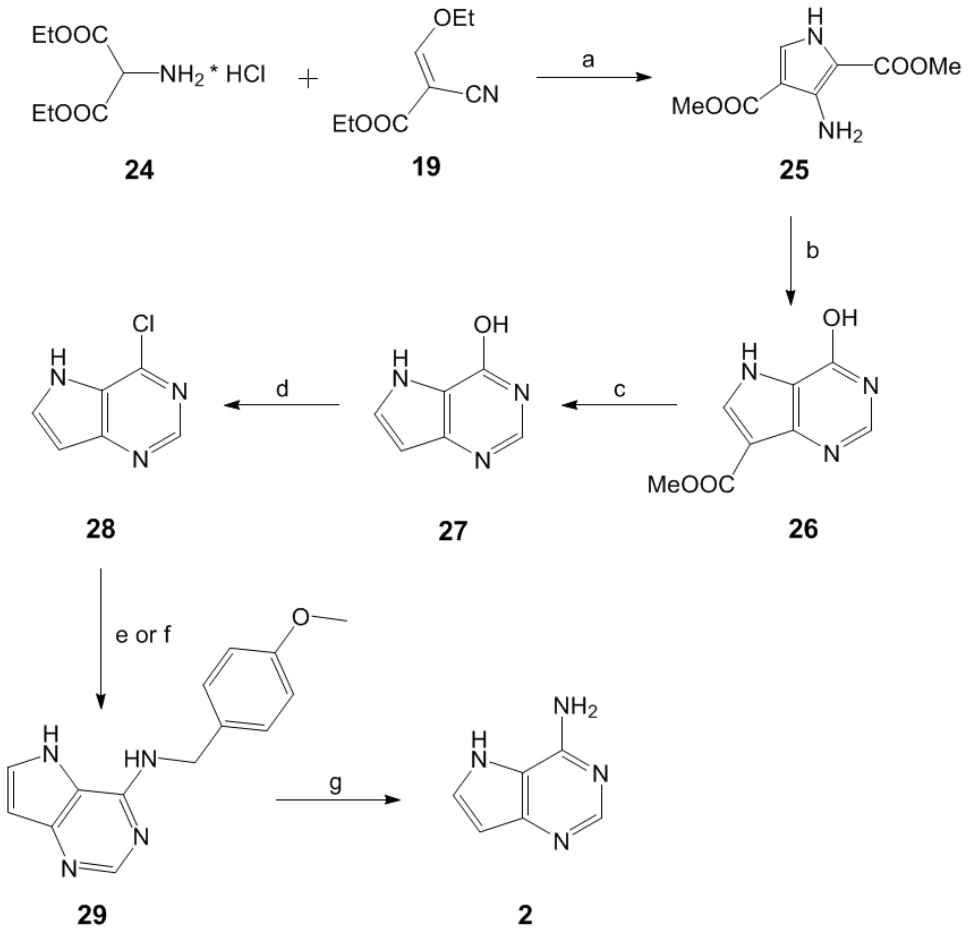

Scheme 9 (a) NaOMe, MeOH, reflux, 4h; (b), formamidine acetate, EtOH, reflux, 24h; (c) KOH, H_2O, reflux, 48h, 20% over 3 steps; (d) $POCl_3$, reflux, 1h, 68% crude; (e) PMBA, EtOH, reflux, 6h; (f) PMBA, DIPEA, reflux, 6h; (g) 10% aq. HCl, reflux, 2h.

Starting form diethyl-2-aminomalonate hydrochloride **24** and ethyl-2-cyano-3-ethoxyacrylate **19** the pyrrole derivative **25** was obtained by refluxing **24** and **19** with sodium methoxide in methanol. Reaction of pyrrole **25** with formamidine acetate in ethanol gave **26**, subsequently the methyl ester moiety was removed by potassium hydroxide in water to afford the 9-deazahypoxanthine **27**[79] in 20% yield over three steps. The hydroxyl group of 9-deazahypoxanthine **27** was replaced with chlorine by reaction with phosphorous oxychloride to afford pyrimidine derivative **28**. The new strategy towards 9-deazaadenine **2** investigated the replacement of the chlorine moiety by 4-methoxy-benzylamine (PMBA) to give **29** followed by the removal of the 4-methoxy-benzyl group to afford **2**.

The reaction of **28** with PMBA was conducted either by using three equivalents of PMBA (Method A) or by using 1.1 equivalent of PMBA and one equivalent of diisopropylethylamine (DIPEA) as base (Method B). NMR and TLC analysis suggested that the reaction itself seemed to work well but the work up was accompanied by huge difficulties; namely the removing of excess PMBA and/or DIPEA. Removal of the excess PMBA was

[79] Furneaux, R.H.; Tyler, P.C. Improved Synthesis of 3*H*,5*H*-pyrrolo[3,2-d]pyrimidines. *J.Org. Chem*. **1999**, *64*, 8411-8412.

attempted by trituration with Et_2O but some PMBA remained in the mixture. Column chromatography and finally recrystallisation from methanol with water afforded **29** of reasonable purity but it was accompanied by huge loss of product on the column. The removal of the PMBA-group of **29** was carried out in three ways: 1) Cleavage with one equivalent of TFA in methanol under reflux for 55h; 2) Cleavage with 10% Pd on carbon, hydrogen in methanol at rt and ambient pressure; 3) Cleavage in 10% aq. HCl under reflux for 2h. The first two attempts were not successful at all but the cleavage with 10% aq. HCl seemed to work reasonably well although similar problems with the purification as described for the previous step were encountered. Although several solvent systems were tried, it was not possible to separate **2** from the cleaved PMBA group and other impurities by chromatography. Recrystallisation from water by adding aq. cNH_4OH also failed several times. Hence, 9-deazaadenine **2** was never isolated as a clean product from this synthetic sequence. Given that the reactions in this route all work reasonably well, the purification of either **29** or **2** needs to be optimized. One possibility may be sublimation, but it could not be tried due to time restrictions.

2.3.3 Synthesis of racemic Amine 9 and racemic Transition State Analogue 11

The synthesis of the racemic transition state analogue **11** started from diallylamine **7**, which was protected as its carboxybenzylcarbamate (Cbz) derivative **30**. Treatment of **30** with Grubb's 1st generation catalyst in DCM afforded the Cbz-protected 2,5-dihydro-1H-pyrrole **31** which was subsequently converted to the bromohydrin **32** with *N*-bromosuccinimide (NBS) and water in DMSO. Conversion of bromohydrin **32** to the epoxide **33** was achieved by reaction with 1M aq. NaOH in MeOH.

The epoxide **33** was opened by introducing various Grignard reagents to afford **34a**, **34b** and **34c**. For **34a** and **34b**, the corresponding Grignard reagents were obtained commercially and added to the epoxide in presence of copper(I)bromide dimethylsulfide complex in THF. Since the batch of the cyclopropyl magnesium bromide was of questionable quality the obtained product was heavily contaminated with impurities. Therefore, **34a** was never isolated but NMR spectra indicated that the desired product had been formed. Compound **34b** was synthesized following the same procedure as for **34a** and the product was obtained in a moderate yield (38%). For **34c** the allyl magnesium bromide was obtained following the general procedure for Grignard reagents and it was reacted with **33** in Et_2O to give **34c** in a moderate yield (40%). Due to time constraints **34b** was not further processed.

Removal of the Cbz-group from **34c** was conducted with 2M KOH in isopropanol to afford the racemic amine **9**. This rather unusual method for the Cbz-removal was chosen, since conventional deprotection by hydrogenation was not possible due to the presence of a double bond and HBr in anhydrous acetic acid was not readily available. Unfortunately,

compound **9** was heavily contaminated during the purification process, due to what was presumed to be a contaminated batch of chromatography solvents. Due to time constraits it was not possible to repeat this synthesis and a previously prepared batch of **34c** was used for the synthesis of **11**. In this batch the amine was protected with a BOC-group and its deprotection was conducted with cHCl in methanol and thus the compound was isolated as the corresponding hydrochloride. The free amine was liberated by elution through a silica column with DCM:MeOH:aq.cNH_4OH = 5:4.5:0.5 (v/v/v) and subsequently processed with 9-deazaadenine **2** and formaldehyde in 1,4-dioxane and water to the transition state analogue **11** (Scheme 10).

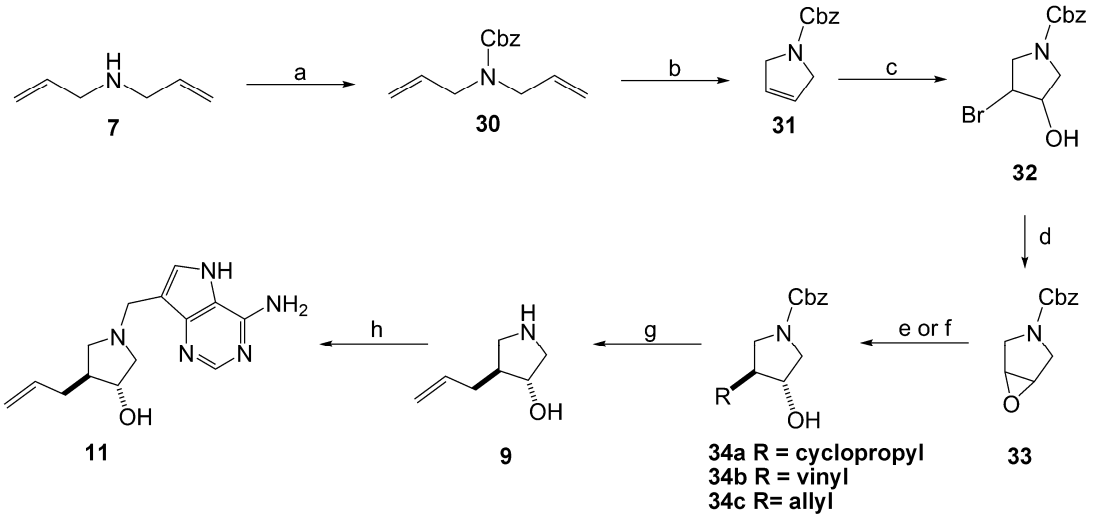

Scheme 10 (a) Cbz-Cl, Et_3N, DCM, 0ºC → rt, 12h, 92%; (b) $(Pcy_2)_2Cl_2Ru$=CHPh, DCM, rt, 24h, 92%; (c) NBS, DMSO, H_2O, 0ºC → rt, 2h; (d) 1M aq. NaOH, MeOH, 0ºC → rt, 24h, 72% (over 2 steps); (e) for **34a** and **34b**: RMgBr, Cu(I)Br*Me_2S, THF, -30ºC → -10ºC, 1h, 0% for **34a** 38% for **34b**; (f) allylbromide, Mg, Et_2O, 2h, reflux then 0ºC, **33**, Et_2O, 40min, 40%; (g) 2M KOH in i-propanol, reflux, 2h; (h) 9-deazaadenine, CH_2O, H_2O, 1,4-dioxane, rt, 12h, 23%.

3.3.4 Biological Results and Inhibition Studies

Transition state analogues **10** and **11** have been tested against human MTAP and bacterial MTANs from *E. coli* and *N. meningitides*. Additionally, a series of other racemic transition state analogues **35**-**40** were enclosed in this study in order to compare their biological activity with the activity of of compounds **10** and **11**. All tested analogs are derivatives of MT-DADMe-Imm-A (Figure 21) with different substituents on position C-4 of the pyrrolidine ring. The substituents are: R = ethyl, both enantiopure and racemic derivatives **10** and **35** respectively as well as R = n-butyl **36**, R = isobutyl **37**, R = pentan-3-yl **38**, R = phenyl **39**, R = cyclohexylmethyl **40**, R = allyl **11**, all racemic (Table 1). For detailed information about the experimental procedures of the inhibition studies, see reference 80.

Table 1: The structures of compounds **10** and **11** and **35**-**40** and their K_i values in nM, *indicates slow onset, as inhibitors for *E. coli* and *N. meningitides* MTANs and human MTAP.

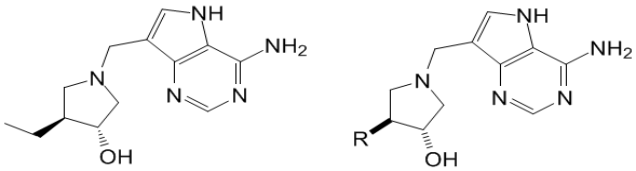

10 **11, 35 - 40**

	R	*E. coli* MTAN	*N. meningitides* MTAN	Human MTAP
10	ethyl	0.31 ± 0.02	2.2 ± 0.3	8.6 ± 1.0
35	ethyl	0.84 ± 0.06	1.4 ± 0.2	> 5 μM
36	n-butyl	0.051 ± 0.003	0.47 ± 0.06	> 5 μM
36	iso-butyl	*0.047 ± 0.009	*0.28 ± 0.06	6.0 ± 0.4
38	pentan-3-yl	0.7 ± 0.1	*0.44 ± 0.08	> 5 μM
39	phenyl	*0.030 ± 0.002	*0.24 ± 0.02	4.3 ± 0.6
40	cyclohexylmethyl	0.059 ± 0.008	*0.31 ± 0.05	> 5 μM
11	allyl	0.35 ± 0.03	3.0 ± 0.2	14.3 ± 1.7

As outlined in section 2.1.1, inhibition of enzymes with transition state analogues usually involves the two-step mechanism of slow-onset tight-binding inhibition. In the first step the competitive reversible binding of the inhibitor ($I^{‡}$) to the active site takes place to form the initial enzyme inhibitor complex ($E{\cdot}I^{‡}$), characterized by the dissociation-constant K_i. The second step involves the usually slow conversion of $E{\cdot}I^{‡}$ to the tight bound complex $EI^{‡}$. The overall equilibrium dissociation constant K_i^* after slow-onset is defined by the overall

[80] (a) Schramm, V.L. et. al. Femtomolar transition state analogue inhibitors of 5'-Methylthioadenosine/S-adenosylhomocysteine nucleosidase from *Escherichia coli*. *J. Biol. Chem*. **2003**, *18*, 18265-18273; (b) Almo, S.C.; Evans, G.B.; Furneaux, R.H.; Schramm, V.L.; Shi, W.; Singh, V.; Tyler, P.C. Picomolar transition state analogue inhibitors of human 5'-Methylthioadenosine phosporylase and X-ray structure with MT-immucillin-A. *Biochemistry* **2004**, *43*, 9-18.

equilibrium dissociation constant: $E + I \leftrightarrow EI^{\ddagger}$.[62] Accordingly, slow-onset tight-binding inhibitors are characterized by their K_i^*-value.

The K_i and K_i^* values for the compounds **10**, **11** and **35**-**40** are given in Table 1. Unless otherwise indicated all values are given in nM. Note that a decrease in number of the K_i and K_i^* values means an increase of inhibitory activity.

A comparison of the K_i-values obtained for *N. meningitides* MTAN with those obtained for *E. coli* MTAN, reveals that the tested compounds are better inhibitors for the *E. coli* MTAN. This result may arise from the nature of the *N. meningitides* MTAN transition state, which is, according to KIE-analysis, an early transition state, with a C1′-N9 distance between 1.47Å and 1.68Å with MTA as substrate.[72] Therefore, late transition state analogues, such as compounds **10** and **11** and **35**-**40**, may not be powerful inhibitors for the *N. meningitides* MTAN. However, the results obtained confirm the results of KIE-analysis and provide further evidence for the proposal that *N. meningitides* MTAN has an early transition state.

The K_i and K_i^* values of the *E. coli* MTAN decrease in number for the compounds with bulkier alkyl moieties, i.e. compounds **36**-**40**, about one order of magnitude, compared to the compounds with smaller alkyl moieties, i.e. compounds **10**, **11** and **35**. This suggests that transition state analogues with large substituents at the pyrrolidine ring induce better binding interactions with the enzyme and thus are better inhibitors. This finding was already indicated by sulfur containing transition state analogues with large substituents.[58] For instance MT-DADMe-ImmA and the 4'-(4-chlorophenyl)thio-derivative of MT-DADMe-ImmA have K_i-values of $2*10^{-3}$nM and $4.7*10^{-5}$nM respectively (Figure 21). [58] Likewise, this trend can also be seen in the K_i and K_i^* values obtained for the *N. meningitides* MTAN.

The comparison of the K_i-values of compounds **35** and **10**, 0.84 ± 0.06nM and 0.31 ± 0.02nM respectively, indicates that the enantiopure inhibitor is recognized better by the enzyme, than its racemic counterpart. This trend has already been observed with sulfur containing transition state analogues, which have been obtained via a similar route to that of compound **10**.[62] Hence, it seems that the transition state analogues should be enantiopure, or at least enantiomerically enriched, to act as powerful inhibitors. The simplified chemical synthesis via the epoxide-ring-opening provides racemic structures and therefore is not suitable to obtain as powerful inhibitors as compared to a more difficult asymmetric synthesis. Nonetheless, the synthetic route towards the racemic transition state analogs enables the fast synthesis of several inhibitors, which can be screened against the target enzymes. Once the most active compounds have been determined, they can be remade in enantiopure form.

The K_i values for human MTAP are quite distributed between the range of nM and µM. All compounds under investigation in this study were found to be less active, than the previously tested the sulfur containing inhibitors. This result suggests that MTAP inhibitors

are required to have a sulfur containing moiety in order to compete with MTAP's natural substrate MTA.

2.4 Summary and Conclusion

Two novel transition state analogue inhibitors **10** and **11** for the human enzyme 5'-methylthioadenosine phosphorylase (MTAP) as well as for the bacterial enzyme 5'-methylthioadenosine nucleosidase (MTAN) have been synthesised. Both enzymes play key roles in metabolic pathways that are involved in carcinogenesis and autoinducer synthesis. Autoinducers are signalling molecules, which are used in intra- and interspecies communication between bacteria (quorum sensing) and are related to bacterial virulence factors. Therefore, both enzymes are targets for the development of new pharmaceuticals, addressing cancer therapy as well as treatment of bacterial infections.

The design of the inhibitors is based on the determination of the enzymes transition state structures by kinetic isotope effect analysis in combination with computational methods.

A key feature of the inhibitors is a hydroxypyrrolidine ring with different functional groups adjacent to the hydroxyl group. Previously synthesised inhibitors for MTAP and MTANs contained thioalkyl groups, which have now been replaced by alkyl moieties in order to simplify the chemical synthesis and to study the influence of this replacement on the inhibitory activity of the target compounds. Compound **11** is part of a series of transition state analogues for which a fast and convenient synthetic strategy employing cheap starting materials was investigated. This route afforded the target compounds as a racemic mixture with presumed *trans*-stereochemistry between the alkyl group and the hydroxy group. Transition state analogue **10** is an enantiopure counterpart to one of the racemic inhibitors. The asymmetric synthesis of **10** was carried out in order to compare its biological activity against the activity of its racemic counterpart as well to prove the *trans*-stereochemistry of the racemic inhibitors.

Together with six other racemic transition state analogues compounds **10** and **11** have been tested against human MTAP and bacterial MTANs from *E. coli* and *N. meningitides*. For the bacterial MTANs the results of this biological evaluation indicate that bulkier alkyl moieties increase the inhibitory activity of the compounds. Furthermore, the enantiopure compound **10** shows a better inhibitory profile than its racemic counterpart. Therefore, the more convenient racemic synthesis does not provide as powerful inhibitors as an asymmetric synthesis. Nonetheless, it can be employed for the rapid synthesis of a library of potential inhibitors, which can be screened against the target enzymes. Once the most active compounds have been found, they can be synthesised in enantiopure form. The inhibitory activity of all tested compounds for *N. meningitides* was not as good as for *E. coli*, which is explained by differences in the transition state structure of the two enzymes. In case of human MTAP the replacement of the sulfur moieties has lead to a decrease of the

inhibitory activity. This result indicates the necessity of the thioalkyl groups on the inhibitors for the successful inhibition of MTAP.

In addition to the synthesis of **10** and **11** also a new synthetic route to 9-deazaadenine was investigated. 9-Deazaadenine is also a structural key feature of the MTAP and MTAN inhibitors, which mimics the purine moiety in the enzymes natural substrate. Although the desired product was obtained, the synthesis was accompanied by difficulties with the purification of the products in the last two steps of the reaction sequence. Hence, the investigated route is not suitable for the synthesis of 9-deazaadenine, unless the purification protocol is optimized, which could not be done due to time restrictions.

In conclusion new transition state analogue inhibitors for MTAP and MTANs have been developed, in order to test the influence of new structural features on the biological activity as well as new synthetic approaches. The data obtained in the biological evaluation allows for better understanding of the transition state structures of the target enzymes and thus points out directions for further investigations towards powerful inhibitors with promising pharmaceutical potential.

2.5 Experimental

2.5.1 Materials and Methods

Unless otherwise stated all chemicals were obtained commercially and used without further purification.

Thin layer chromatography was performed on silica gel 60 F_{254} aluminium sheets (Merck) visualized under UV light and/or with Ehrlich's reagent (*p*-(*N,N*-dimethylamino)benzaldhyde in cHCl/EtOH) or potassium permanganate solution (0.5% w/w potassium permanganate in 1M sodium hydroxide) and subsequent heating. Column chromatography was carried out using Davisil LC60A 40-63 micron silica. Analytical HPLC was performed on an Agilent 1100 instrument, eluting with a 0.1%w/w TFA in H_2O : MeOH = 97:3 → 50 : 50 → 97:3 gradient over 30min through a Phenomenex® Synergi 4µ polar RP 80A, 250 x 4.6mm column.

^{1}H-NMR spectra were recorded either on a Brucker Avance 300MHz at 300.13MHz or on a Brucker Avance III 500MHz spectrometer at 499.84MHz. ^{13}C-NMR spectra were recorded at 125.68MHz on a Brucker Avance III 500MHz spectrometer. For ^{1}H-spectra chemical shifts are reported in ppm from tetramethylsilane with the solvent signal, resulting from incomplete deuteration, as internal standard. For ^{13}C-NMR spectra chemical shifts are reported with the ^{13}C resonance of the deuterated solvent as internal standard. The data is reported as follows: chemical shift, integration, multiplicity (s = singlet, d = doublet, t = triplet, dd = doublet-doublet, ddd = doublets of doublets of doublets, m = multiplett), coupling constants (if appropriate) and assignment.

Optical rotations were obtained from a Perkin-Elmer 241 polarimeter using a cell of path length 1.0dm and are given in 10^{-1}deg cm^2 g^{-1}.

Melting points (mp) are uncorrected and were obtained on a Stuart SMP3 apparatus. Positive electro spray ionization high resolution and low resolution mass spectra (ESI-HRMS/ESI-LRMS) were recorded on a Waters Q-TOF Premier Mass Spectrometer.

pH-Assessments were done with Macherey-Nagel REF 921 10 pH-Fix 0-14 stripes.

Please note that for convenience the nomenclature as well as the numbering of the compounds is not IUPAC-conform.

2.5.2 Experimental Procedures

(3*R*,4*R*)-4-(Benzoyloxy)methyl-1-*tert*-butoxycarbonyl-3-hydroxypyrrolidine (13). A solution of (3*R*,4*R*)-1-*tert*-butoxycarbonyl-3-hydroxy-4-(hydroxymethyl)pyrrolidine (**12**)[62] (4.10g, 19mmol) and dibutyltin oxide (5.17g, 21mmol) in toluene (60mL) was refluxed in a Dean-Stark apparatus for 1h. The solution was cooled to 5ºC and benzoyl chloride (2.2ml, 19mmol) was added drop wise while the temperature was kept below 10ºC. The solution was stirred at rt overnight. The solvent was removed under reduced pressure and the residue was purified by column chromatography to give the title compound **13** as yellow oil (2.48g, 7.7mmol, 41%).

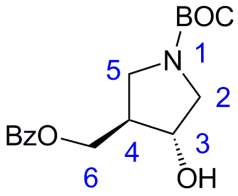

TLC-S:	$CHCl_3$: MeOH = 3 : 1
CC-S:	CH : EtOAC = 6 : 4
Yield:	40.9%
MW:	321.37g*mol^{-1}

^{1}H-NMR (500MHz, $CDCl_3$): δ = 7.98 (2H, d, Bz), 7.60-7.57 (1H, m, Bz), 7.47-7.44 (2H, m, Bz), 4.35-4.28 (2H, m, H-6, H-6'), 4.28-4.22 (1H, m, H-3), 3.73-3.62 (2H, m, H-2, H-5), 3.34-3.22 (2H, m, H-2', H-5'), 2.57-2.52 (1H, m, H-4), 1.46 (9H, s, BOC). ^{13}C-NMR (125MHz, $CDCl_3$): δ = = 166.7 (Bz), 154.6 (BOC), 133.3, 129.8, 129.7, 128.5 (Bz), 79.8 (BOC), 72.2, 71.5 (C-3), 64.2, 64.1 (C-6), 52.8, 52.6 (C-2), 47.0, 46.5 (C-4), 45.8, 45.3 (C-5), 28.5 (BOC).

(3*R*,4*R*)-4-(Benzoyloxy)methyl-1-*tert*-butoxycarbonyl-3-(*tert*-butyldimethylsilyloxy)-pyrrolidine (14). To a solution of compound **13** (2.48g, 7.7mmol) and 1H-imidazole (2.10g, 31mmol) in dry DMF (5ml, 65mmol) *tert*-butylchlorodimethylsilane (2.33g, 15mmol) was added and the mixture was stirred at rt for 12h. The solution was diluted with toluene (50mL) and washed with water twice (50mL each). The water was extracted with toluene (20mL each) twice and the combined organic phases were washed with brine, dried with $MgSO_4$ and concentrated under reduced pressure to afford the title compound **14** as yellow oil (3.31g, 7.6mmol, 98.7% crude).

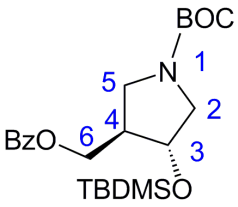

TLC-S:	CH : EtOAC = 1 : 1
Yield:	98.7% crude
MW:	435.63g*mol^{-1}

^{1}H-NMR (500MHz, $CDCl_3$): δ = 8.04-8.01 (2H, m, Bz), 7.60-7.56 (1H, m, Bz), 7.48-7.43 (2H, m, Bz), 4.37-4.33 (1H, m, H-3), 4.28-4.20 (2H, m, H-6, H-6'), 3.73-3.68 (1H, m, H-5), 3.66-3.57 (1H, m, H-2), 3.33-3.17 (2H, m, H-2', H-5'), 2.54-2.47 (1H, m, H-4), 1.46 (9H, s, BOC), 0.85 (9H, s, TBDMS), 0.05 (6H, s, TBDMS).

(3*R*,4*R*)-1-*tert*-Butoxycarbonyl-3-(*tert*-butyldimethylsilyloxy)-4-hydroxymethyl pyrrolidine (15). To a solution of compound **14** (3.31g crude) in MeOH (0.3mL) sodium methoxide (1.8mL, 7.9mmol, 25%w/w in MeOH) was added and the mixture was stirred at rt for 3h. The mixture was diluted with $CHCl_3$ (40mL), washed with water twice (20mL each) and dried with $MgSO_4$. The solvent was removed under reduced pressure and the remaining material was subjected to purification by column chromatography, which afforded compound **15** as yellow oil (1.20g, 3.6mmol, 47%).

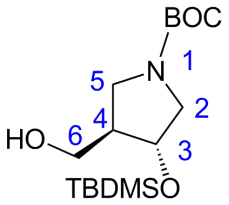

TLC-S:	CH : EtOAC = 4 : 6
CC-S:	CH : EtOAC = 7:3 → 4 : 6
Yield:	47.0%
MW:	331.52g*mol^{-1}

^{1}H-NMR (500MHz, $CDCl_3$): δ = 4.20-4.14 (1H, m, H-3), 3.69-3.51 (4H, m, H-2, H-5, H-6, H-6'), 3.18-3.12 (2H, m, H-2', H-5'), 2.31-2.23 (1H, m, H-4), 1.46 (9H, s, BOC), 0.88 (9H, s, TBDMS), 0.08-0.07 (6H, m, TBDMS). ^{13}C-NMR (125MHz, $CDCl_3$): δ = 154.8 (BOC), 79.4 (BOC), 72.8, 72.2 (C-3), 62.7, 62.5 (C-6), 53.3, 52.7 (C-2), 49.0, 48.5 (C-4), 46.4, 46.0 (C-5), 28.7 (BOC), 25.9 (TBDMS), 18.1 (TBDMS), -4.5 (TBDMS).

(3*R*,4*S*)-1-*tert*-Butoxycarbonyl-3-(*tert*-butyldimethylsilyloxy)-4-formylpyrrolidine (16). Method A. Compound **15** (0.25g, 0.7mmol) was dissolved in dry DCM (4.4mL, 69mmol) under argon atmosphere and cooled to -78ºC. DMSO (0.3mL, 3.7mmol) and subsequently trifluoroacetic anhydride (0.4mL, 3mmol) were added and the mixture was stirred for 1h at -74ºC. Et_3N (0.6mL, 4.5mmol) was added and after stirring for 30min at -78ºC the reaction was quenched with water (8mL) and diluted with DCM (10mL). The organic phase was washed with water (10mL each) 3 times and brine (10mL), dried with $MgSO_4$ and concentrated *in vacuo*. The residue was purified by column chromatography to afford the aldehyde **16** as yellow oil (0.15g, 0.5mmol, 59.6%).

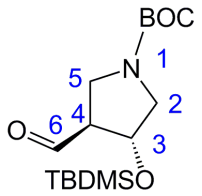

TLC-S:	CH : EtOAC = 2 : 1
CC-S:	CH : EtOAC = 9:1 → 1 : 1
Yield:	59.6%
MW:	329.51g*mol^{-1}

^{1}H-NMR (500MHz, $CDCl_3$): δ = 9.66 (1H, s, H-6), 4.54-452 (1H, m, H-3), 3.68-3.44 (3H, m, H-2, H-2',H-5), 3.19 (1H, m, H-5'), 2.97-2.96 (1H, m, H-4), 1.43 (9H, s, BOC), 0.86 (9H, s, TBDMS), 0.06 (6H, s, TBDMS). ^{13}C-NMR (125MHz, $CDCl_3$): δ = 198.9 (C-6), 153.4 (BOC), 79.0 (BOC), 70.7, 70.1 (C-3), 58.3, 57.6 (C-4), 52.9, 52.8 (C-2), 42.7 (C-5), 28.4 (BOC), 25.6 (TBDMS), 17.9 (TBDMS), -5.6 (TBDMS).

(3*R*,4*S*)-1-*tert*-Butoxycarbonyl-3-(*tert*-butyldimethylsilyloxy)-4-formylpyrrolidine (16). Method B. To a suspension of Dess-Martin periodinane (1.54g, 3.6mmol) in dry DCM (30mL) compound **15** (1.1g, 3.3mmol) was added and the mixture was stirred at rt for 2.5h. After dilution with Et_2O (150mL) the mixture was washed with a mixture of $NaHCO_3$ and $Na_2S_2O_3$ (100ml, saturated aq. $NaHCO_3$: 10% aq. $Na_2S_2O_3$, v/v 1:1) twice. The organic phase was dried with $MgSO_4$ and concentrated under reduced pressure. Column chromatography of the resulting residue afforded **16** as pale yellow oil (0.98g, 3.0mmol, 90%).

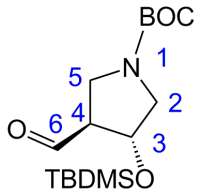

TLC-S:	CH : EtOAC = 2 : 1
CC-S:	CH : EtOAC = 9 : 1 → 8 : 2
Yield:	90%
MW:	329.51g*mol^{-1}

NMR-Data are given in the section: **(3*R*,4*S*)-1-*tert*-Butoxycarbonyl-3-(*tert*-butyldimethylsilyloxy)-4-formylpyrrolidine (16). Method A.**

(3*R*,4*S*)-1-*tert*-Butoxycarbonyl-3-(*tert*-butyldimethylsilyloxy)-4-vinylpyrrolidine (17). Methyltriphenylphosphonium bromide was co-evaporated with toluene 3 times then dried under high vacuum for 3h and stored over P_2O_5 in a desiccator for 72h. THF was dried by distillation over NaH (60% in mineral oil) directly before use. To a suspension of methyltriphenylphosphonium bromide (2.44g, 6.8mmol) in THF (10mL), n-BuLi (1.6M in hexane, 4.3mL, 6.8mmol) was added drop wise and the resulting bright orange solution was stirred under argon atmosphere at 0ºC. After 30min the reaction mixture was allowed to come to rt and this solution was added drop wise to a solution of aldehyde **16** (0.98g, 3.0mmol) in THF (10mL) at -78ºC. The resulting mixture was stirred at -78ºC for 1h and

consecutively at rt for 2.5h. The reaction was quenched with water (3mL) and extracted with DCM (100mL). The organic phase was washed with saturated. aq. $NaHCO_3$ (100ml) and with water (100mL), dried with $MgSO_4$ and concentrated under reduced pressure. Column chromatography of the remaining residue afforded the title compound **17** as colourless oil (0.87g, 2.7mmol, 89%).

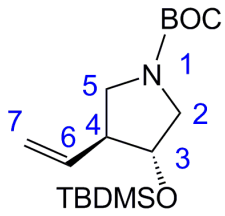

TLC-S:	CH : EtOAC = 9 : 1
CC-S:	CH : EtOAC = 9 : 1
Yield:	89%
MW:	327.53g*mol^{-1}

^{1}H-NMR (500MHz, $CDCl_3$): δ = 5.69-5.62 (1H, m, H-6), 5.13-5.07 (2H, m, H-7, H-7'), 4.01-3.97 (1H, m, H-3), 3.64-3.59 (1H, m, H-5), 3.57-3.49 (1H, m, H-2), 3.22-3.14 (1H, m, H-2'), 3.12-3.07 (1H, m, H-5'), 2.66-2.61 (1H, m, H-4), 1.45 (9H, s, BOC), 0.86 (9H, s, TBDMS), 0.04 (6H, s, TBDMS). ^{13}C-NMR (125MHz, $CDCl_3$): δ = 154.7, 154.6 (BOC), 136.8 (C-6), 117.0 (C-7), 79.4 (BOC), 75.7, 75.0 (C-3), 52.9, 52.5 (C-2), 51.0, 50.2 (C-4), 48.7, 48.2 (C-5), 28.6 (BOC), 25.9 (TBDMS), 18.1 (TBDMS), -4.2 (TBDMS). ESI-HRMS for $C_{17}H_{33}NO_3Si$ $[MNa]^+$ calcd: 350.2127, found: 350.2128; LRMS for $C_{17}H_{33}NO_3Si$ $[MNa]^+$: 350 (100%).

(3*R*,4*S*)-1-*tert*-Butoxycarbonyl-3-(*tert*-butyldimethylsilyloxy)-4-ethylpyrrolidine (18).
Compound **17** (0.87g, 2.7mmol) was dissolved in EtOH (25mL), Pd/C (10%, 0.5g) was added and the mixture was stirred under hydrogen atmosphere for 15h. After filtration the solution was concentrated under reduced pressure to afford **18** as yellow oil (0.77g, 2.3mmol, 88% crude). The product was used in the next step without purification.

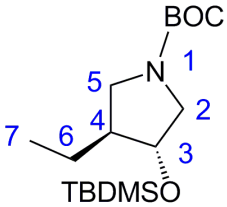

Yield:	88% crude
MW:	329.55g*mol^{-1}

^{1}H-NMR (500MHz, $CDCl_3$): δ = 3.90-3.89 (1H, m, H-3), 3.61-3.58 (1H, dd, $J_{5,5'}$ = 9.2Hz, $J_{5,4}$ = 6.3Hz H-5), 3.54-3.46 (1H, dd, $J_{2,2'}$ = 9.4Hz, H-2), 3.12-3.05 (1H, dd, H-2'), 3.02-3.92 (1H, dd, H-5'), 1.90-1.89 (1H, m, H-4), 1.45 (9H, s, BOC), 1.22-1.15 (2H, m, H-6, H-6'), 0.93 (3H, t, $J_{7,6,6'}$ = 7.2Hz, H-7), 0.88 (9H, s, TBDMS), 0.06 (6H, s, TBDMS). ^{13}C-NMR (125MHz, $CDCl_3$): δ = 154.9 (BOC), 79.3 (BOC), 75.7, 75.0 (C-3), 53.2, 52.8 (C-2), 49.2, 48.4 (C-4), 48.7, 47.8 (C-5), 28.7 (BOC), 25.9 (TBDMS), 24.3 (C-6), 18.1 (TBDMS), 12.4 (C-7), -4.5 (TBDMS).

(3*R*,4*S*)-4-Ethylpyrrolidin-3-ol (8). Compound **18** (0.77g, crude) was dissolved in TFA (25mL) and stirred at rt for 14h. After removing the TFA under reduced pressure, the residue was taken up in water (50mL) and washed with $CHCl_3$ (50mL each) twice. The aqueous layer was concentrated *in vacuo* and purification of the remaining material by column chromatograpy afforded the deprotected pyrrolidine **8** as yellow oil (0.205g, 1.8mmol, 76%).

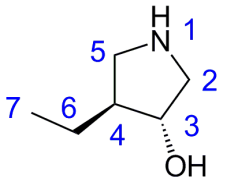

TLC-S:	DCM : MeOH : aq. cNH_4OH = 5 : 4.5 : 0.5
CC-S:	DCM : MeOH : aq. cNH_4OH = 5 : 4.5 : 0.5
Yield:	76%
MW:	115.17g*mol^{-1}

^{1}H-NMR (500MHz, MeOD): δ = 3.90-3.88 (1H, ddd, $J_{3,2}$ = 5.4Hz, $J_{3,2'}$ = 3.4Hz, $J_{3,4}$ = 3.6Hz, H-3), 3.19-3.16 (1H, dd, $J_{5,4}$ = 7.6Hz, $J_{5,5'}$ = 11.3Hz, H-5), 2.94-2.91 (1H, dd, $J_{2,2'}$ = 11.9Hz, H-2), 2.75-2.71 (1H, dd, H-2'), 2.47-2.43 (1H, dd, $J_{5',4}$ = 6.3Hz, H-5'), 1.83-1.77 (1H, m, $J_{4,6}$ = 6.5Hz, $J_{4,6'}$ = 6.5Hz, H-4), 1.51-1.43 (1H, m, $J_{6,7}$ = 7.4Hz, $J_{6,6'}$ = 13.6Hz, H-6), 1.28-1.21 (1H, m, $J_{6',7}$ = 7.4Hz, H-6'), 0.93 (3H, t, H-7). ^{13}C-NMR (125MHz, MeOD): δ = 78.1 (C-3), 54.7 (C-2), 51.6 (C-5), 51.0 (C-4), 26.3 (C-6), 12.9 (C-7). ESI-HRMS for $C_6H_{13}NO$ $[MH]^+$ calcd: 116.1075, found: 116.1080; LRMS for $C_6H_{13}NO$ $[MH]^+$: 116 (100%); $[\alpha]_D^{21}$= + 5.04 (c = 1.2, MeOH).

(3*R*,4*S*)-1-[(9-Deaza-adenin-9-yl)methyl]-4-ethyl-3-hydroxypyrrolidine (10). Pyrrolidine **8** (0.044g, 0.38mmol) was dissolved in H_2O (1.4mL, 78mmol). Subsequently 1,4-dioxane (0.7mL, 8.1mmol), formaldehyde solution (0.05mL, 0.7mmol) and 9-deazaadenine (0.05g, 0.4mmol) were added and the mixture was stirred at rt for 60h. The product was subjected to purification by column chromatography twice to afford the title compound **9** as off white solid (0.07g, 0.26mmol, 67%).

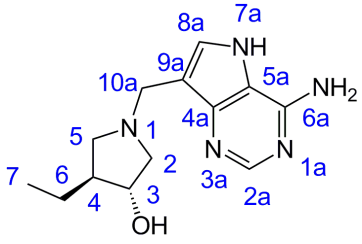

TLC-S:	DCM : MeOH : aq. conc. NH_4OH = 5 : 4.8 : 0.2
CC-S:	DCM : 7N NH_3 in MeOH = 8 : 2 and
	DCM: MeOH : aq. conc. NH_4OH = 5 : 4.5 : 0.5
Yield:	67%
MW:	261.32g*mol^{-1}

^{1}H-NMR (500MHz, MeOD): δ = 8.15 (1H, s, H-8a), 7.50 (1H, s, H-2a), 3.86-3.76 (2H, dd, *J* = 13.4, 24.8Hz, H-10a, H-10a'), 3.87-3.84 (1H, ddd, $J_{3,2}$ = 6.3Hz, $J_{3,2'}$ = 3.9Hz, $J_{3,4}$ = 4.3Hz, H-3), 3.08-3.04 (1H, dd, $J_{5,5'}$ = 9.5Hz, $J_{5,4}$ = 8.1Hz, H-5), 2.77-2.74 (1H, dd, $J_{2,2'}$ = 10.4Hz, H-2),

2.70-2.68 (1H, dd, H-2'), 2.21-2.17 (1H, dd, $J_{5',4}$ = 7.9Hz, H-5'), 1.90-1.84 (1H, m, $J_{4,6,6'}$ = 6.9Hz, H-4), 1.59-1.51 (1H, m, $J_{6,7}$ = 7.4Hz, H-6), 1.38-1.29 (1H, m, $J_{6',7}$ = 7.4Hz, H-6'), 0.94-0.91 (3H, t, H-7). ^{13}C-NMR (125Mhz, MeOD): δ = 152.1 (C-6a), 150.9 (C-2a), 147.1 (C-4a), 130.1 (C-8a), 115.1 (C-5a), 112.5 (C-9a), 77.4 (C-3), 62.4 (C-2), 59.3 (C-5), 50.3 (C-10a), 49.1 (C-4), 27.0 (C-6), 12.8 (C-7). ESI-HRMS for $C_{13}H_{19}N_5O$ $[MH]^+$ calcd: 262.1668, found: 262.1665; LRMS for $C_{13}H_{19}N_5O$ $[MH]^+$: 262 (100%); $[\alpha]_D^{21}$= + 3.48 (c = 1.0, MeOH); Purity by HPLC: 98%. mp: decomposition above 220°C.

Ethyl 2-(*Z/E*)-cyano-3-(cyanomethylamino)acrylate (20). Sodium acetate (14.5g, 177mmol) was added to a stirred suspension of aminoacetonitrile bisulfate (9.16g, 59mmol) in MeOH (130mL) at rt. After 10min ethyl(ethoxymethylene)cyanoacetate (10.7g, 63mmol) was added and the mixture was stirred at rt for 3.5h. The solvent was removed under reduced pressure and the residue was diluted with saturated aq. $NaHCO_3$ (200mL) and extracted with EtOAc (200mL each) 3 times. The combined organic phases were washed with brine (200mL), dried with $MgSO_4$ and concentrated *in vacuo* to afford the title compound **18** as a yellow solid (11g, 61mmol, 97% crude) with a *Z/E*-ratio of 1.3 : 1. The product was used in the next step without purification.

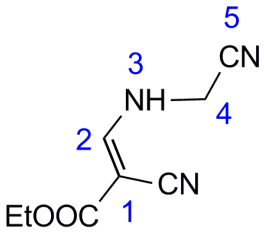

TLC-S:	DCM : MeOH = 9.5 : 0.5
Yield:	97% crude
MW:	179.18g*mol^{-1}

^{1}H-NMR (300MHz, MeOD): δ = 8.07 (1H, s, H-2, *E*-isomer), 7,69 (1H, s, H-2, *Z*-isomer), 4.78 (2H, s, H-4), 4.27-4.17 (2H, m, $COOC\underline{H_2}CH_3$), 1.32-1.27 (3H, m, $COOCH_2C\underline{H_3}$).

Ethyl 2-(*Z/E*)-cyano-3-((cyanomethyl)(methoxycarbonyl)amino)acrylate (21).
Triethylamine (11.2mL, 80mmol) was added drop wise to a mixture of compound **20** (11g crude) and methyl chloroformate (6.2mL, 80mmol) in dry DCM (134mL) at such a rate that the temperature was kept below 40°C. After stirring the mixture at rt for 3h the reaction was refluxed for 12h and subsequently quenched with saturated aq. $NaHCO_3$ (40mL). The organic layer was washed consecutively with water (50mL each) twice, with 10% aq. HCl (50mL each) twice and with sat. aq. $NaHCO_3$ (40mL each) twice. The combined organic layers were dried over $MgSO_4$ and concentrated under reduced pressure to afford the title compound **21** as a dark red syrup (11.9g, 82% crude) with a *Z/E*-ratio of 5.6 : 1. The material was used in the next step without purification.

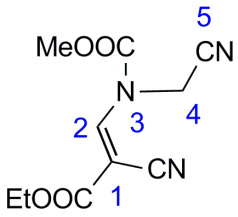

TLC-S: DCM : MeOH = 9.5 : 0.5
Yield: 82% crude
MW: 237.21g*mol^{-1}

^{1}H-NMR (300MHz, MeOD): δ = 9.15 (1H, s, H-2, *E*-isomer), 8,62 (1H, s, H-2, *Z*-isomer), 5.11 (2H, s, H-4), 4.35-4.29 (2H, m, $COOCH_2CH_3$), 4.01 (3H, s, $COOCH_3$) 1.36-1.32 (3H, m, $COOCH_2CH_3$).

Ethyl 4-amino-5-cyano-1*H*-pyrrole-3-carboxylate (22). DBU (3.9mL, 27mmol) was added drop wise to a solution of **21** (11.9g crude) in dry DCM (100mL) at rt under argon atmosphere. The reaction mixture was first stirred at rt for 3.5h and kept under reflux for 12h. HCl (10%, 35mL) was added at rt and the organic layer was washed with saturated aq. $NaHCO_3$ (50mL). The organic layer was dried over $MgSO_4$ and concentrated under reduced pressure to afford the title compound **22** as a black solid (11.1g, 123% crude). The product was used in the next step without purification.

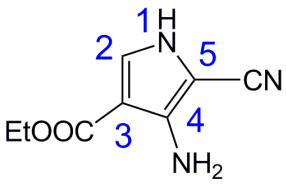

TLC-S: DCM : MeOH = 9.5 : 0.5
Yield: 123% crude
MW: 179.18g*mol^{-1}

^{1}H-NMR (300MHz, MeOD): δ = 7.35 (1H, s, H-2), 8.11 (1H, s, H-8), 4.25-4.29 (2H, dd, $COOCH_2CH_3$), 1.28 (3H, t, $COOCH_2CH_3$)

Ethyl 4-amino-5*H*-pyrrolo[3,2-d]pyrimidine-7-carboxylate (23). Compound **22** (6.7g crude) was dissolved in EtOH (35mL) and formamidine acetate (6.7g, 65mmol) was added portion wise. The resulting mixture was refluxed for 18h, cooled to 0℃ and the title compound **21** was filtered off as a black solid (2.95g, 38% crude). The product was used without further purification.

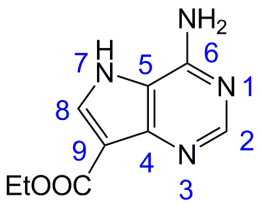

TLC-S: DCM : MeOH = 9.5 : 0.5
Yield: 38% crude
MW: 206.20g*mol^{-1}

^{1}H-NMR (300MHz, d_6-DMSO): δ = 8.19 (1H, s, H-2), 8.11 (1H, s, H-8), 4.27-4.20 (2H, dd, COOC<u>H</u>$_2$CH$_3$), 1.29 (3H, t, COOCH$_2$C<u>H</u>$_3$)

5*H*-Pyrrolo[3,2-d]pyrimidin-4-amine (9-deazaadenine) (2). Compound **23** (2.95g crude) and KOH (2.6g, 47mmol) were refluxed in water (30mL) for 48h. After cooling to rt conc. HCl (40mL) and charcoal (2.9g) were added and the suspension was refluxed again for 20min and filtered hot through celite. The filtrate was concentrated under reduced pressure and the remaining material was dissolved in hot water and the pH was adjusted to 12 by adding aq. conc. NH_4OH. The mixture was cooled to 0℃ and filtrated, wh ich afforded compound **2** as an off white solid (0.13g, 7% crude).

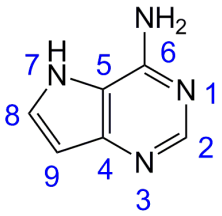

TLC-S: DCM : MeOH = 9.5 : 0.5
Yield: 7% crude
MW: 134.14g*mol^{-1}

^{1}H-NMR (300MHz, d_6-DMSO): δ = 8.08 (1H, s, H-2), 7.50 (1H, s, H-8), 6.33 (1H, s, H-9).

Dimethyl 3-amino-1*H*-pyrrole-2,4-dicarboxylate (25). A solution of diethyl-2-aminomalonate hydrochloride **24** (250g, 1180mmol), sodium methoxide (195g, 3544mmol 30%w/w solution in MeOH) and ethyl-2-cyano-3-ethoxyacrylate **19** (200g, 1181mmol) in MeOH (2.1L) was refluxed for 4h. Acetic acid (150mL) was added at rt and the mixture was concentrated under reduced pressure. The residue was dissolved in water (2L) and the title compound **25** was filtered off as a brown solid (133g, 672mmol, 56% crude). The product was used in the next step without purification.

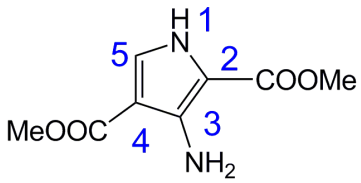

Yield: 56% crude
MW: 198.18g*mol^{-1}

^{1}H-NMR (300MHz, d_6-DMSO): δ = 7.23 (1H, s, H-5), 3.73 (3H, s, COOC<u>H</u>$_3$), 3.70 (3H, s, COOC<u>H</u>$_3$).

Methyl 4-hydroxy-5*H*-pyrrolo[3,2-d]pyrimidine-7-carboxylate (26). A suspension of compound **25** (132g crude) and formamidine acetate (139g, 1331mmol) in ethanol (1.8L) was refluxed for 25h. The mixture was diluted with water (700mL) and compound **26** (76.2g,

394mmol, 60%) was obtained by filtration of the hot reaction mixture. The product was used in the next step without purification.

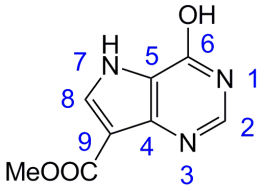

Yield: 60% crude

MW: 193.60g*mol^{-1}

^{1}H-NMR (300MHz, d_6-DMSO): δ = 7.91 (1H, s, H-8), 7.78 (1H, s, H-2), 3.77 (3H, s, COOC$\underline{H}_3$).

5*H*-Pyrrolo[3,2-d]pyrimidin-4-ol (27). KOH (88g, 1577mmol) was added to a solution of **26** (76.2g crude) in water (1L). After refluxing the solution for 44h charcoal (10g) was added and the resulting mixture was stirred for 10min. The solids were removed by filtration of the hot suspension. Acetic acid (120mL) was added to the filtrate at rt and the product was filtered off and washed with saturated aq. $NaHCO_3$ (200mL). Compound **27**, a dark grey solid (31.6g, 234mmol, 60% crude) was used in the next step without further purification.

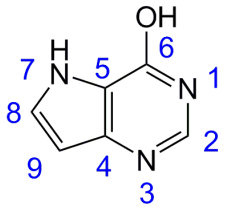

Yield: 60% crude

MW: 135.12g*mol^{-1}

^{1}H-NMR (300MHz, d_6-DMSO): δ = 7.77 (1H, s, H-2), 7.35 (1H, d, $J_{8,9}$ = 2.8Hz, H-8), 6.36 (1H, d, H-9).

4-Chloro-5*H*-pyrrolo[3,2-d]pyrimidine (28). Compound **27** (1.1g crude) was refluxed in $POCl_3$ (3.3mL, 35mmol) for 1h. The solvent was removed under reduced pressure and the residue was poured into ice water. From this mixture compound **28** (0.84g, 5.4mmol, 68% crude) was obtained as a brown solid by filtration. The product was used in the next step without purification.

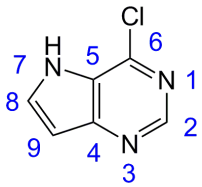

Yield: 68% crude

MW: 153.57g*mol^{-1}

^{1}H-NMR (300MHz, d_6-DMSO): δ = 8.63 (1H, s, H-2), 7.99 (1H, d, $J_{8,9}$ = 3.2Hz, H-8), 6.74 (1H, d, H-9).

***N*-(4-Methoxybenzyl)-5*H*-pyrrolo[3,2-d]pyrimidin-4-amine (29) Method A.** To a suspension of **28** (0.72g crude) in EtOH (4.5mL), 4-methoxybenzylamine (1.85mL, 14.1mmol) was added. The mixture was refluxed for 6h, cooled to rt, diluted with EtOH (5mL) and was stirred with Amberlyst® A21 for 12h (ion exchanger was washed with EtOH prior to use). Charcoal (0.05g) was added, the mixture was refluxed for 20min, filtered hot through celite and the solvent was removed under reduced pressure. The residue was purified by column chromatography. For further purification the product was triturated with Et_2O and finally crystallized from MeOH with water 3 times to afford **29** as a brown solid (0.15g, 0.60mmol, 13% yield).

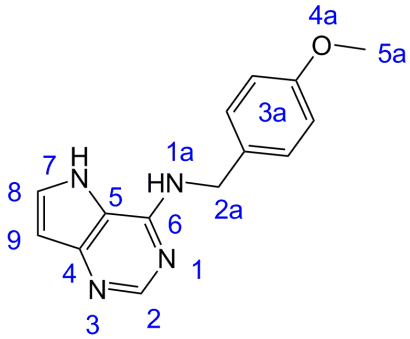

CC-S: DCM : MeOH : aq. NH_4OH = 97 : 2.5 : 0.5
Yield: 13%
MW: 241.29g*mol^{-1}

^{1}H-NMR (500MHz, d_6-DMSO): δ = 8.16 (1H, s, H-2), 7.47 (1H, d, $J_{8,9}$ = 3.0Hz, H-8), 7.33-7.31 (2H, m, H-3a), 6.92-6.90 (2H, m, H-3a), 6.36 (1H, d, H-9), 4.65 (2H, d, *J* = 5.5Hz, H-2a), 3.73 (3H, s, H-5a).

***N*-(4-Methoxybenzyl)-5*H*-pyrrolo[3,2-d]pyrimidin-4-amine (29). Method B.** To a solution of **28** (0.5g, 3.3mmol) in EtOH (3mL) *N,N*-diisopropylethylamine (0.57mL, 3.3mmol) and 4-methoxybenzylamine (0.43mL, 3.3mmol) were added and mixture was refluxed for 5h. The work up was the same as described in method A but the product could never be isolated in satisfying purity.

***N*-Benzyloxycarbonyl-*N,N*-diallylamine (30).** The reaction was carried out by Alistair Longshaw (ail/09/41).* The crude material was received and filtered through celite and washed with EtOAc. Removal of the solvent in vacuo afforded the title compound **30** as yellow oil (25.6g, 111mmol, crude). The product was used in the next step without further purification.

* IRL Carbohydrate Chemistry Team

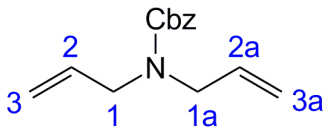

TLC-S: CH : EtOAC = 9.5 : 0.5

MW: 231.29g*mol^{-1}

^{1}H-NMR (300MHz, $CDCl_3$): δ = 7.39-7.23 (5H, m, Cbz), 5.82-5.73 (2H, m, H-2, H-2a), 5.20-5.10 (6H, m, H-3, H-3', H-3a, H-3a', Cbz), 3.89 (4H, m, H-1, H-1', H-1a, H-1a').

1-Benzyloxycarbonyl-2,5-dihydro-1*H*-pyrrole (31). Compound **30** (25.6g, 111mmol) was dissolved in DCM (500mL), Grubb's catalyst 1st gen. (1.1g, 1.34mmol) was added and the mixture was stirred under argon atmosphere at rt for 24h. The solvent was removed under reduced pressure and the residue was purified by column chromatography to afford the title compound **31** as a yellow oil (13.2g, 65mmol, 58%).

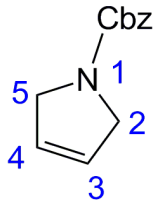

TLC-S: CH : EtOAC = 9.5 : 0.5

CC-S: CH : EtOAC = 9.8 : 0.2 → 9.6 : 0.4 → 9 : 1

Yield: 58%

MW: 203.24g*mol^{-1}

^{1}H-NMR (500MHz, $CDCl_3$): δ = 7.40-7.29 (5H, m, Cbz), 5.83-5.75 (2H, m, H-3, H-4), 5.17 (2H, s, Cbz), 4.23-4.18 (4H, m, H-2, H-2', H-5, H-5').

1-Benzyloxycarbonyl-3-bromo-4-hydroxypyrrolidine (32). Compound **31** (0.21g, 1.03mmol) was dissolved in DMSO (3.3mL). Subsequently water (0.14mL, 8mmol) and NBS (0.23g, 1.27mmol) were added at 0℃ and the mixture was stirred at 0℃ for 1h and 30min at rt. The reaction mixture was diluted with water (50mL) and was extracted with EtOAc (50mL each) 3 times. The combined organic layers were washed with brine (50mL), dried over $MgSO_4$ and the solvent was removed under reduced pressure to afford the title compound **32** as a colourless oil (0.31g, 1.04mmol, 101% crude). The product was processed further without purification.

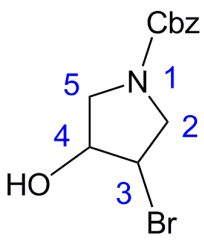

TLC-S: CH : EtOAC = 4 : 1

Yield: 101% crude

MW: 298.13g*mol^{-1}

^{1}H-NMR (500MHz, $CDCl_3$): δ = 7.37-7.30 (5H, m, Cbz), 5.16 (2H, s, Cbz), 4.51-4.50 (1H, s, H-4), 4.15-4.09; 3.99-3.82 (4H, m, H-2, H-2', H-5, H-5'), 3.52-3.46 (1H, m, H-3).

Benzyl 6-oxa-3-azabicyclo[3.1.0] hexane-3-carboxylate (33). To a solution of **32** (1.03mmol - assuming 100% yield from previous reaction) in MeOH (3.4mL) aq. NaOH (0.06mL, 1.6mmol, 1M) was added at 0℃. After 20min the ice bath was removed and the mixture was stirred at rt for 12h. After removal of the solvent *in vacuo* the remaining residue was dissolved in water and extracted into EtOAc (50mL each) 3 times. The combined organic layers were washed with brine (50mL) and dried over $MgSO_4$. The solvent was removed under reduced pressure and column chromatography of the residue afforded the title compound **33** as yellow oil (0.17g, 0.75mmol, 72% over 2 steps).

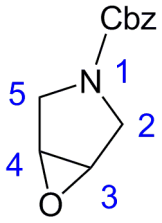

TLC-S:	CH : EtOAC = 3 : 2
CC-S:	CH : EtOAC = 3 : 2
Yield:	72%
MW:	219.24g*mol^{-1}

^{1}H-NMR (300MHz, $CDCl_3$): δ = 7.37-7.30 (5H, m, Cbz), 5.14-5.08 (2H, dd, *J* = 12.3, 17.9Hz, Cbz), 3.91-3.83 (2H, m, H-2, H-5), 3.69-3.67 (2H, m, H-4, H-3), 3.41-3.37 (2H, m, H-2', H-5'). ^{13}C-NMR (125MHz, $CDCl_3$): δ = 155.4, 136.8, 128.6, 128.2, 128.1, 67.0 (Cbz), 55.6, 55.1 (C-3, C-4), 47.4, 47.2 (C-2, C-5); ESI-HRMS for $C_{12}H_{13}NO_3$ $[MNa]^+$ calcd: 242.0793; found: 242.0791; ESI-LRMS for $C_{12}H_{13}NO_3$ $[MNa]^+$: 242 (100%).

1-Benzyloxycarbonyl-3-hydroxy-4-vinylpyrrolidine (34b). To a solution of compound **31** (0.142 g, 0.65mmol) and copper(I) bromide dimethyl sulfide complex (0.02g, 0.08mmol) in dry THF (5mL) vinyl magnesium bromide (3.2mL, 3.2mmol, 1M in THF) was added drop wise at -35ºC. The mixture was slowly warmed to -10ºC over a period of 2.5h. The reaction was quenched by adding 10% aq. NH_4OH (10mL). The layers were separated and the aqueous layer was extracted with Et_2O (50mL each) twice. The combined organic layers were dried over $MgSO_4$ and concentrated under reduced pressure. The residue was purified by column chromatography to afford the title compound **32b** as yellow oil (0.06g, 0.24mmol, 38%).

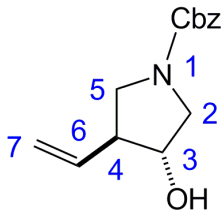

TLC-S:	DCM : EtOAC = 4 : 1
CC-S:	DCM : EtOAC = 4 : 1
Yield:	38%
MW:	247.29g*mol^{-1}

^{1}H-NMR (500MHz, $CDCl_3$): δ = 7.37-7.31 (5H, m, Cbz), 5.77-5.63 (1H, m, H-6), 5.24-5.14 (4H, m, Cbz, H-7, H-7'), 4.16-4.09 (1H, m, H-3), 3.79-3.69 (2H, m, H-5, H-2), 3.38-3.27 (2H, m, H-2', H-5'), 2.77-2.65 (1H, m, H-4). ^{13}C-NMR (125MHz, $CDCl_3$): δ = 155.1, 136.9 (Cbz), 136.1, 136.0 (C-6), 128.6, 128.1, 127.9 (Cbz), 117.5, 117.4 (C-7), 74.9, 74.2 (C-3), 67.0 (Cbz), 52.6, 52.2 (C-2), 50.4, 49.8 (C-4), 48.9, 48.7 (C-5). ESI-HRMS for $C_{14}H_{17}NO_3$ $[MNa]^+$ calcd: 270.1106, found: 270.1104; ESI-LRMS for $C_{14}H_{17}NO_3$ $[MNa]^+$: 270 (100%).

1-Benzyloxycarbonyl-4-allyl-3-hydroxypyrrolidine (34c). Compound **33** (0.130g, 0.59mmol) was dissolved in dry Et_2O (2mL). This solution was added drop wise to a suspension of allylmagnesium bromide in Et_2O (8mL) at 0ºC. The allylmagnesium bromide was generated *in situ* from allyl bromide (0.8g, 6.6mmol) and Mg (0.37g, 15mmol) by refluxing in Et_2O (10mL) for 2h. After stirring for 40min the reaction was quenched with aq. HCl (6mL, 1M). The layers were separated and the aqueous layer was extracted with Et_2O (50mL each) twice. The combined organic layers were dried over with $MgSO_4$, concentrated under reduced pressure and the residue was purified by column chromatography to afford the title compound **32c** as yellow oil (0.06g, 0.3mmol, 40%).

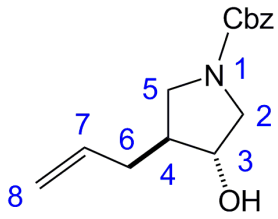

TLC-S:	DCM : EtOAC = 4 : 1
CC-S:	DCM : EtOAC = 4 : 1 → 7 : 3
Yield:	40%
MW:	261.31g*mol^{-1}

^{1}H-NMR (500MHz, $CDCl_3$): δ = 7.38-7.29 (5H, m, Cbz), 5.84-5.74 (1H, m, H-7), 5.14 (2H, s, Cbz), 5.11-5.06 (2H, m, H-8, H-8'), 4.14-4.08 (1H, m, H-3), 3.73-3.68 (1H, m, H-5), 3.68-3.64 (1H, m, H-2), 3.36-3.32 (1H, m, H-2'), 3.23-3.17 (1H, m, H-5'), 2.22-2.14 (2H, m, H-6, H-6'), 2.10-2.02 (1H, m, H-4). ^{13}C-NMR (125MHz, $CDCl_3$): δ = 155.2, 136.9 (Cbz), 135.7 (C-7), 128.6, 128.1, 128.0 (Cbz), 117.1 (C-8), 74.9, 74.1 (C-3), 67.0 (Cbz), 53.0, 52.6 (C-2), 49.3, 49.0 (C-5), 45.7, 45.1 (C-4), 35.6 (C-6). ESI-HRMS for $C_{15}H_{19}NO_3$ $[MNa]^+$ calcd: 284.1263, found: 284.1258; ESI-LRMS for $C_{15}H_{19}NO_3$ $[MNa]^+$: 284 (100%).

4-Allylpyrrolidin-3-ol (9). Compound **34c** (0.06g, 0.3mmol) was refluxed in a mixture of KOH and isopropanol (3.6mL, 2M) for 2h. The mixture was dry loaded onto silica and purification was attempted with DCM:MeOH:aq.cNH_4OH = 5:4.5:0.5 (v/v/v). Due to contaminated solvent **9** could not be isolated pure from this experiment. Therefore, a previously prepared batch of **34c**[75] was used for the synthesis of **11**. In this batch the amine was protected with a BOC group and its deprotection was conducted with conc. HCl in

MeOH to give compound 9 as the corresponding hydrochloride. The free amine was liberated by elution through a silica column with DCM:MeOH:aq.cNH$_4$OH = 5:4.5:0.5 (v/v/v).

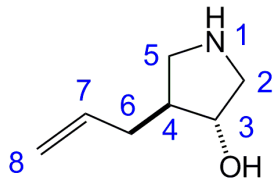

TLC-S:	DCM : MeOH : aq.cNH$_4$OH = 5 : 4.5 : 0.5
CC-S:	DCM : MeOH : aq.cNH$_4$OH = 5 : 4.5 : 0.5
MW:	127.18g*mol^{-1}

^{1}H-NMR (500MHz, MeOD): δ = 5.87-5.79 (1H, ddd, $J_{7,6}$ = 3.6Hz, $J_{7,8}$ = 6.8Hz, $J_{7,8'}$ = 17.0Hz, H-7), 5.10-5.02 (2H, m, H-8, H-8'), 4.00-3.98 (1H, ddd, $J_{3,2}$ = 5.3Hz, $J_{3,2'}$ = 3.2Hz, $J_{3,4}$ = 2.2Hz, H-3), 3.24-3.20 (1H, dd, $J_{5,4}$ = 7.1Hz, $J_{5,5'}$ = 11.5Hz, H-5), 3.05-3.01 (1H, dd, $J_{2,2'}$ = 12.1Hz H-2), 2.83-2.80 (1H, dd, H-2'), 2.60-2.56 (1H, dd, $J_{5',4}$ = 5.5Hz, H-5'), 2.27-2.20 (1H, m, $J_{4,6}$ = 6.7 H-4), 2.09-1.99 (2H, m, H-6). ^{13}C-NMR (125MHz, MeOD): δ = 137.6 (C-7), 116.7 (C-8), 77.3 (C-3), 54.3 (C-2), 51.0 (C-5), 48.3 (C-4), 37.3 (C-6).

4-Allyl-1-[(9-deaza-adenin-9yl)methyl]-3-hydroxy-pyrrolidine (11). Compound **34c** (0.04g, 0.4mmol) was dissolved in water (1.2mL, 65mmol). Subsequently 1,4-dioxane (0.6mL, 8mmol), formaldehyde solution (0.04mL, 0.7mmol) and 9-deazaadenine (0.04g, 0.3mmol) were added and the mixture was stirred at rt for 12h. The product was purified by column chromatography twice to afford the title compound **11** as off white solid (0.02g, 0.07mmol, 23%).

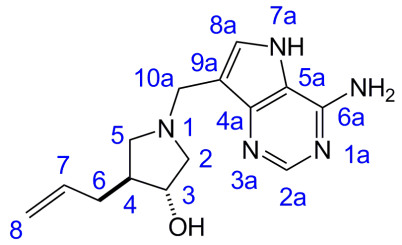

TLC-S:	DCM : MeOH : aq. cNH$_4$OH = 5 : 4.8 : 0.2
CC-S:	DCM : 7N NH$_3$ in MeOH = 9 : 1 → 8 : 2 → 7 : 3 → 6 : 4
	DCM: MeOH : aq. cNH$_4$OH = 5 : 4.9 : 0.1
Yield:	23%
MW:	273.33g*mol^{-1}

^{1}H-NMR (500MHz, MeOD): δ = 8.15 (1H, s, H-2a), 7.49 (1H, s, H-8a), 5.83-5.74 (1H, m, $J_{7,8}$ = 6.8Hz, $J_{7,8'}$ = 17.0Hz, $J_{7,6}$ = 3.6Hz, H-7), 5.04-4.95 (2H, m, H-8, H-8'), 3.90-3.88 (1H, ddd, $J_{3,2}$ = 6.3Hz, $J_{3,2'}$ = 4.1Hz, $J_{3,4}$ = 2.2Hz, H-3), 3.86-3.78 (2H, dd, J = 13.5, 24.8Hz, H-10a, H-10a'), 3.04-3.00 (1H, dd, $J_{5,4}$ = 7.5Hz, $J_{5,5'}$ = 9.9Hz, H-5), 2.81-2.79 (1H, dd, $J_{2,2'}$ = 10.4, H-2), 2.70-2.67 (1H, dd, H-2'), 2.30-2.24 (1H, m, H-6), 2.27-2.24 (1H, dd, $J_{5',4}$ = 7.2Hz, H-5'), 2.08-2.01 (2H, m, H-4, H-6'). ^{13}C-NMR (125MHz, MeOD): δ = 152.1 (C-6a), 151.0 (C-2a), 147.0 (C-4a), 138.0 (C-7), 130.1 (C-8a), 116.3 (C-8), 115.1 (C-5a), 112.5 (C-9a), 76.8 (C-3), 62.2 (C-2), 59.0 (C-5), 49.1 (C-10a), 48.0 (C-4), 38.2 (C-6). ESI-HRMS for $C_{14}H_{19}N_5O$ [MH]$^+$ calcd:

274.1668, found: 274.1661. HPLC: 95%; ESI-LRMS for $C_{14}H_{19}N_5O$ $[MH]^+$: 274 (100%); 95.3% purity by HPLC. mp: decomposition above 220℃.

3 Appendix

^{13}C-NMR Spectra of the Amadori products

β-D-Galactopyranosyl-(1→5)-1-(*N,N*-dibenzyl)amino-1-deoxy-α-D-*gluco*-hept-2-ulopyranose (25)

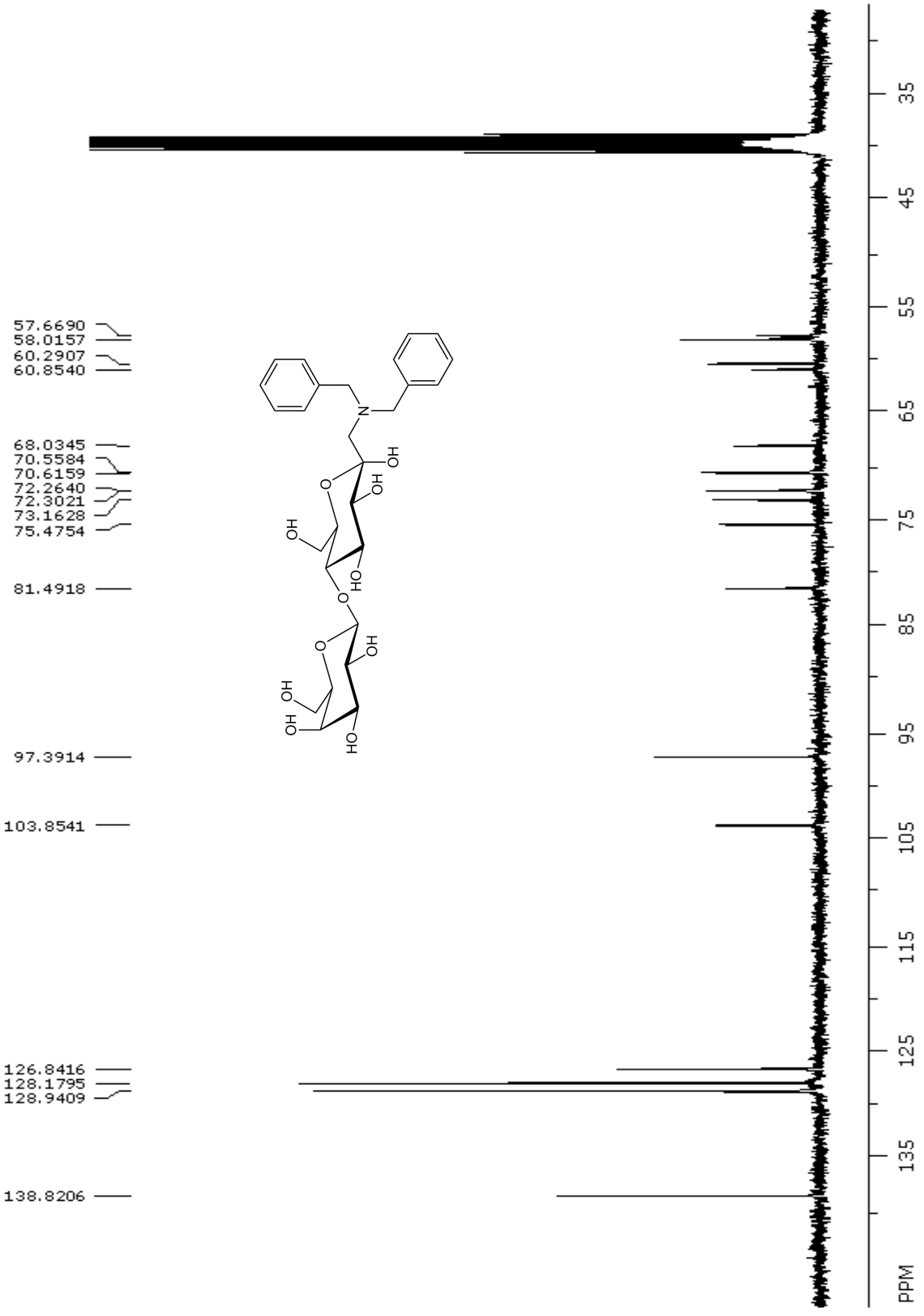

β-D-Glucopyranosyl-(1→5)-1-(*N,N*-dibenzyl)amino-1-deoxy-α-D-*gluco*-hept-2-ulopyranose (26)

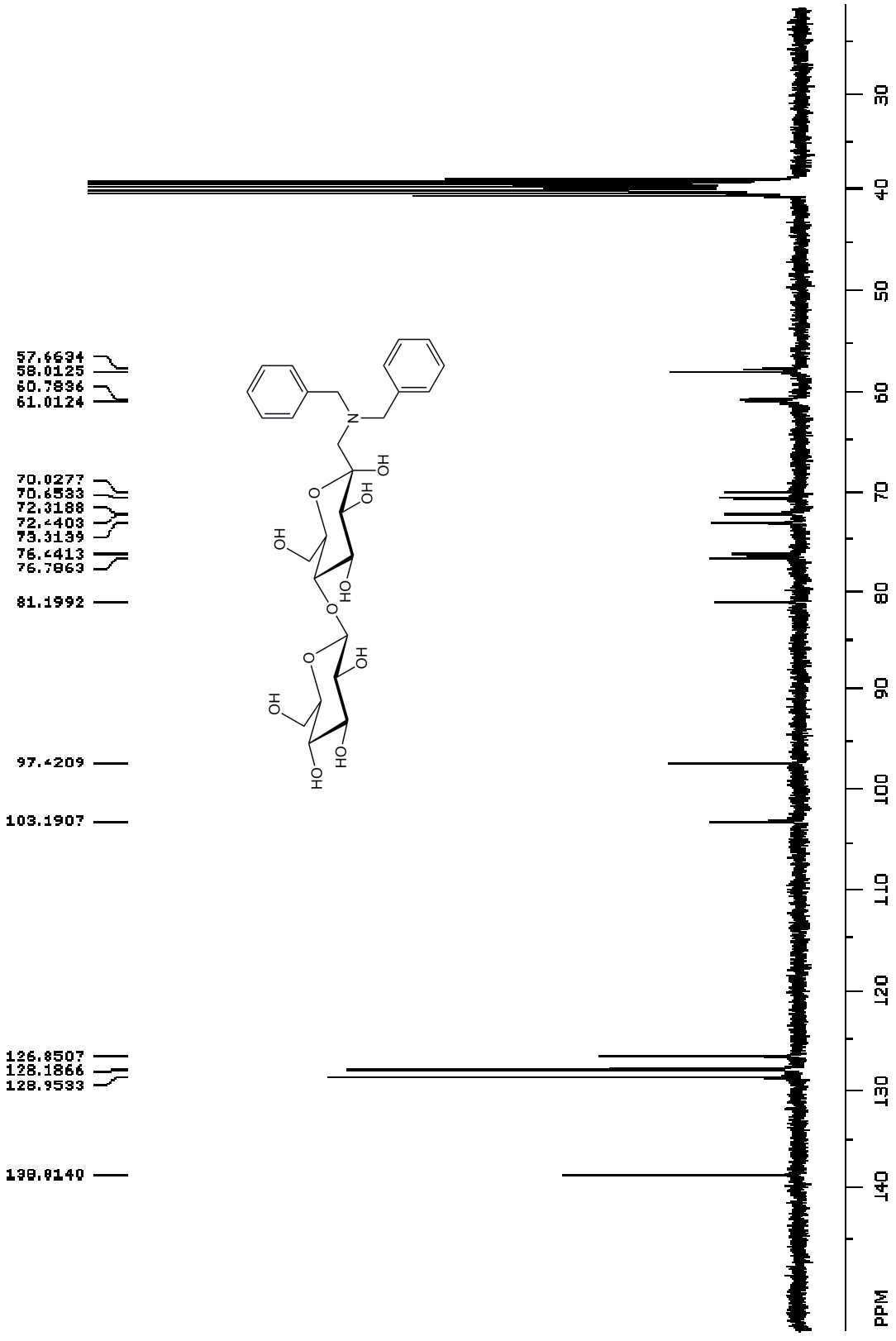

β-D-Galactopyranosyl-(1→5)-1-(*N,N*-dibenzyl)amino-1-deoxy-2-*N*-[1,3-dimethyl-2,4,6 (1H,3H,5H)-trioxopyrimidine-5-ylidene]methylamino-2-deoxy-α-D-*gluco*-hept-2-ulopyranose (27)

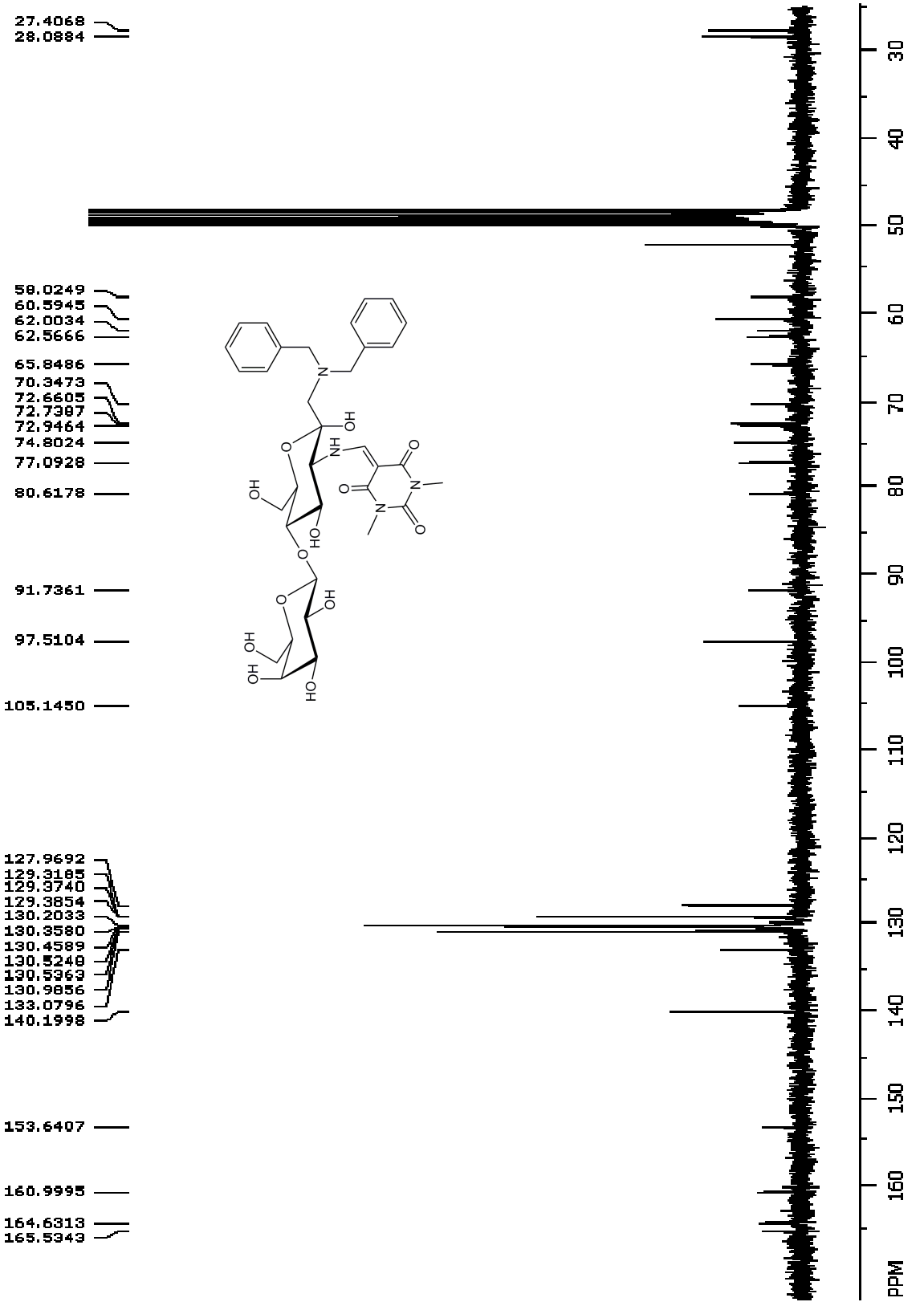

2',3',4',6'-Tetra-*O*-acetyl-α-D-glucopyranosyl-(1→5)-3,4,7-tri-*O*-acetyl-1-(*N*-methoxycarbonylpentyl)amino-1-*N*,2-*O*-carbonyl-1-deoxy-(1→4)-α,β-D-*gluco*-hept-2-ulopyranose (31)

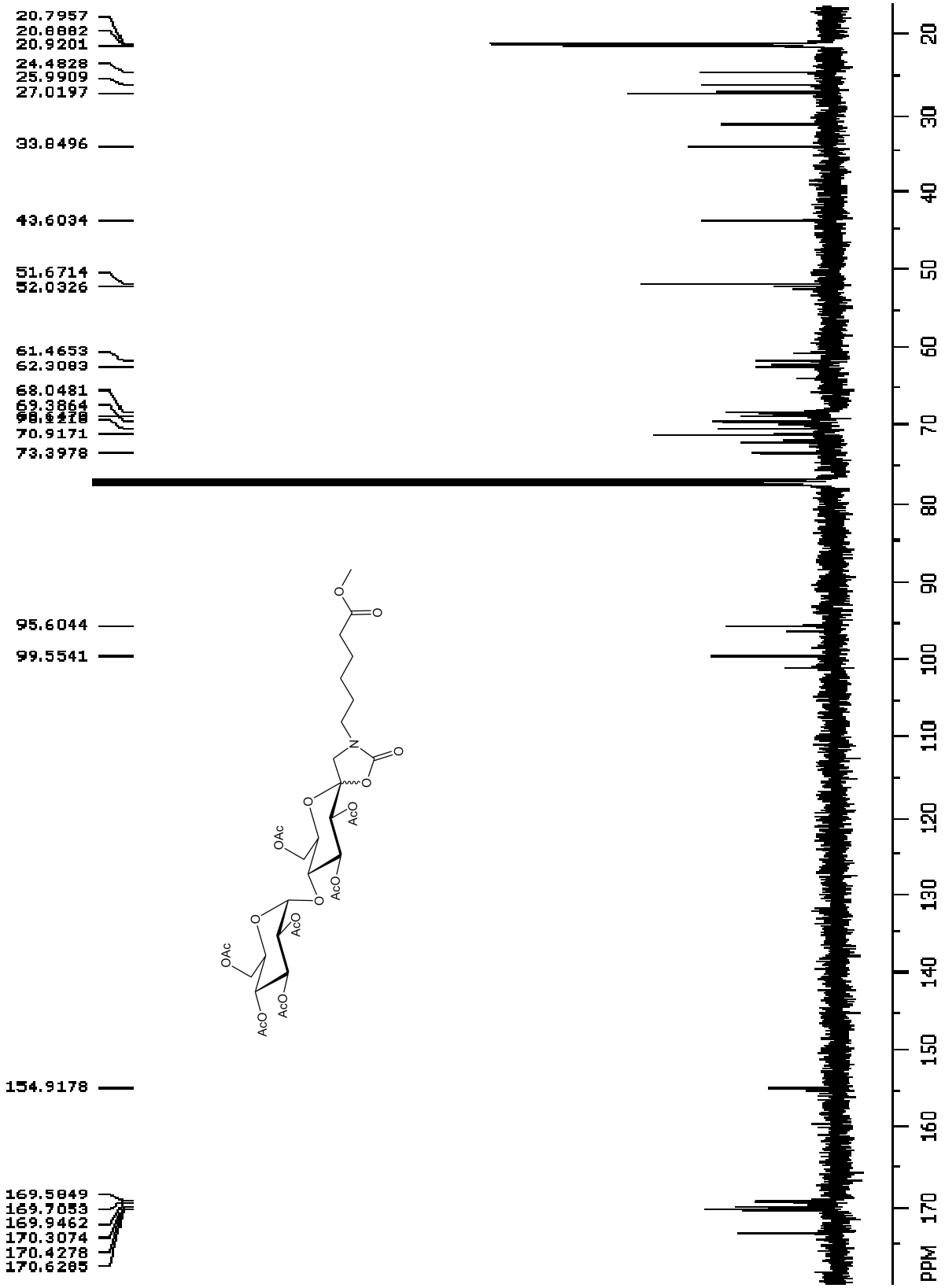

4 Curriculum Vitae

Florian Adanitsch

Born October 24, 1985 in Graz, Austria

Education

1992-1996	Primary School: Volkschule Leutschach
1996-2004	Grammar School: BG/BRG Leibnitz
June 2004	University Entry Certificate, “with distinction”
Oct. 2004-present	Graz University of Technology, undergraduate studies in Technical Chemistry
March 2009-present	Diploma Thesis: **“Synthesis of Biological Active Carbohydrates and Analogues”**, advisor: Assoc. Prof. Dipl.-Ing. Dr. *techn*. Tanja M. Wrodnigg, Institute of Organic Chemistry, Graz University of Technology. In collaboration with Dr. Peter C. Tyler, Industrial Research Limited, Lower Hutt, New Zealand).

Stay abroad

March 2009-June 2009	Wellington, New Zealand. Undergraduate coworker of Dr. Peter C. Tyler at the Carbohydrate Chemistry Team of Industrial Research Limited, Lower Hutt.

Internship

Jul 2007-Aug 2007	Graz University of Technology, Institute of Organic Chemistry. Advisor: Assoc. Prof. Dipl.-Ing. Dr. *techn*. Tanja M. Wrodnigg.
Jul 2008-Aug 2008	DSM Fine Chemicals, Linz, Austria, Department for Research and Development.

5 Publications

Publications in Journals

Adanitsch, F.; Pototschnig, G.; Wrodnigg, T.M. Synthesis of *C*-glycosyl Type Glycoconjugates of important Carbohydrates by the Amadori Rearragement. In preparation for the *Journal of Carbohydrate Chemistry*

Posters at Conferences

Adanitsch, F.; Evans, G.B.; Longshaw, A.I.; Tyler, P.C. The Synthesis of Hydroxypyrrolidine Cores for Incorporation into Immucillins. *15th European Carbohydrate Symposium, EUROCARB XV,* Vienna , Austria, **July 19 – 24, 2009**.

Adanitsch, F.; Evans, G.B.; Longshaw, A.I.; Tyler, P.C. Hydroxypyrrolidine Cores synthesised for the Incorporation into Immucillins. *13. Österreichische Chemietage der GÖCH,* Vienna, Austria, **August 24-27, 2009**.

Oral Presentations

Wrodnigg, T.M.; Adanitsch, F.; Steiner, A.J.; Stütz, A.E. Iminoalditole als Chaperone für die Therapie lysosomaler Speicherkrankheiten. *12. Österreichischer Kohlenhydratworkshop,* Universität für Bodenkultur, Vienna, Austria, **February 21, 2008**.

Adanitsch, F.; Wrodnigg, T.M. Amadori Rearrangements of Glycosylated Heptoses. *14. Österreichischer Kohlenhydratworkshop,* Universität für Bodenkultur, Vienna, Austria, **February 11, 2010**.